OCEAN DRILLING PROGRAM

LEG 181 PRELIMINARY REPORT

SOUTHWEST PACIFIC GATEWAYS

Dr. Robert Carter
Co-Chief Scientist, Leg 181
Department of Geology
James Cook University
Townsville
QLD 4811
Australia

Dr. I.N. McCave
Co-Chief Scientist, Leg 181
Department of Earth Sciences
University of Cambridge
Downing Street
Cambridge CB2 3EQ
United Kingdom

Dr. Carl Richter
Staff Scientist, Leg 181
Ocean Drilling Program
Texas A&M University Research Park
1000 Discovery Drive
College Station, Texas 77845-9547
U.S.A.

Dr. Jack Baldauf
Deputy Director
Science Operations
ODP/TAMU

Dr. Carl Richter
Leg Project Manager
Science Services
ODP/TAMU

November 1998

This informal report was prepared from the shipboard files by the scientists who participated in the cruise. The report was assembled under time constraints and is not considered to be a formal publication that incorporates final works or conclusions of the participating scientists. The material contained herein is privileged proprietary information and cannot be used for publication or quotation.

Preliminary Report No. 81

First Printing 1998

Distribution

Electronic copies of this publication may be obtained from the ODP Publications Home Page on the World Wide Web at http://www-odp.tamu.edu/publications

D I S C L A I M E R

This publication was prepared by the Ocean Drilling Program, Texas A&M University, as an account of work performed under the international Ocean Drilling Program, which is managed by Joint Oceanographic Institutions, Inc., under contract with the National Science Foundation. Funding for the program is provided by the following agencies:

Australia/Canada/Chinese Taipei/Korea Consortium for the Ocean Drilling
Deutsche Forschungsgemeinschaft (Federal Republic of Germany)
Institut Français de Recherche pour l'Exploitation de la Mer (France)
Ocean Research Institute of the University of Tokyo (Japan)
National Science Foundation (United States)
Natural Environment Research Council (United Kingdom)
European Science Foundation Consortium for the Ocean Drilling Program (Belgium, Denmark, Finland, Iceland, Italy, The Netherlands, Norway, Spain, Sweden, Switzerland, and Turkey)
Marine High-Technology Bureau of the State Science and Technology Commission of the People's Republic of China

The following scientists were aboard the JOIDES Resolution for Leg 181 of the Ocean Drilling Program:

Co-Chief Scientist
Robert Carter
Department of Geology
James Cook University of North Queensland
Townsville, QLD 4811
Australia
Work Phone: (61) 7-47814536
Fax: (61) 7-47251501
Internet: bob.carter@jcu.edu.au

Co-Chief Scientist
I.N. McCave
Department of Earth Sciences
University of Cambridge
Downing Street
Cambridge CB2 3EQ
United Kingdom
Work Phone: (44) 1223-333422
Fax: (44) 1223-333450
Internet: mccave@esc.cam.ac.uk

Staff Scientist
Carl Richter
Ocean Drilling Program
Texas A&M University Research Park
1000 Discovery Drive
College Station, TX 77845-9547
U.S.A.
Internet: carl_richter@odp.tamu.edu
Work: 409-845-2522
Fax: 409-845-0876

Paleontologist (radiolarians)
Yoshiaki Aita
Department of Geology
Faculty of Agriculture
Utsunomiya University
350 Mine
Utsunomiya 321-8505
Japan
Work Phone: 81-28-649-5427
Fax: 81-28-649-5428
Internet: aida@cc.utsunomiya-u.ac.jp

Sedimentologist
Christophe Buret
Département des Sciences de la Terre
Université de Lille I
Cité Scientifique Bât. SN5
Villeneuve d'Ascq Cedex 59655
France
Work Phone: 33-3-2043-4125
Fax: 33-3-2043-4910
Internet: Christophe.buret@univ-lille1.fr
Mailing Address:
Université de Picardie Jules Verne
Département de Géologie
33, rue Saint Leu
80 039 AMIENS CEDEX
France
Work Phone: 33-3-2282-7608
Internet: christophe.buret@sc.u-picardie.fr

Observer (New Zealand)/Sedimentologist
Lionel Carter
National Institute of Water and Atmosphere
P.O. Box 14-901 Kilbirnie
Wellington
New Zealand
Work Phone: 64-4-386-0300
Fax: 64-4-386-2153
Internet: l.carter@niwa.cri.nz

Paleontologist (nannofossils)
Agata Di Stefano
Instituto di Geologia e Geofisica
Università di Catania
Corso Ialia 55
Catania 95129
Italy
Work phone: (39) 95-719-5713
Fax: (39) 95-719-5712
Internet: distefan@mbox.unict.it

Paleontologist (diatoms)
Juliane Fenner
Bundesanstalt für Geowissenschaften und Rohstoffe
Stilleweg 2
Hannover 30655
Federal Republic of Germany
Work Phone: (49) 511-643-2510
Fax: (49) 511-643-2304

LDEO Logging Trainee
Patrick Fothergill
Department of Geology
University of Leicester
Borehole Research
Leicester LE1 7RH
United Kingdom
Work Phone:
Fax: (44) 116-252-3918
Internet: paf10@le.ac.uk

Paleontologist (foraminifers)
Felix Gradstein
Saga Petroleum a.s.
Kjorboveien 16, P. O. Box 490
Sandvika 1301
Norway
Work Phone: (47) 67-126-141
Fax: (47) 67-126-585
Internet: felix.gradstein@saga.no

Sedimentologist
Ian Hall
Department of Earth Sciences
University of Cambridge
Downing Street
Cambridge CB2 3EQ
United Kingdom
Work Phone: (44) 1223-333442
Fax: (44) 1223-333450
Internet: ih10006@esc.cam.ac.uk

LDEO Logging Scientist
David Handwerger
Department of Geology and Geophysics
University of Utah
1460 East 135 South, Rm 719
Salt Lake City, UT 84112
U.S.A.
Work Phone: (801) 585-5328
Fax: (801) 581-7065
Internet: dahandwe@mines.utah.edu

Stratigraphic Correlator
Sara Harris
Sea Education Association
P.O. Box 6
Woods Hole, MA 02543
U.S.A.
Work Phone: 800-552-3633
Internet: sharris@oce.orst.edu
Shipping Address:
Sea Education Association
171 Woods Hole Road
Falmouth, MA 02540
U.S.A.

Observer (New Zealand)/Paleontologist (foraminifers)
Bruce Hayward
Geology Department
Symonds Street
University of Auckland
Private Bag 92019
Auckland
New Zealand
Work Phone: (64) 9-373-7999
Fax: (64) 9-373-7435
Internet: b.hayward@auckland.ac.nz

Paleomagnetist
Shouyun Hu
Department of Geology
University of California, Davis
Davis, CA 95616
U.S.A.
Fax: 530-752-0951

Sedimentologist
Leah Joseph
Department of Geological Sciences
University of Michigan
2534 C.C. Little Bldg.
425 East University
Ann Arbor, MI 48109-1063
Work Phone: (734) 647-7925
Fax: (734) 763-4690
Internet: ljoseph@umich.edu

Inorganic Geochemist
Boo Keun Khim
Research Institute of Oceanography
Seoul National University
Shillim-dong San56-1
Kwanak-Gu
Seoul 151-742
Korea
Work Phone: (82) 2-880-6496
Home Phone: (82) 343-424-0139
Fax: (82) 2-872-0311
Internet: bkkocean@plaza.snu.ac.kr

Physical Properties Specialist
Yir-Der Lee
Department of Oceanography
Texas A&M University
O&M Building
College Station, TX 77843
Work Phone: (409) 862-9133/
(409)-255-3558
Fax: (409) 862-6331
Internet: eddy@ocean.tamu.edu

Physical Properties Specialist
Lynn Millwood
Department of Geology
University of Texas at Arlington
500 Yates, Room 107
P.O. Box 19049
Arlington, TX 76019-0049
U.S.A.
Work Phone: (817) 272-2987
Fax: (817) 272-2628
Internet: idm8510@omega.uta.edu

Organic Geochemistry
Joachim Rinna
Institut für Chemie und Biologie des Meeres
(ICBM)
Carl von Ossietzky Universität, Oldenburg
Postfach 2503
Carl von Ossietzky Straße
Oldenburg 26111
Germany
Work Phone: (49) 441-798-3415
Fax: (49) 441-798-3404
Internet: j.rinna@ogc.icbm.uni-oldenburg.de

Sedimentologist
Gerald Smith
Department of Geology
876 Natural Science Complex
State University of New York, Buffalo
Buffalo, NY 14260
U.S.A.
Work: (716) 645-6800, ext 2470
Fax: (716) 645-3999
Internet: stratigrapher@msn.com

Inorganic Geochemist
Atushi Suzuki
Address until 14 December 1998:
Australia Insitute of Marine Sciences
PMB, No. 3, Townsville Mail Centre
Townsville, Queenland Q4810
Australia
Work: 61-747-53-4211
Fax: 61-747-72-5852
Internet: asuzuki@aims.gov.au
Address after 14 December 1998:
Marine Geology Department
Geological Survey of Japan
1-1-3 Higashi, Tsukuba, Ibaraki, 305
Japan
Work Phone: 81-298-54-3773
Fax: 81-298-54-3765
Internet: a_suzuki@gsj.go.jp

Stratigraphic Correlator
Graham Weedon
Department of Environment, Geography and Geology
University of Luton
Park Square
Luton, Bedfordshire LU1 3JU
United Kingdom
Work: (44) 1582-734-111, ext 2528
Fax: (44) 1582-489-212
Internet: graham.weedon@luton.ac.uk

Paleontologist (nannofossils)
Kuo-Yen Wei
Department of Geology
National Taiwan University
245 Choushan Road
Taipei 10770
Taiwan, Republic of China
Work Phone: (886) 2-23691163
Fax: (886) 2-23636095
Internet: weiky@ms.cc.ntu.edu.tw

Paleomagnetist
Gary Wilson
Byrd Polar Research Center
Ohio State University
1090 Carmack Road
Columbus, OH 43210-1002
U.S.A.
Work: (614) 292-6531
Fax: (614) 292-4697
Internet: wilsongs@geology.ohio-state.edu

Sedimentologist
Amelie Winkler
GEOMAR
Research Center for Marine Geosciences
Wischhofstraße 1-3
Gebäude 4
Kiel 24148
Federal Republic of Germany
Work: (49) 431-600-2844
Fax: (49) 431-600-2941
Internet: awinkler@geomar.de

SCIENTIFIC REPORT

ODP LEG 181 LEG SUMMARY: SOUTHWEST PACIFIC GATEWAYS

INTRODUCTION

The circulation of cold, deep Antarctic Bottom Water (AABW) is one of the controlling factors in the Earth's heat budget and, ultimately, climate. Today, forty percent of the flux of cold bottom-water entering the major ocean basins does so through the Southwest Pacific Ocean, as a thermohaline Deep Western Boundary Current (DWBC) (Warren, 1981). The cold water in the DWBC is derived through dense waters sinking around Antarctica and through the entrainment and mixing of deep Atlantic and Indian ocean waters by the wind-driven Antarctic Circumpolar Current (ACC). At the approach to the Pacific Ocean, filaments of the ACC pass around and through gaps in the Macquarie Ridge to reunite further east and flow northeast along the eastern edge of the New Zealand microcontinent (Fig. F1A). Early in its journey, where it flows northeast along the edge of the Campbell Plateau, the DWBC is reinforced by the ACC. At the southern edge of the Bounty Trough (46°S), the ACC veers east and continues across the Pacific, whereas the DWBC flows on north at depths between ~4500 and 2000 m, across the Bounty Fan, around the eastern end of the Chatham Rise, northwestward across the northern boundary of the Hikurangi Plateau, to finally turn north and flow toward the equator along the Tonga-Kermadec Trench. Higher in the water column, north-spreading Antarctic Intermediate Water (AAIW), formed by subduction at the Antarctic Convergence (AAC), bathes the top and eastern upper flank of the Campbell Plateau in depths of 400–1500 m.

Earlier Research

Despite the key location of eastern New Zealand at the gateway for major water flows into the Pacific Ocean, no previous ODP drilling has been accomplished in the region. Of the four earlier DSDP sites (Fig. F2), only one—Site 594 in the inner Bounty Trough, which penetrated a thick sequence of hemipelagic muds and nannofossil chalks dated to the late Early Miocene—was cored with the Advanced Piston Corer. Results from this site yielded important information regarding the synchroneity of glaciations between the hemispheres (Nelson et al., 1985), the history of supply of AAIW, and the position through time of the Subtropical Convergence (STC) and the SAF (Nelson et al., 1986, 1993). The three other DSDP sites were Sites 275 and 276, which were rotary drilled at locations on the edge of the Campbell Plateau where active erosion has removed a large part of the record, and Site 277, on the western edge of the Campbell Plateau, where an exceptional Paleogene–Neogene isotope record was recovered (Shackleton and Kennett, 1975). New research into the late Quaternary oceanographic, climatic, and sedimentary history of offshore eastern New Zealand has burgeoned over the last two decades (e.g., Carter and Mitchell, 1987;

Barnes, 1992; Fenner et al., 1992; Carter et al., 1994; Carter and McCave, 1994, 1997; L. Carter et al., 1995, 1996; R. Carter et al., 1996; McCave and Carter, 1997; Thiede et al., 1997; Weaver et al., 1997, 1998. This work notwithstanding, the lack of cored offshore drill holes means that we remain ignorant of the post–mid-Cenozoic paleoceanography for most of the region, apart from occasional studies from the western shallow water and onland edge of the basin (Ward and Lewis, 1975; Carter, 1985; L. Carter et al., 1996; R. Carter et al., 1996). Recent seismic studies have delineated the offshore structure moderately well (Lewis et al., 1985; Barnes, 1994; R. Carter et al., 1994, 1996; Lewis, 1994; Barnes and de Lepinay, 1997), and this is the region that we must now search for the record of the inception and evolution of the large ACC and the Pacific DWBC current systems.

Background and Objectives of Leg 181

In summary, our knowledge of Southwest Pacific ocean history, and in particular the development of the ACC-DWBC system, is extremely poor. Leg 181 therefore drilled seven holes in the eastern New Zealand region in order to attempt to reconstruct the stratigraphy, paleohydrography, and dynamics of the DWBC and related water masses. The sites composed a transect of water depths from 393 to 4460 m and spanned a latitudinal range from 39°S to 51°S. Leg 181 drilling has provided the data that are needed to study a range of problems in Southern Ocean Neogene paleohydrography, sedimentology, paleoclimatology, and micropaleontology.

Tectonic Creation of the Southern Ocean

The origin of the modern thermohaline ocean circulation system must postdate the tectonic creation of a continuous Southern Ocean. Particularly important for the origin of the ACC-DWBC was the opening of the Australian-Antarctic (South Tasman) and South American-Antarctic (Drake Passage) deep-water flow gateways (Molnar et al., 1975; Lawver et al., 1992). The South Tasman gateway, including the Balleny Fracture Zone (Lonsdale, 1988), opened to deep water in the early Oligocene (~32 Ma), thereby allowing connection between the Indian and Pacific Oceans for the first time (Kennett et al., 1972; Kennett, 1977). Later, at ~20 Ma (earliest Miocene), the opening of Drake Passage (Boltovskoy, 1980) allowed the establishment of the full circum-Antarctic ocean circulation. During the critical late Eocene to Miocene period, the New Zealand Plateau was located downcurrent from the evolving South Tasman gateway (Watkins and Kennett, 1971), directly in the path of the evolving ACC-DWBC system (Fig. F3).

Geological Setting

The evolution of the ACC-DWBC system took place during the Oligocene and earliest Miocene (32–20 Ma), when plate movements created the first deep-water oceanic gaps south of Australia and South America. The stratigraphic record of these events, and of the development of the modern ACC-DWBC, occurs in Cenozoic sediments located on and just east of the New Zealand microcontinental plateau (Fig. F4). South Island New Zealand is today transected by the Alpine Fault boundary between the colliding Australian and Pacific plates, but the greater part of

eastern New Zealand has been unaffected by major tectonic events since the phase of Late Cretaceous rifting that created the south Pacific Ocean and first delineated the New Zealand Pacific continental margin. In short, since the Late Cretaceous, eastern New Zealand, which includes the submerged continental crust of Campbell Plateau and Chatham Rise, separated by the rift re-entrant of the Bounty Trough, has been a trailing-edge passive margin, and subject to thermotectonic subsidence and marine transgression (Cotton, 1955; Carter, 1988a).

The geological history of eastern New Zealand therefore consists of Late Cretaceous rift-valley filling (Bishop and Laird, 1976), followed by peneplanation and a marine transgression that reached its climax in the Oliocene, when almost the entire New Zealand plateau was submerged, terrigenous sources were flooded or buried, and regional carbonate sedimentation reigned supreme (Suggate et al., 1978). In the west, tectonic activity associated with the development of the transform plate boundary through New Zealand started in the late Eocene (Turnbull, 1985; Turnbull and Uruski, 1995; Sutherland, 1995), and, by the copious volumes of early Miocene terrigenous sediment from mountains along the Alpine Fault were being shed eastward into the Canterbury Basin, where they built the progradational sedimentary prism that underlies the modern coastal lowland and continental shelf of eastern South Island (Carter and Norris, 1976; Norris et al., 1978). Mountain building accelerated, and, presumably, sediment yields increased, at ~6.5 Ma in the late Miocene, when a shift in the pole of rotation resulted in a stronger element of collision across the Alpine Fault boundary (Walcott, 1998). These various plate boundary events had only minor effects in the eastern (offshore) parts of the New Zealand plateau (Fig. F4B). Apart from localized episodes of volcanism and mild folding-faulting associated with changes in regional stress patterns (e.g., Oliver et al., 1950; Carter, 1988b; Carter et al., 1994; Campbell et al., 1993), stasis or very slow postrift subsidence continued, and major sources of terrigenous sediment were absent. Sediment accumulation on highs was either precluded by strong water motion (e.g., Chatham Rise) or consisted of biopelagic chalk and ooze (e.g., Campbell Plateau), and terrigenous sedimentation was restricted to lows (e.g., Bounty Channel-Fan complex) or to sites adjacent to the prograding eastern New Zealand sediment prism (e.g., DSDP Site 594; Kennett, von der Borch, et al., 1986).

Oceanography: Deep Currents

The supply of deep water to the Pacific Ocean is dominated by a single source, the deep western boundary current (DWBC) that flows north out of the Southern Ocean along the east side of the Campbell Plateau-Chatham Rise-Hikurangi Plateau, east of New Zealand (Figs. F1, F5). The volume transport of the DWBC is ~20×10^6 m^3 s^{-1} (Sv), which composes ~40% of the total input of deep water to the world's oceans (Warren, 1973; 1981). A secondary, but minor, flow of ~3 Sv of deep-water flows north into the Peru-Chile basin (Lonsdale, 1976). The magnitude of DWBC flow, and the low temperature of the water involved, are major determinants of the oceanography of the Pacific Ocean and of the global heat balance. Monitoring the DWBC flow at its entry into the Pacific is a key area where the "global salt conveyor" hypothesis (Gordon, 1986; Broecker et al., 1990; Schmitz, 1995) can be tested, as the flow thereafter is believed to spread out

to fill the Pacific. Some water upwells and returns at shallower depths across the Indian Ocean and on to the Atlantic, whereas other waters return south as North Pacific Deep Water (NPDW).

The supply of cold water to the deep Pacific from the main generating regions in the Weddell and Ross Seas is modulated by the ACC, which mixes these waters with North Atlantic Deep Water (NADW) in the South Atlantic to form Circumpolar Deep Water (CDW). Deep water output to the Pacific therefore carries the combined signatures of Southern Ocean processes in the region of deep water formation, chemical composition related to Southern Ocean gas exchange, and NADW. Despite its turbulent passage around Antarctica, CDW is not completely mixed, and a distinct NADW salinity maximum can be recognized at depths of 2800 m (at 55°S) deepening northward to 3400 m (at 28°S). In the Southwest Pacific, the DWBC comprises three main divisions: lower CDW, a mixture of bottom waters generated around Antarctica, in particular cold Weddell Sea Deep Water; salinity-maximum middle CDW, representing the NADW core; and strongly nutrient-enriched and oxygen-depleted upper CDW, mainly derived from Indian Ocean outflow added to Pacific outflow returning through Drake Passage (Fig. F5). The DWBC has its upper boundary at depths around 2000–2500 m. On the eastern side, the DWBC is overlain between 2550 and 1450 m depth by south-flowing NPDW, marked by an oxygen minimum and high silica. Regionally, both DWBC and NPDW are overlain by low salinity, AAIW (Figs. F1B, F5).

The ACC-DWBC enters the Southwest Pacific around and through gaps in the Macquarie Ridge complex before passing along the 3500 m high margin of the Campbell Plateau. Near the mouth of the Bounty Trough, the ACC uncouples and continues its eastward path, whereas the DWBC flows north around the eastern end of Chatham Rise and through Valerie Passage, where a small part of the flow diverges through gaps in the Louisville Seamount chain (McCave and Carter, 1997). Valerie Passage, the 250-km-wide gap between the Chatham Rise and the Louisville Ridge, therefore marks the gateway to the Pacific for the DWBC (Warren, 1973).

Oceanography: Shallow Fronts

In the shallower ocean, the seas east of South Island are crossed by two major frontal systems that exhibit intensified meridional gradients in temperature, salinity and density (Fig. F1). At around 55°S, but then curling north around the southeastern corner of the Campbell Plateau to almost 50°S, the east-flowing ACC is bounded to the north by the Subantarctic Front (SAF) (Orsi et al., 1995). South of the SAF, the annual mean surface-water temperature is <10°C, and the nutrient-rich polar ocean is rich in both phosphate and silica. The SAF is also the site where low-salinity AAIW is subducted rapidly from the surface northward to depths around 1000 m. The observations of Bryden and Heath (1985), together with global circulation models (Carter and Wilkins, in press), indicate that another unnamed front may extend east into the Pacific from the south side of the Bounty Trough. This front, at about latitude 46°S, probably marks the northern limit of the ACC east of New Zealand, rather than the 56°S SAF that is usually taken as the ACC limit (e.g., Orsi et al., 1995).

About ten degrees of latitude north of the SAF, the Subtropical Convergence (STC) separates

subantarctic water of salinity 34.5 and an annual mean surface-temperature range of 8°–15°C from subtropical water with salinity >35 and an annual mean temperature range of >15°C. East-flowing currents occur on both sides of the STC, the warm East Cape Current (a continuation of the East Australian current) on the north side, and the cold West Wind Drift on the south. However, these current systems are most active several degrees of latitude away from the STC, and sluggish flow is therefore characteristic of the frontal region itself. Eastward flow on the south side of the STC is augmented by the Southland Current (derived from the Tasman Current being deflected by wind-drift around the south end of South Island), which flows north along the eastern South Island continental shelf and then turns east along the southern side of the crest of Chatham Rise. Heat transfer from the equator to the pole takes place across the SAF and STC by a combination of wind drift and dynamic eddying, with a cold return flow at depth in the DWBC. In the open ocean, as demonstrated in the Indian Ocean sector of the Southern Ocean, these fronts may migrate backward and forward by up to 6° of latitude during a glacial/interglacial cycle (e.g., Howard and Prell, 1992). However, modern seasonal movements of the front of at least 2° of latitude occur also, as for example for the STC east of New Zealand (Chiswell, 1994). In contrast to the oceanic mobility of the STC, several authors have shown that east of South Island the STC probably remained fixed to the shallow Chatham Rise throughout at least the most recent climatic cycle (Fenner et al., 1992; Nelson et al., 1993; Weaver et al., 1998).

The pronounced bathymetry around New Zealand exercises a controlling influence on the disposition of both deep currents and oceanic frontal zones. Notably, the ACC and DWBC are steered around or through gaps in Macquarie Ridge, and are then guided northward along the eastern escarpment of the Campbell Plateau. Concomitantly, in near-surface waters, the SAF, and the ACC with it, is forced north around and along the southeastern corner of the Campbell Plateau, and the position of the STC is probably controlled by eastward currents both north and south of the Chatham Rise. Some sites on Leg 181 were chosen in order to track whether or not past changes in the position of these fronts has occurred.

Sedimentary Record of the ACC-DWBC

Sediments on the eastern New Zealand margin at shelf to upper bathyal depths (50–1000 m) are known to have been strongly affected by currents since at least the late Oligocene (Ward and Lewis, 1975; Carter, 1985; L. Carter et al., 1996). This evidence for strong paleoflows, together with the confirmation that substantial Antarctic glaciation commenced at least as early as the early Oligocene (Shackleton and Kennett, 1975; Barrett, 1996; Barron, Larsen, et al., 1989) implies that Pacific hydrography has been fundamentally affected by an evolving circumpolar current and western boundary current system since the middle Cenozoic.

To reconstruct the paleoflow of the DWBC and overlying current system requires drill sites through thick, undisturbed, fine-grained sediment masses constructed under the influence of the current. Seismic records indicate the presence of candidate sediment drifts at many points along the eastern edge of the New Zealand Plateau, in water and paleowater depths between 300 and 5500 m (Carter and McCave, 1994; L. Carter et al., 1996). There are, however, five possible origins for

any particular body of sediment: (1) deposition as part of the deepening- and fining-upward rift-drift cycle that characterizes New Zealand's Cretaceous to Oligocene history; (2) transport into the area via the DWBC (e.g., subantarctic diatoms present in the drifts at 40°S; Carter and Mitchell, 1987); (3) biopelagic snow; (4) airfall rhyolitic and andesitic ash, which derives from explosive Miocene–Holocene explosive arc volcanism in New Zealand (Ninkovich, 1968; van der Lingen, 1968; Lewis and Kohn, 1973; Nelson et al., 1985; Froggatt et al., 1986; Froggatt and Lowe, 1990; Shane, 1990; Shane and Froggatt, 1991; Carter et al., 1995; Shane et al., 1995, 1996), and which, over the last 20 k.y., has been input at rates up to one-third that of fluvial terrigenous sediment (Carter et al., 1995); and (5) terrigenous sediment that is derived from uplifting mountains in New Zealand, after the inception of the modern Alpine Fault plate boundary (i.e., Miocene–Holocene Otakou Group equivalents; cf. Fig. 4A) and transported into the path of the DWBC by turbidity currents traveling down the Solander, Bounty, and Hikurangi channel systems. Each of these sediment sources can be constrained, and the sedimentary dynamics and transport paths of the modern system are moderately well delineated (e.g., Carter and Carter, 1993; Carter and McCave, 1997; Lewis, 1994). In contrast, little is known regarding the geologic record or history of the DWBC.

The Eastern New Zealand Oceanic Sedimentary System (ENZOSS)

The available seismic records suggest that the DWBC has been active along the eastern New Zealand margin since at least the Miocene, and probably since the middle Oligocene (32 Ma) (Carter and McCave, 1994). Starting at ~24 Ma, abundant terrigenous material was shed from rising mountains along the Alpine Fault plate boundary (Vella, 1962; Norris et al., 1978) and fed through the eastern South Island shelf into the Solander, Bounty and Hikurangi channel systems. Sediment supply accelerated at ~6.5 Ma in the late Cenozoic, when collision increased along the plate boundary (Walcott, 1998; cf. Kennett, von der Borch, et al., 1986), and supply to the deep sea was probably enhanced again from the start of major glacial lowstands at ~2.6 Ma onward. Much of this sediment ultimately became entrained in the DWBC drift system, which carries it northward to be eventually subducted into the Kermadec Trench.

Sediment is delivered into the DWBC through two newly described transport conduits, the Bounty (Carter and Carter, 1993) and Hikurangi (Lewis, 1994) channel-fan systems. A third feeder channel, Solander, is poorly known, but extends for >450 km before discharging into the DWBC at Emerald Basin between Macquarie Ridge and the western side of Campbell Plateau (L. Carter et al., 1996; Carter and McCave, 1997; Schuur et al., in press). The Hikurangi Fan has been termed a "fan-drift" by Carter and McCave (1994) because it apparently represents the extreme case of a fan whose thickness and facies pattern are directly remolded by a deep current into the form of a sediment drift. In contrast, the Bounty Fan, located in a bathymetric embayment, has retained its fan morphology and has developed directly across the path of the DWBC, the only evidence of modern drift formation being scour of the northern fan and redeposition of material as a series of small, discrete ridges (Carter and Carter, 1993). Compared to Hikurangi Fan Drift, Bounty Fan has formed in a region where the DWBC is inferred to be slowed (1) by the lack of

forcing by the shallower water stream of the ACC, which continues east across the Pacific just south of Bounty Trough; and (2) the loss of the topographic steering, and current acceleration, provided by the steep eastern slope of the Campbell Plateau, which ceases abruptly at Bollons Seamount, again at the southern edge of the Bounty Trough. However, six years of satellite sea-surface temperature data, summarized by Carter et al. (1998), indicates that meanders from the ACC periodically affect the outer Bounty Trough, and the water motions that accompany them may also play a role in current-winnowing on the lower Bounty Fan.

During the later Cenozoic, the two described abyssal fans have been supplied with sediment by turbidites passing through the Bounty and Hikurangi channels, each of which is over 1000 km long. Hikurangi Channel heads in the Kaikoura Canyon, only a few hundred meters from shore, and less than 10 km from the rapidly rising, 2.5-km-high Seaward Kaikoura Mountains (Lewis, 1994). The Hikurangi system is therefore active today, in interglacial times. In contrast, the Solander and Bounty Channels head in a number of canyons that indent the edge of the continental shelf. The Bounty and Solander Systems may therefore be sea-level (i.e., climatically) controlled, with most sediment being fed into them during glacial lowstands, whereas in interglacials the same sediment stream is diverted along the inner shelf, some of it reaching the Hikurangi System via the Kaikoura Canyon (Carter and Herzer, 1979).

Eastern New Zealand is thus the site of a major recycling system, whereby sediment is shed from uplifting mountains along the Australian/Pacific plate boundary and provided to the deep sea via several major submarine channel systems. Once at abyssal depths, the sediment is re-entrained by the ACC and DWBC, and passed north along the edge of the Campbell Plateau, around the tip of the Chatham Rise, westward along the foot of the Hikurangi Plateau, to finally arrive in the Hikurangi-Kermadec trench, where it is subducted, melted and enters the cycle again as juvenile volcanic rock. Remarkably, and largely because of the effects of the plate boundary, the two small islands of New Zealand supply two percent of the world’s sediment load to the oceans (Milliman and Syvitski, 1992); it is this sediment load that is then entrained in what L. Carter et al. (1996) have termed the Eastern New Zealand Oceanic Sedimentary System (ENZOSS) (Fig. F6).

Recent publications (Carter and Carter, 1993; Lewis, 1994; Carter and McCave, 1994; L. Carter et al., 1996) have delineated the ENZOSS region, between the Solander Trough and the Kermadec Trench, east of the modern Australian-Pacific plate boundary, as an integrated sediment source-transport-sink area. During the latter half of the Cenozoic, sediment from mountains along the New Zealand plate boundary has been transported through deep-sea channel/fan systems, delivered into the path of the DWBC, entrained northward within this current system and finally consumed by subduction at the same plate boundary after a transport path of up to 3500 km.

PRINCIPAL RESULTS

Site 1119

Hole 1119A

Position: 44°45.33234´S, 172°23.59772´E
Start hole: 0345 hr, 23 August 1998
End hole: 1020 hr, 23 August 1998
Time on hole: 6.58 hr
Seafloor (drill pipe measurement from rig floor, mbrf): 406.50
Distance between rig floor and sea level (m): 11.00
Water depth (drill pipe measurement from sea level, m): 395.50
Total depth (from rig floor, mbrf): 412.50
Total penetration (mbsf): 6.00
Coring totals: type: APC; number: 1; cored: 6.00 m; recovered: 100.17%
Formation: lithostratigraphic Unit I: olive gray silty sand and greenish gray silty clay

Hole 1119B

Position: 44°45.33234´S, 172°23.59772´E
Start hole: 1015 hr, 23 August 1998
End hole: 0020 hr, 24 August 1998
Time on hole: 14.08 hr
Seafloor (drill pipe measurement from rig floor, mbrf): 407.80
Distance between rig floor and sea level (m): 11.00
Water depth (drill pipe measurement from sea level, m): 396.80
Total depth (from rig floor, mbrf): 563.60
Total penetration (mbsf): 155.80 mbsf
Coring totals: type: APC; number: 17; cored: 155.80 m; recovered: 105.56%
Formation: lithostratigraphic Unit I: 0–92 mbsf; olive gray silty sand and greenish gray silty clay
lithostratigraphic Unit II: 92–155.8 mbsf; olive gray silty sand and greenish gray silty clay

Hole 1119C

Position: 44°45.33188´S, 172°23.61420´E
Start hole: 0020 hr, 24 August 1998
End hole: 1915 hr, 26 August 1998
Time on hole: 66.92 hr
Seafloor (drill pipe measurement from rig floor, mbrf): 407.20
Distance between rig floor and sea level (m): 11.00
Water depth (drill pipe measurement from sea level, m): 396.20
Total depth (from rig floor, mbrf): 902.00

Total penetration (mbsf): 494.80
Coring totals: type: APC; number: 17; cored: 160.30 m; recovered: 108.28%
type: XCB; number: 35; cored: 334.50 m; recovered: 80.32%
Formation: lithostratigraphic Unit I: 0–92 mbsf; olive gray silty sand and greenish gray silty clay
lithostratigraphic Unit II: 92–404 mbsf; olive gray silty sand and greenish gray silty clay
lithostratigraphic Unit III: 404–494.72 mbsf; greenish gray silty clay

Site 1119 is located 96 km east of the eastern shoreline of New Zealand's South Island, offshore from Timaru, within the Canterbury Basin. The site was drilled in a water depth of 393 m on the upper slope, 5 km seaward of the edge of the continental shelf. Further seaward the slope levels out onto Campbell Plateau at 800–1000 m. Clinoform reflectors within the Miocene–Holocene represent earlier positions of the prograding shelf-slope. The reflectors define a shore-parallel zone of Pliocene–Pleistocene sediment drifts which prograded landward and accreted to the edge of the shelf.

Site 1119 was drilled to sample the upper slope sediments and underlying sediment drifts. A copious source of sediment is required to build the drifts. Site 1119 samples will allow the provenance of the upper drift sediments to be established, paleocurrent velocities to be inferred, and the late Pliocene–Pleistocene history of the important AAIW water mass to be reconstructed close to its source. The sand-rich intervals encountered in the hole may allow inferences to be made regarding relative sea-level change during this period.

Hole 1119A comprised a single 6.01-m-long core taken for mudline sampling. APC penetration, with essentially full core recovery and little disturbance, was then achieved to a depth of 155.8 mbsf (Hole 1119B) and 160.3 mbsf (Hole 1119C) successively (Table T1). Hole 1119C continued to a depth of 494.8 mbsf using the XCB. Throughout the APC core sections, core voids were common in the sands and silts, resulting from the discharge of gas that caused core expansion. Core recovery was 105% for Hole 1119B and 89% for Hole 1119C.

The 494.8 m of sediment cored is subdivided into three lithologic units (Fig. F7). The upper 246.8 m (Unit I) comprises repetitive, sharp-based, silty sand–silty clay couplets. Silty sand beds are usually <2 m thick and have an olive gray color, coarse texture with shell debris, and small amounts of glauconite. Many microfossils are reworked. The silty clays form thick greenish gray beds (usually >4 m), with mica and scattered macrofossils (including double valves of the subantarctic scallop *Zygochlamys delicatula).* Nannofossils occur in most samples, radiolarians have sporadic distribution, pyrite is a common accessory mineral, and sponge spicules are prominent. Toward the bottom of lithostratigraphic Unit I, bathyal gastropods appear in the silty muds (e.g., *Ellicea*), indicating deepening conditions for the sedimentary couplets with depth in the hole: the sequence as a whole indicates shallowing-upward conditions. Foraminifers and nannoplankton indicate deeper, warmer conditions during deposition of the silty sands (sediment-starved upper slope during interglacial highstands), and deposition of silty-clay intervals in relatively shallower, colder water on a nearshore upper slope during glacial lowstands. The basic

nature of the Unit I sedimentary couplets was apparently controlled by sea-level change, but seismic records show that all but the uppermost parts of Unit I (shallower than 50 m) have a drift geometry. However, the marked sedimentary and environmental cyclicity of Unit I is similar to that already described from Pliocene–Pleistocene sediments nearby on land.

Unit II comprises Subunits IIA from 246.8 to 318.4 mbsf and IIB from 318.4 to 428 2 mbsf. It also contains sedimentary rhythms that differ from the couplets of Unit I. The upper part, Subunit IIA, contains doubly-graded silty-sand/silty-clay units (A-Bt-A), with continuous gradation between components. The sands have increased calcite content and sometimes show incipient cementation. Nannofossils are more frequent than in Unit I. The lower part of Unit II (IIB) contains sharp-based sand-silty clay couplets (A-Bc) similar to those of Unit I, but in which the sandstones have less terrigenous material, and include significant amounts of broken shell, benthic foraminifers, and nannofossils. The sands have sharp bases beneath which are muds displaying sand-filled burrows of *Thalassinoides* and *Chondrites.* Whole-valve molluscs, conspicuous in the overlying unit, are rare.

The lowest gradational A-Bt-A motif occurs in the bottom part of Core 181-1119C-34X (the base of Subunit IIA), below which the sharp-based sand-mud couplets continue downhole intermittently to the base of Core 181-1119C-43X (428.2 mbsf, base of Subunit IIB). We interpret the double graded-motif as the deeper water manifestation of the climatic and sea-level changes that produced the sharp-based silty sand-silty clay couplets in Unit I. The sharp-based silty sand-silty clay couplets of Subunit IIB are more difficult to interpret. They may have a similar origin to their counterparts in Unit I, or they may be redeposited (i.e., turbidites). X-radiography will be a great help in making this distinction.

Unit III occurs from 428.2 mbsf to the bottom of the hole and comprises mostly massive, pale olive gray silty clay with occasional burrows, which is similar to the inferred glacial silty clays of Units I and II. Unit III contains very thin beds and laminae of light gray sediments that smear slides suggest are mud turbidites. The trace fossil *Zoophycos* occurs scattered throughout, macrofossils and shell fragments are almost absent, and interbeds of olive sand are completely absent. This unit corresponds with the presence of a large sediment drift on the deep seismic line through Site 1119, and we interpret Unit III sediments as deposits of the deeper slopes of the Canterbury drifts. Microfaunas from Unit III are consistent with deeper water depths than are those from Units I and II.

Preliminary paleontological data indicate that the Unit I/II boundary is ~1 Ma (early Castlecliffian), the Unit II/III boundary ~2 Ma (early Nukumaruan), and the bottom of hole ~2.6 Ma (late Pliocene, perhaps as old as late Waitotaran) old. These ages are drawn from cycle counting and faunal evidence. A shipboard paleomagnetic reversal chronology could not be determined unambiguously because of a combination of low intensities and magnetic overprints. The average sedimentation rate across the section is therefore ~20 cm/k.y., with lower rates during interglacials (sand), and considerably higher rates during glacials (silt and clay).

Despite the widely varying sedimentation rates and the presence of random core gaps resulting from degassing, an excellent spliced MST record for the two APC cores was achieved for Site

1119, based on magnetic susceptibility and natural gamma records. Cyclicity that matches the observed sediment couplets is apparent in both the smoothed magnetic susceptibility and, to a lesser degree, the natural gamma ray records. In other physical property data a distinct increase in vane shear strength is noted at ~85 mbsf, which may correlate with an observed seismic discontinuity and indicate a hiatus.

Carbonate concentrations are in the wide range of 0.5% and 75%, indicating strongly variable environmental conditions during sediment deposition (Fig. F7). In contrast, the average concentration of total organic carbon is 0.34% with small variations, which is low for coastal sediments. This may be a result of dilution either by carbonate or, during times with low carbonate supply, by enhanced terrigenous clastic material.

Interstitial water profiles show that the sulfate reduction zone occurs at 20 mbsf. There are increases in alkalinity, ammonium, and phosphate concentration in this zone. These increases are controlled by the degradation of sedimentary organic matter in a shallow marine environment. Sulfate concentrations are near zero from 20.15 through 472.3 mbsf, suggesting enhanced diagenetic processes, including the dissolution of magnetic minerals throughout the sequence. The decreases in calcium and magnesium concentrations in the sulfate reduction zone suggest the precipitation of diagenetic carbonate promoted by the rapid increase in alkalinity.

Downhole logging at Site 1119 included runs of the following tools: triple combination, Geologic High-Resolution Magnetic Tool (GHMT), and Formation MicroScanner (FMS-sonic). Downhole conditions were irregular below 160.3 m because of damage to the wall during drilling, and some data dropouts occur. After the GHMT tool run, the bottom 20 m of the hole collapsed because of cavings or swelling mud, and, as a result, the data from the two later tool strings do not contain this portion of the hole. The poor hole conditions affected the lithodensity and neutron porosity tools, making interpretation of the data difficult. The sonic tool was also affected by the poor conditions, but to a lesser degree, and the data obtained from it were used to create integrated travel times for interpretation of seismic survey data at this site. The resistivity, susceptibility, and gamma ray tools recorded good logs with cyclic signals.

Site 1120

Hole 1120A

Position: 50°3.80333´S, 173°22.30042´E

Start hole: 0045 hr, 28 August 1998

End hole: 0600 hr, 28 August 1998

Time on hole: 5.25 hr

Seafloor (drill pipe measurement from rig floor, mbrf): 553.90

Distance between rig floor and sea level (m): 11.00

Water depth (drill pipe measurement from sea level, m): 542.90

Total depth (from rig floor, mbrf): 558.50

Total penetration (mbsf): 4.60

Coring totals: type: APC; number: 1; cored: 4.60 m; recovered: 100%

Formation: lithostratigraphic Unit I: 0–4.6 mbsf; foraminifer nannofossil ooze and nannofossil foraminifer ooze

Hole 1120B

Position: 50°3.80333´S, 173°22.30042´E
Start hole: 0600 hr, 28 August 1998
End hole: 2020 hr, 28 August 1998
Time on hole: 14.33 hr
Seafloor (drill pipe measurement from rig floor, mbrf): 555.20
Distance between rig floor and sea level (m): 11.00
Water depth (drill pipe measurement from sea level, m): 544.20
Total depth (from rig floor, mbrf): 743.20
Total penetration (mbsf): 188.00
Coring totals: type: APC; number: 8; cored: 68.30 m; recovered: 92.55%
type: XCB; number: 13; cored: 119.70 m; recovered: 69.59%
Formation: lithostratigraphic Unit I: 0–4.6 mbsf; foraminifer nannofossil ooze and nannofossil foraminifer ooze
lithostratigraphic Unit II: 4.6–11.5 mbsf; foraminifer nannofossil ooze
lithostratigraphic Unit III: 11.5–54.9 mbsf; foraminifer nannofossil ooze
lithostratigraphic Unit IV: 54.9–184.55 mbsf; nannofossil ooze

Hole 1120C

Position: 50°3.81546´S, 173°22.29950´E
Start hole: 2020 hr, 28 August 1998
End hole: 0613 hr, 29 August 1998
Time on hole: 33.88 hr
Seafloor (drill pipe measurement from rig floor, mbrf): 556.90
Distance between rig floor and sea level (m): 11.00
Water depth (drill pipe measurement from sea level, m): 545.90
Total depth (from rig floor, mbrf): 601.50
Total penetration (mbsf): 44.60
Coring totals: type: APC; number: 5; cored: 44.60 m; recovered: 100.78%
Formation: lithostratigraphic Unit I: 0–4.6 mbsf; foraminifer nannofossil ooze and nannofossil foraminifer ooze
lithostratigraphic Unit II: 4.6–11.5 mbsf; foraminifer nannofossil ooze

Hole 1120D

Position: 50°3.82210´S, 173°22.30042´E
Start hole: 0613 hr, 29 August 1998
End hole: 0600 hr, 1 September 1998

Time on hole: 47.78 hr
Seafloor (drill pipe measurement from rig floor, mbrf): 556.90
Distance between rig floor and sea level (m): 11.00
Water depth (drill pipe measurement from sea level, m): 545.90
Total depth (from rig floor, mbrf): 777.60
Total penetration (mbsf): 220.70
Total length of drilled intervals (m): 157.40
Coring totals: type: XCB; number: 9; cored: 63.30 m; recovered: 104.53%
Formation: lithostratigraphic Unit IV: 157.4–220.7 mbsf; nannofossil ooze

Site 1120 is located ~650 km southeast of Stewart Island on the eastern flank of Pukaki Rise, near the middle of the Campbell Plateau, in 543 m deep water. The seismic succession is punctuated by seven conspicuous reflectors (from top to bottom = reflectors A–F), which probably represent unconformities. Few basement highs remained on the Campbell Plateau to shed terrigenous sediment after late Cretaceous rifting of the eastern plateau margin and subsequent erosion, and the entire succession above reflector E (probably Paleocene) is apparently biopelagic carbonate. Times of water-mass change, perhaps accompanied by current activity and sublevation, are indicated by changes in seismic character that take place across younger reflectors D to A, the target of Site 1120 drilling.

Site 1120 was drilled to establish the age of the major unconformities in the Campbell Plateau sequence and to determine the evolution of the shallow parts of the ACC where it sweeps past and over the southeast corner of the Plateau. The analysis of seafloor magnetic anomalies suggests that the ACC had its inception in the Oligocene, at ~32 Ma, when Australia separated from Antarctica and allowed partial circumpolar flow. At this time, the Campbell Plateau was situated immediately down-current from the opening southern ocean and was therefore exposed to vigorous current activity. It was anticipated that reflector B would be of middle to late Miocene age and correlate with either or both the sharp cooling of Antarctica recorded isotopically at 15–14 Ma, and a phase of known volcanism and minor faulting in eastern South Island, New Zealand, between ~13–10 Ma.

Four holes that recovered a sedimentary section spanning the last 23 m.y. were cored with the APC/XCB at Site 1120 to a maximum depth of 220.7 mbsf (Table T2). Hole 1120A consists of one single mudline core. Twenty-one cores were taken with the APC/XCB at Hole 1120B from 0 to 188.0 mbsf before operations were put on standby because of excessive heave. After waiting on weather, five cores were taken with the APC at Hole 1120C to 44.6 mbsf before a broken wireline and deteriorating weather conditions ended operations. Hole 1120D was drilled to 157.4 mbsf and cored with the XCB to 220.7 mbsf when operations had to be terminated because of the excessive heave.

Site 1120 penetrated a succession of calcareous biogenic oozes that downsection become less siliciclastic, less foraminifer rich, and contain less distinct bedding. Bioturbation ranges from moderate to heavy throughout the core, with identifiable traces of *Zoophycos*, *Palaeophycus*, and

Planolites. The lithology is visually monotonous and featureless for most of the section. However, using subtle changes in composition determined from smear slides, four units were identified (Fig. F8). The uppermost lithology (Unit I, 0–4.6 mbsf) comprises glacial-interglacial cycles in alternating beds of foraminifer-oozes and nannofossil-foraminifer oozes. Unit II (4.6–11.5 mbsf) is separated from Unit I by an unconformity and comprises a foraminifer nannofossil ooze with glauconite and rare pyrite concretions. Unit III (11.5–54.9 mbsf) is a foraminifer nannofossil ooze similar to Unit II. The lowermost unit (54.9–221.12 mbsf) is a foraminifer-bearing nannofossil ooze. Foraminifers are less abundant in this unit than in overlying beds, and neither glauconite nor siliceous sponge spicules were observed.

The section is punctuated by a number of significant paraconformities, the first of which lay just at 4.5 mbsf, separating stratified cycles of darker and lighter white ooze of late Pleistocene age from slightly compacted, brownish foraminiferal ooze of middle Pleistocene age below. Another paraconformity may occur at around 13 mbsf, corresponding to a reflection on the site survey 3.5-kHz profile, and a change in microfaunas to latest Miocene (5–6 Ma). Between ~13 and 170 mbsf occurs an expanded section of middle and late Miocene age (13.6–6 Ma), apparently without breaks across minor seismic discontinuities at 61 and 98 mbsf. Another probable unconformity, marked by reflector B on seismic reflection profiles, is located at ~170 mbsf, where nannofossil evidence suggests a biostratigraphic break may occur.

The stratigraphic thickness is very low in the Pleistocene and Pliocene, and the presence of major hiatuses indicates that intensified water mass movements occurred across the Campbell Plateau during this time. The relatively complete middle to late Miocene section that underlies corresponds to sedimentation rates of 1–2 cm/k.y. over the period ~5.5 to 16 Ma, and indicates quieter, undisturbed biopelagic conditions. The lowest part of the core is of early Miocene age (18–23 Ma), and has a slower sedimentation rate, consistent with current influence. The occurrence of the usually long-ranging *Sphenolithus heteromorphus* in only one core (between 167 and 177 mbsf) suggests that up to 2–3 m.y. of late early Miocene and early middle Miocene sediment may be either missing at an unconformity or represented by condensed sedimentation.

Benthic foraminifers indicate that the site has been bathyal throughout the Neogene–Quaternary. Evidence from all planktonic microfossil groups consistently indicates that during the Pleistocene the surface waters and intermediate water masses above the Campbell Plateau were cold. In the Miocene section, changes in the composition of calcareous microfossils reflect cyclic alternations between warmer and colder conditions. The planktonic foraminifers and calcareous nannofossils show a general trend toward colder faunas and floras from the early-middle to the middle-late Miocene.

Physical sediment properties were determined both by high-resolution MST core logging and by index property measurements. Magnetic susceptibility, GRAPE density, natural gamma-ray intensity, and digital reflectance data measured with the Minolta Spectrophotometer reveal cyclicities, which were used for stratigraphic correlation in the top 50 mbsf. Detailed hole-to-hole comparisons demonstrated nearly complete recovery of the sedimentary sequence down to 50 meters composite depth (mcd), with a gap in the continuous record at 19 mcd.

A shipboard paleomagnetic reversal chronology could not be determined because of a combination of low intensities and magnetic overprints.

The profiles of interstitial water constituents are controlled by simple diagenetic diffusion processes, which show slightly increasing alkalinity, chloride, calcium, lithium, and silica concentrations and decreasing potassium and magnesium trends with depth, and no signatures of sulfate reduction. This results from the uniform lithology (carbonate oozes) throughout the hole. The dominant chemical reactions were dissolution of carbonate, silica diagenesis, the possible precipitation of dolomite, and ion-exchange reactions in clay minerals.

Site 1121

Hole 1121A

Position: 50°53.87581´S, 176°59.86176´E
Start hole: 2225 hr, 1 September 1998
End hole: 1555 hr, 2 September 1998
Time on hole: 17.50 hr
Seafloor (drill pipe measurement from rig floor, mbrf): 4503.10
Distance between rig floor and sea level (m): 11.10
Water depth (drill pipe measurement from sea level, m): 4492.00
Total depth (from rig floor, mbrf): 4511.50
Total penetration (mbsf): 8.40
Coring totals: type: APC; number: 1; cored: 8.40 m; recovered: 99.64%
Formation: lithostratigraphic Subunit IA (0–8.40 mbsf): yellow to yellowish brown silty or sandy clay and grayish brown and light yellowish brown silt, silty sand, and sand beds

Hole 1121B

Position: 50°53.87581´S, 176°59.86176´E
Start hole: 1555 hr, 2 September 1998
End hole: 1045 hr, 4 September 1998
Time on hole: 42.83 hr
Seafloor (drill pipe measurement from rig floor, mbrf): 4499.00
Distance between rig floor and sea level (m): 11.10
Water depth (drill pipe measurement from sea level, m): 4487.90
Total depth (from rig floor, mbrf): 4638.70
Total penetration (mbsf): 139.70
Coring totals: type: APC; number: 3; cored: 23.00 m; recovered: 129.04%
type: XCB; number: 14; cored: 4.60 m; recovered: 49.85%
Formation: lithostratigraphic Subunit IA (0–15.2 mbsf): yellow to yellowish brown silty or sandy clay and grayish brown and light yellowish brown silt, silty sand, and sand beds

lithostratigraphic Subunit IB (15.2–32.7 mbsf): pale yellow and light yellowish brown clay with fragments of chert layers and nodules
lithostratigraphic Subunit IIA (32.7–35.07 mbsf): white nannofossil ooze with a subordinate content of diatoms, radiolarians, sponge spicules, and silicoflagellates
lithostratigraphic Subunit IIB (35.07–119.4 mbsf): light greenish nannofossil diatom ooze
lithostratigraphic Subunit IIC (119.4–132.7 mbsf): light greenish gray nannofossil ooze
lithostratigraphic Subunit IID (132.7–139.7 mbsf): greenish gray nannofossil-bearing clay

Site 1121 is located on the Campbell Drift under the combined effect of the DWBC and ACC in the Southwest Pacific. Drilling at this site showed that, contrary to the generally accepted view, the sediment accumulation defined by topography and seismic reflection profiles is not a Neogene contourite drift.

The sediment body drilled lies along the foot of the 3000-m-high eastern escarpment of Campbell Plateau and is ~800 km long. The underlying crust dates from the rifting of Campbell Plateau from Marie Byrd Land at 85 Ma. Immediately overlying that crust is up to 1.1 s (~1000 m) of sediment presumed to be a wedge of nonmarine clastics followed by latest Cretaceous and Paleogene marine sediments and Neogene contourites. In particular, Carter and McCave (1997) surmised that the uppermost sequence of closely spaced reflectors (<160 m thick) was of Pliocene–Pleistocene age. A short gravity core from the site has yielded an abundant assemblage of upper Pleistocene and reworked older foraminifers. This sequence, presumed to carry a record of ACC and DWBC history, was the drilling target. The objectives were to obtain well-dated records of isotopic properties of oxygen and carbon that would show the shifts of the Subantarctic Front, the onset of and changes in the inflow of Circumpacific Deep Water, and, through grain-size analysis, document changes in the vigor of the deep circulation.

Two holes that recovered a sedimentary section spanning the last 63 m.y. were cored with the APC/XCB at Site 1121 to a maximum depth of 139.7 mbsf (Table T3). Hole 1121A consists of one single mudline core. Seventeen cores were taken with the APC/XCB at Hole 1121B from 0 to 139.7 mbsf with 62.9% recovery when operations were terminated.

The cored section is divided into two units, each subdivided (Fig. F9). Subunit IA (0–15 mbsf) is mottled silty and sandy clay with conspicuous manganese nodules. Subunit IB (15–32.7 mbsf) is a relatively uniform yellow siliceous clay with cherts as nodules and (broken) layers. This unit is possibly of Neogene age, and represents a residual deposit with a very slow net sedimentation rate (~1 m/m.y.). It is the residue of significant erosion by the ACC/DWBC some time after the Paleocene. Unit II includes four subunits dominated by varying mixtures of siliceous and nannofossil-bearing ooze with up to 50% carbonate. The unit is extensively bioturbated and contains common chert below 71 mbsf. The lithologic features indicate deep marine deposition of pelagic biogenic material close to the CCD in the order of 15–30 m/m.y. The inferred erosion in

the upper part of the section is corroborated by the ratio of shear strength to overburden pressure which, with values over 0.5 in the upper 20 mbsf, is indicative of overconsolidation. Chert in the lower part of the section precludes similar measurements in the Paleocene Unit II which is probably also overcompacted.

The uppermost 3 mbsf of the section contains a condensed sequence dated by using diatoms as late Pleistocene over early Pleistocene over late Pliocene in the top meter, underlain by 2 m of early late Pliocene. Foraminifers and coccoliths in the top meter are of middle to late Pleistocene age. The remainder of the upper 32 mbsf composing Unit I yielded a few upper Neogene nannofossils and reworked (?)Paleocene radiolarians. From 32 mbsf to the bottom of the hole (Unit II) the sequence provides for the first time in the southwest Pacific a continuous record of the late early to late Paleocene. This includes all major microfossil groups including nannofossils, diatoms, radiolarians, and benthic foraminifers. Radiolarian zones RP4, 5, and 6, nannofossil zones NP4, 5, 6, and 8, benthic foraminiferal zone CD1, and diatom *Hemiaulus incurvus* Zone are present in the record. This has provided tight control on an equally good magnetostratigraphic record in the Paleocene section where magnetochrons C27r, C27n, C26n, and C25r are recognized. The upper condensed section also contains a number of reversals but, apart from the tentative recognition of the Gauss Chron, the biostratigraphic control is not adequate to place them somewhere within the Oligocene to Pliocene, where they probably reside. The combined age data allow specification of sedimentation rates in the order of 15–30 m/m.y. in the Paleocene and ~1 m/m.y. in the Neogene.

The profiles of interstitial water constituents show local fluctuations suggesting dominantly lithologic control rather than a simple diffusion process of diagenetic fluids. The primary chemical reactions may be silica diagenesis, dissolution of carbonate, and possibly ion-exchange reactions of clay minerals. In particular, relatively high concentrations of dissolved silica in the interval between ~35 and 120 mbsf are related to the dissolution of biosiliceous sediments.

Site 1122

Hole 1122A

Position: 46°34.78088´S, 177°23.60962´W

Start hole: 2254 hr, 5 September 1998

End hole: 0415 hr, 7 September 1998

Time on hole: 29.35 hr

Seafloor (drill pipe measurement from rig floor, mbrf): 4446.20

Distance between rig floor and sea level (m): 11.20

Water depth (drill pipe measurement from sea level, m): 4435.00

Total depth (from rig floor, mbrf): 4570.10

Total penetration (mbsf): 123.90

Coring totals: type: APC; number: 8; cored: 75.80 m; recovered: 96.97%
type: XCB; number: 5; cored: 48.10 m; recovered: 29.02%

Formation: lithostratigraphic Subunit IA (0–22.7 mbsf): light brownish gray silty clay
lithostratigraphic Subunit IB (22.71–109.35 mbsf): greenish gray silty clay with

interbedded dark greenish gray and greenish gray sand and fine sand turbidites
lithostratigraphic Subunit IC (109.35–123.90 mbsf): dark greenish gray silt and very fine sand turbidites, which are intercalated in grayish green and greenish gray silty clay

Hole 1122B
Position: 46°34.78088´S, 177°23.60962´W
Start hole: 0415 hr, 7 September 1998
End hole: 0625 hr, 7 September 1998
Time on hole: 2.17 hr
Seafloor (drill pipe measurement from rig floor, m mbrf): 4441.00
Distance between rig floor and sea level (m): 11.20
Water depth (drill pipe measurement from sea level, m): 4429.80
Total depth (from rig floor, mbrf): 4450.50
Total penetration (mbsf): 9.50
Coring totals: type: APC; number: 1; cored: 9.50 m; recovered: 103.26%
Formation: lithostratigraphic Subunit IA (0–9.5 mbsf): light brownish gray silty clay
Hole 1122C
Position: 46°34.78020´S, 177°23.62152´W
Start hole: 0625 hr, 7 September 1998
End hole: 0800 hr, 12 September 1998
Time on hole: 121.58 hr
Seafloor (drill pipe measurement from rig floor, mbrf): 4443.00
Distance between rig floor and sea level (m): 11.20
Water depth (drill pipe measurement from sea level, m): 4431.80
Total depth (from rig floor, mbrf): 5070.40
Total penetration (mbsf): 627.40
Coring totals: type: APC; number: 13; cored: 103.70; recovered: 103.33%
type: XCB; number: 55, cored: 523.70 m; recovered: 46.65%
Formation: lithostratigraphic Subunit IA (0–22.7 mbsf): light brownish gray silty clay
lithostratigraphic Subunit IB (22.71–109.35 mbsf): greenish gray silty clay with interbedded dark greenish gray and greenish gray sand and fine sand turbidites
lithostratigraphic Subunit IC (109.35–261.7 mbsf): dark greenish gray silt and very fine sand turbidites, which are intercalated in grayish green and greenish gray silty clay
lithostratigraphic Subunit ID (261.7–389.9 mbsf): greenish gray and gray silty clay interbedded with dark greenish gray very fine sand and silt turbidites
lithostratigraphic Subunit IIA (389.9–472.3 mbsf): greenish gray to light greenish gray silty clay with interbeds of dark gray or dark greenish gray fine sand and silt beds

lithostratigraphic Subunit IIB (472.3–550.4 mbsf): dark greenish gray to greenish gray silty clay interspersed with light brownish gray to gray, nannofossil-rich layers
lithostratigraphic Subunit IIIA (550.4–580.62 mbsf): green to greenish gray clayey silt to silty clay with interbeds of greenish to greenish gray fine sand and silt beds and white to gray nannofossil-bearing foraminifer sands
lithostratigraphic Subunit IIIB (580.62–617.85 mbsf): greenish gray fine sand with intraclasts of silty clay and abundant wood fragments (debris flow) and greenish gray to dark greenish gray fine sand-bearing siltstones and light greenish gray foraminifer-bearing nannofossil chalks

Site 1122 is located ~830 km east of South Island, in a water depth of 4430 m on the north bank levee of the abyssal Bounty Fan. The fan is located in the most seaward axial deep of the Bounty Trough, a rift basin formed in the Late Cretaceous during the separation of New Zealand and Antarctica across the newly forming mid-Pacific Rise. The Bounty Channel feeds sediment along the axis of the trough and into the path of the Pacific DWBC, which flows north along 80-m.y.-old oceanic crust of the Southwest Pacific abyssal plain. Subsidence calculations indicate that Site 1122 was situated at depths of ~4700 m in the early Miocene, subsequently shoaling to ~4400 m today because of late Cenozoic sediment deposition. The seismic line through the fan shows that the channel here has over 300 m of incision, with a higher north bank levee, of which the upper parts are composed of a spectacular series of climbing sediment waves, deposited from turbidity current overspill.

Three holes that recovered a sedimentary section spanning the last 16 m.y. were cored with the APC/XCB at Site 1122 to a maximum depth of 627.4 mbsf (Table T4). Hole 1122A was cored with the APC to 75.8 mbsf and deepened with the XCB to 124.0 mbsf. One failed mudline core was taken at Hole 1122B. Thirteen cores were taken with the APC at Hole 1122C from 0 to 103.7 mbsf. The hole was deepened with the XCB to 627.4 mbsf. In an attempt to log Hole 1122C the triple combination was deployed but was unable to pass the bit by more than 12 m. It was decided to recover the logging tool in rapidly deteriorating weather conditions and to terminate operations at the site because of the heavy seas and high winds.

Drilling confirmed that the upper ~300 m of the sediment pile is composed of rhythmic late Pleistocene sand turbidites (Fig. F10), deposited at a high rate of more than 40 cm/k.y. Recovery ranged from good when the turbidite sands were separated by regular muds and cored by APC, to very poor where they were inferred to be dominated by sand and cored XCB. Between 300 and 450 mbsf, the turbidite sequence changed into late Pliocene to middle Pleistocene current-worked sands, and muds that are inferred to have been deposited under the influence of the DWBC, possibly reinforced by the ACC. A substantial 8-m.y.-long condensed sequence or unconformity exists at ~470–500 mbsf, below which current-influenced sands and muds of late Miocene age (10–18 Ma), with a sedimentation rate of ~5 cm/k.y., were penetrated. Accompanying microfaunas show a shift to less diverse foraminifer assemblages, suggestive of the incursion of colder waters and also of the appearance of Subantarctic diatom floras. The lower part of the

Miocene sediments contains abundant coarser grained sand, carbonized wood fragments, and transported shallow-water foraminifers, consistent with the onlap of these sediments onto the angular unconformity observed on the seismic profile. Because of drilling difficulties, the hole terminated just above this unconformity, though poor core recovery and the unfortunate lack of a sonic log makes it difficult to be certain how far above.

Site 1122 yielded an excellent high-resolution record of the input of middle upper Pleistocene sediment into the deep western boundary current and probably ACC system. The site contained some significant surprises. Preliminary analysis shows that (1) turbidite deposition on the fan levee continued through both glacial and interglacial periods, although the frequency was higher in glacials; (2) the major reflecting horizons seen on the seismic profile do not correspond to oxygen isotope stage stratigraphy, and (3) an unexpectedly young age (~0.7 Ma) for the change from DWBC-influenced sedimentation to New Zealand-derived turbidite/fan levee-influenced sedimentation. Seven major tephra horizons were located at Site 1122, and, together with the excellent paleomagnetic record and close micropaleontologic controls, these will provide a tight chronostratigraphic framework for more detailed studies.

A complete magnetostratigraphy was determined in the uppermost 440 mbsf of the APC/XCB section at Site 1122 after AF demagnetization at 20 mT (Fig. F10). All chrons from the Brunhes (C1n) to the onset of C2r.1n (Reunion) at 2.14 Ma could be identified. In the upper Miocene section, below the major unconformity, Chrons C5r.1n and C5r.2n were determined.

Physical sediment properties were determined both by high-resolution MST core logging and by index property measurements. Natural gamma-ray intensity indicates clay mineral concentration and varies strongly between sand and clay layers. Magnetic susceptibility, gamma-ray attenuation porosity evaluator (GRAPE) density, and digital reflectance data measured with the Minolta Spectrophotometer reveal cyclicities, which were used for stratigraphic correlation. Detailed hole-to-hole comparisons demonstrated nearly complete recovery of the sedimentary sequence down to 83 mcd with a gap in the continuous record at 73 mcd.

The primary controlling factor on the interstitial water chemistry at Site 1122 is sulfate reduction and methane genesis, which governs alkalinity, phosphate, and ammonia concentration. In contrast to the complete utilization of sulfate in the upper part of the core, the reappearance of increasing sulfate levels in the middle of the section represents an approach to the original sulfate concentration during sediment deposition, possibly because of a lack of sufficient metabolizable organic matter and to low sedimentation rates. Other significant chemical profiles are magnesium and calcium, from which we may deduce the lateral transport of magnesium-rich fluid during the dissolution of carbonate. The general chemical zonations of interstitial waters at Site 1122 correspond to those of lithostratigraphic units and paleontological age divisions—in particular, the sharp reduction of methane at 260 mbsf, which coincides with the base of the highly pyritized turbidites of the mud wave sequence. The calcium carbonate concentration varies between 0 and 77% indicating strong environmental changes during sediment deposition. Organic carbon contents averages 0.24% and shows also strong variations with the sedimentary facies. The

organic carbonate concentration is low for marine environments and may reflect the dilution of the organic matter either by marine carbonate or terrigenous detritus.

Site 1123

Hole 1123A

Position: 41°47.1743´S, 171°29.9401´W
Start hole: 1848 hr, 13 September 1998
End hole: 2355 hr, 14 September 1998
Time on hole: 29.12 hr
Seafloor (drill pipe measurement from rig floor, mbrf): 3301.40
Distance between rig floor and sea level (m): 11.30
Water depth (drill pipe measurement from sea level, m): 3290.10
Total depth (from rig floor, mbrf): 3459.50
Total penetration (mbsf): 158.10
Coring totals: type: APC; number: 17; cored: 158.10 m; recovered: 100.34%
Formation: lithostratigraphic Subunit IA (0–158.62 mbsf): greenish gray to white clayey nannofossil ooze

Hole 1123B

Position: 41°47.1598´S, 171°29.9387´W
Start hole: 2355 hr, 14 September 1998
End hole: 0955 hr, 19 September 1998
Time on hole: 106.00 hr
Position: 41°47.1598´S, 171°29.9387´W
Seafloor (drill pipe measurement from rig floor, mbrf): 3301.10
Distance between rig floor and sea level (m): 11.30
Water depth (drill pipe measurement from sea level, m): 3289.80
Total depth (from rig floor, mbrf): 3790.10
Total penetration (mbsf): 489.00
Coring totals: type: APC; number: 17; cored: 155.40 m; recovered: 102.79%
type: XCB; number: 35; cored: 333.60 m; recovered: 87.43%
Formation: lithostratigraphic Subunit IA (0–181.9 mbsf): greenish gray to white clayey nannofossil ooze
lithostratigraphic Subunit IB (181.9–256.59 mbsf): white clayey nannofossil chalk interbedded with greenish gray clayey nannofossil chalk
lithostratigraphic Unit II (256.59–450.8 mbsf): light greenish gray clayey nannofossil chalk
lithostratigraphic Subunit IIIA (450.8–488.66 mbsf): light greenish gray and greenish gray clayey nannofossil chalk and nannofossil mudstone

Hole 1123C
Position: 41°47.1466´S, 171°29.9405´W
Start hole: 0955 hr, 19 September 1998
End hole: 1000 hr, 24 September 1998
Time on hole: 120.08 hr
Seafloor (drill pipe measurement from rig floor): 3301.50 mbrf
Distance between rig floor and sea level: 11.40 m
Water depth (drill pipe measurement from sea level): 3290.10 m
Total depth (from rig floor): 3934.30 mbrf
Total penetration: 632.80 mbsf
Coring totals: type: APC; number: 16; cored: 151.50 m; recovered: 101.45%
type: XCB; number: 17; cored: 158.40 m; recovered: 85.69%
Formation: lithostratigraphic Subunit IA (0–151.79 mbsf): greenish gray to white clayey nannofossil ooze
lithostratigraphic Subunit IIIA (484–542.9 mbsf): light greenish gray and greenish gray clayey nannofossil chalk and nannofossil mudstone
lithostratigraphic Subunit IIIB (542.9–550.5 mbsf): greenish gray plastically deformed clasts of clayey nannofossil chalk
lithostratigraphic Subunit IIIC (550.5–587.2 mbsf): greenish gray plastically deformed clasts of clayey nannofossil chalk
lithostratigraphic Unit IV (587.2–632.8 mbsf): white to light greenish gray micritic limestone

Site 1123 is located 410 km northeast of the Chatham Islands, on the deep northeastern slopes of Chatham Rise. The site was drilled in a water depth of 3290 m. The holes penetrated a major sediment drift occurring between 169°W and 175°W at depths of 2200–4500 m. The drift is thicker than 0.6 s above 3500 m water depth, and has been deposited where the DWBC decelerates after passing through Valerie Passage. The drift is well defined by three seismic reflectors. Before drilling, the basal one (707 ms) was interpreted to be of middle Oligocene age. The upper sediments at this site comprise a 0.2 s thick sequence of (hemi)pelagic drape. On 3.5-kHz records, at the surface the drape formed a series of irregular, vertically-climbing mud waves. Parallel reflectors within this drape probably represent muddy calcareous pelagites and purer calcareous pelagites. The anticipated presence of a substantial carbonate record back to the middle Oligocene made Site 1123 a prime site at which to evaluate the evolution of the DWBC system, including information on the NADW component of flow. It was expected that the upper part of the sequence would contain a record of volcanic ashes derived from North Island, New Zealand. The objectives of Site 1123 were thus to (1) test the coherence of the paleoclimatic record with Milankovitch cyclicity; (2) determine the evolution of circum-Antarctic ocean circulation, with particular reference to periods of tectonic opening of critical seaways and climatic events (e.g., growth of Antarctic ice at 15–14 Ma); (3) evaluate grain-size signals (flow speed) to determine water-mass

movement to estimate the velocity behavior of the DWBC; and (4) determine paleoproductivity and location of the Sub-Tropical Convergence and paleohydrography of Circumpolar Deep Water (including the NADW component).

Three holes that recovered a sedimentary section spanning the last 20 m.y. were cored with the APC/XCB at Site 1123 to a maximum depth of 632.8 mbsf (Table T5). Seventeen cores were taken at Hole 1122A with the APC to 158.1 mbsf. Hole 1123B was cored with the APC to 155.4 mbsf and deepened with the XCB to 489.0 mbsf. Logging was conducted from the bottom of the hole at 489 mbsf to the bit at 84 mbsf. Three standard tool-string configurations were run: the triple combination, the FMS-sonic (two passes), and the GHMT. The condition of the borehole was good and the quality of the data is excellent. Hole 1123C was cored with the APC to 151.5 mbsf and deepened by drilling ahead to 484.0 mbsf. One XCB core was obtained from 230.0 to 239.6 mbsf to provide overlap with an interval of poor recovery in Hole 1123B. XCB coring resumed and advanced from 484.0 mbsf to the modified depth objective of 632.8 mbsf with excellent recovery.

Triple APC coring resulted in a complete composite section for the upper 150 mbsf containing the major volcanic ashes from New Zealand of the last 4.2 m.y. (Fig. F11). Splicing was based on color reflectance and magnetic susceptibility. The ashes are surprisingly variable in thickness over the 20-m distance between holes, a possible coring artifact.

The stratigraphic sequence is remarkably uniform over the upper 450 mbsf. Subdivision is made only on the basis of more frequent ashes in the upper section and a change from ooze to chalk lower down. The well-known seismic reflector ‘Y’ is here evidenced by only a small step in velocity and density at around 145 mbsf depth caused by compaction. The dominant lithology is a pale greenish-gray ooze/chalk with a carbonate content oscillating around 65% (±15%). In the upper 40 mbsf of the section the color cyclicty detected visually and by spectrophotometer can be closely matched to isotopic stratigraphy and dated thereby. This agrees with magnetostratigraphy in placing the Matuyama/Brunhes boundary at 32 mbsf (Fig. F11) with implied sedimentation rate of 4.1 cm/k.y. The entire sequence shows cyclic properties, magnetic susceptibility, and/or reflectance, and/or GRAPE, sometimes all three. It is also apparent in the lower resolution gamma radiation record. The lower part of the drift sequence has higher magnetic susceptibility, is darker green from chlorite input, but retains the clear cyclicity seen in the Pleistocene.

The sequence is extraordinarily well dated by 113 microfossil datum points and every single magnetic polarity shift (plus two new ones) back to Chron C6n or 20 Ma on the scale of Berggren et al. (1995). We have ~100% recovery over the 0–11 and 16–20 Ma intervals. Recovery of this sequence ended with a substantial hiatus from Chrons C6n to C12r, at ~32 Ma, with 12.5 m.y. missing. This is the Marshall Paraconformity, regional marker of the middle Oligocene environmental and sea level change. Beneath that is early Oligocene to Eocene micritic limestone, deposited at an average sedimentation rate of 2 cm/k.y., about half the Neogene rate. Only the upper Pleistocene foraminiferal assemblages show little influence of dissolution. Miocene and Pliocene samples are somewhat impoverished in planktonic and also in benthic taxa, with many test fragments at some levels suggesting the area was swept by corrosive bottom waters. This was

not the case in the Eocene and early Oligocene where planktonic-dominated assemblages are found. The Neogene planktonic foraminifers are clearly from the warmer waters north of the Subtropical Convergence. The light/dark sedimentary cyclicity is reflected as warm/cold cycles in planktonic foraminifers and possible productivity changes in diatom abundances. Upper Neogene diatoms show a mixture of local (warm water) forms and subantarctic forms from Bounty Trough or further south. This aspect to the flora is lacking in the beds below the Marshall Paraconformity. The evidence all points to the DWBC starting after 30 Ma.

The physical properties records are excellent, showing cyclicity at several long and short wavelengths in magnetic susceptibility, density, gamma radiation, and color reflectance. Overall properties are uniform or gently increasing down to 450 mbsf, then increase sharply in a unit overlying the unconformity at 587 mbsf. This uniformity and small scale variability are also seen in the downhole logs, from which good information was obtained on acoustic velocities, magnetic susceptibility, resistivity, gamma radiation, and density down to 486 mbsf.

Most of the recovered sediments are carbonate dominated with carbonate concentrations between 10.3% and 84.3% and an average of 57.5% (Fig. F11). Organic carbon contents are twice the average of deep sea sediments. The organic material seems to be heavily oxidized, probably by microbial reworking during sedimentation or early diagenesis. As a result of these processes sufficient metabolizable organic matter is virtually absent, indicated by low sedimentary methane concentrations and moderate sulfate concentrations in the pore water.

Interstitial water compositions are dominantly controlled by the high carbonate content of the sediments. Sulfate reduction occurs moderately in the upper part of the hole, probably related to the relatively high organic carbon content (~0.5%) compared to normal deep-sea carbonate sediments. Sulfate decreases gradually with depth to 13 mM at ~200 mbsf, below which it remains almost constant. Alkalinity shows a small maximum value of 8.5 mM at 107 mbsf. Carbonate diagenetic reactions are inferred from the profiles of dissolved calcium, magnesium, and strontium. The variation of dissolved silica in the lower part of the hole may possibly imply changes of paleoproductivity.

Downhole logging measurements were taken in Hole 1123B, using the triple combination, the FMS-sonic, and the GHMT. Borehole conditions were good and the data quality is excellent. A successful correlation was made between core and log-based magnetic susceptibility. The results were used to position missing sections of core. The sonic velocity data were used to construct a set of integrated travel times, in order to calculate the depth to major seismic reflectors. Distinct logging units were recognizable within the downhole measurements, reflecting fluctuating sedimentary conditions through time.

From all points of view this site is set to become the Neogene standard for the southwest Pacific and to define the properties of the water flowing into this ocean for the last 20 m.y.

Site 1124

Hole 1124A

Position: 39°29.9014´S, 176°31.8938´W

Start hole: 1748 hr, 24 September 1998
End hole: 0305 hr, 25 September 1998
Time on hole: 9.28 hr
Seafloor (drill pipe measurement from rig floor, mbrf): 3979.00
Distance between rig floor and sea level (m): 11.50
Water depth (drill pipe measurement from sea level, m): 3967.50
Total depth (from rig floor, mbrf): 3988.50
Total penetration (mbsf): 9.50
Coring totals: type: APC; number: 1; cored: 9.50 m; recovered: 100.11%
Formation: lithostratigraphic Subunit IA (0–9.5 mbsf): nannofossil silty clay

Hole 1124B
Position: 39°29.9014´S, 176°31.8938´W
Start hole: 0305 hr, 25 September 1998
End hole: 1745 hr, 26 September 1998
Time on hole: 38.67 hr
Seafloor (drill pipe measurement from rig floor, mbrf): 3978.10
Distance between rig floor and sea level (m): 11.50
Water depth (drill pipe measurement from sea level, m): 3966.60
Total depth (from rig floor, mbrf): 3988.00
Total penetration (mbsf): 9.90
Coring totals: type: APC; number: 2; cored: 9.90 m; recovered: 99.90%
Formation: lithostratigraphic Subunit IA (0–9.88 mbsf): nannofossil silty clay

Hole 1124C
Position: 39°29.9014´S, 176°31.8938´W
Start hole: 1745 hr, 26 September 1998
End hole: 1630 hr, 30 September 1998
Time on hole: 94.75 hr
Seafloor (drill pipe measurement from rig floor, mbrf): 3978.00
Distance between rig floor and sea level (m): 11.50
Water depth (drill pipe measurement from sea level, m): 3966.50
Total depth (from rig floor, mbrf): 4451.10
Total penetration (mbsf): 473.10
Coring totals: type: APC; number: 14; cored: 132.00 m; recovered: 102.12%
type: XC; number: 35; cored: 333.10 m; recovered: 89.76%
Formation: lithostratigraphic Subunit IA (8–60.74 mbsf): nannofossil silty clay
lithostratigraphic Subunit IB (60.74–178.4 mbsf): silty clay grading into nannofossil silty clay intercalated with clayey nannofossil ooze grading into nannofossil ooze
lithostratigraphic Subunit IC (178.4–294 mbsf): clay-bearing nannofossil chalk

intercalated with clayey nannofossil chalk and nannofossil mudstone
lithostratigraphic Unit II (294–411.5 mbsf): nannofossil chalk with interbeds and laminae of clay-bearing nannofossil chalk that grades downcore through a nannofossil-bearing mudstone to a plain mudstone
lithostratigraphic Unit III (411.5–419.8 mbsf): clayey nannofossil chalk
lithostratigraphic Unit IV (419.8–429.09 mbsf): mudstone
lithostratigraphic Unit V (429.09–463.42 mbsf): nannofossil bearing mudstone
lithostratigraphic Unit VI (467.4–473.21 mbsf): nannofossil bearing mudstone

Hole 1124D
Position: 39°29.8841´S, 176°31.8917´W
Start hole: 1630 hr, 30 September 1998
End hole: 2330 hr, 1 October 1998
Time on hole: 31.00 hr
Seafloor (drill pipe measurement from rig floor, mbrf): 3978.00
Distance between rig floor and sea level (m): 11.50
Water depth (drill pipe measurement from sea level, m): 3966.50
Total depth (from rig floor, mbrf): 4133.60
Total penetration (mbsf): 155.60
Coring totals: type: APC; number: 14; cored: 133.00 m; recovered: 99.13%
Formation: lithostratigraphic Subunit IA (22.5–60.74 mbsf): nannofossil silty clay
lithostratigraphic Subunit IB (60.74–155.5 mbsf): silty clay grading into nannofossil silty clay intercalated with clayey nannofossil ooze grading into nannofossil ooze

Site 1124 is located ~600 km due east of New Zealand's North Island on the 250-km long ridge of Rekohu Drift. The main Rekohu sequence consisting principally of inferred Miocene drift sediments overlies older sediments beneath seismic reflector X and is thought to be onlapped by overbank turbidites from the Hikurangi Channel above diffuse reflector Y. By correlation with other sections, the Unit B sediments (between X and Y) at this site before drilling were believed to be calcareous pelagites. Unraveling the evolution of the Rekohu Drift is critical to understanding the development of Hikurangi Channel, and the injection of sediment into the DWBC. Rekohu Drift has clearly acted as an effective barrier to eastward dispersal of terrigenous sediment from Hikurangi Channel, which turns abruptly to the left (N) against the drift, during the Pliocene–Pleistocene. The channel is thought to have originally flowed to the north along the New Zealand margin into Kermadec Trench and then been diverted to flow eastward by a major slide off Hawkes Bay in the late Pliocene. It was hoped that Site 1124 would yield a mainly carbonate record of the Miocene paleohydrography of the DWBC, and (if it penetrated unconformity X) important information on the middle Cenozoic initiation of the system. The objectives of Site 1124 were thus to determine: (1) the Miocene evolution of the DWBC and associated water masses, (2)

provenance of sediment in the DWBC system and, (3) the Neogene volcanic history of the North Island.

Hole 1124A consists of a failed mudline core. The bit was raised by 5 m and Hole 1124B was spudded. The core barrel was retrieved with a shattered liner and no core. The second APC core achieved incomplete stroke and required retrieval of the BHA with the stuck core barrel to the surface. Hole 1124C was washed to 8.0 mbsf where XCB coring was initiated. The hole was cored with the XCB from 8.0 to 27.2 mbsf and deepened with the APC to 159.2 mbsf and with the XCB to 473.1 mbsf (Table T6). The hole was logged from total depth to 78 mbsf with the triple combination, the FMS-sonic, and the GHMT. Hole 1124D was drilled ahead to 22.6 mbsf with the XCB and deepened with the APC to refusal at 155.6 mbsf.

An excellent and complete spliced record was obtained for 17.7 to 174 mcd from Holes 1124C and 1124D. The uppermost 11.7 mcd is also complete in Cores 181-1124A-1H and 1124B-1H and 2H, but coring difficulties caused by ashes lost the small section between 11.7 and 17.7 mcd. The B/M boundary is located at 33 mcd (Fig. F12), however, and it will be straightforward to estimate the resulting time gap in the middle Pleistocene, which may be only ~100 k.y. The coring problems suggest considerable lateral variability in ash thickness and cementation over the short distances between holes (~20 m).

The sequence here has been divided into six lithostratigraphic units. Units I and II, which compose the drift sequence, occupy the top 412 mbsf. These units are pale greenish gray ooze and chalk showing cyclicity in color, GRAPE, and magnetic susceptibility. Ash beds are increasingly common upsection from the late Miocene to Holocene sediments, which encompass the top 200 mbsf. The drift sequence is broken by an unconformity with a hiatus of ~4 m.y. within the lower Miocene (23–19 Ma). Beneath this is a thick (110 m) upper Oligocene section overlying the Marshall Paraconformity at 412 mbsf, across which there is a 5 m.y. hiatus (32–27 Ma). Beneath this are four thin units of contrasting character: lower Oligocene nannofossil chalk (Unit III), middle Eocene brown to dark brown mudstone (Unit IV), Paleocene nannofossil chalk with zeolitic interbeds (Unit V), and Upper Cretaceous cherty zeolitic mudstone with nannofossils (Unit VI), the first three being separated by two hiatuses and the last two by the K/T boundary. Unfortunately the boundary section itself is missing between cores though it shows clearly on the FMS and other downhole logs as a resistivity high and magnetic susceptibility low. Carbonate contents are variable, averaging 36% but ranging from 0% to 88%. The lowest values are found in the middle and upper Miocene, between 100 and 300 mbsf. The organic carbon content is normal for deep-sea sediment, averaging 0.31%. The Eocene brown mudstone (Unit IV) which superficially resembles the facies of the Waipawa Black Shale on land, also has a low organic carbon content of 0.26 to 0.44 wt%.

Despite poor preservation of all groups in the Oligocene and Miocene, 66 microfossil datum points (49 above the middle Oligocene) have been recognized, giving a reasonably well-constrained age-depth curve. Planktonic foraminifers are too poorly preserved—only thick-shelled species survive—for assessment of warm/cold assemblages. However the diatoms represent a warm subtropical flora. The upper Neogene, but not upper Oligocene/lower Miocene,

contains reworked Eocene forms. As other indicators suggest the deep current was flowing vigorously, this may point to opening of a source to the south supplying Bounty Trough or scouring of Chatham Rise. Corrosion of foraminifers clearly sets in after the Marshall Paraconformity compared with specimens in underlying strata, evidence of a new bottom-water source.

Magnetostratigraphy was particularly good for the spliced interval of Holes 1124C and 1124D (30–170 mcd). All subchrons of the Matuyama, Gauss, Gilbert, and C3r-C4r inclusive were recognized in the upper part of the record. However, a strong magnetic overprint was encountered between 180 and 280 mbsf preventing unambiguous polarity determination over that interval. Magnetic intensities were very weak in the Oligocene, but increased in the Paleocene and around the Cretaceous/Tertiary (K/T) boundary where C29r was identified spanning the K/T boundary interval. Shore-based research should allow polarity and environmental magnetism to be determined for the whole record at Site 1124.

The Upper Cretaceous-Paleocene siliceous zeolitic mudstones were deposited at an average rate of 5 m/m.y., and the rates for the succeeding two unconformity-bounded Eocene and lower Oligocene sections are indeterminate. Above the Marshall Paraconformity, the thick upper Oligocene–lower Miocene (~27–23 Ma) section accumulated at ~27 m/m.y. The middle and upper Miocene sections accumulated steadily at 10 m/m.y., slowing down (or possibly a brief hiatus) around 9.5 to 8.5 Ma. A sharp increase in sedimentation at 2 Ma and continuing at ~38 m/m.y. possibly records the Hikurangi channel switching toward the drift and contributing fine tails of turbidity currents to it. This provides a possible age for the emplacement of the very large Ruatoria slide off eastern New Zealand.

Physical properties are very uniform in two intervals, 20–178 and 178–280 mbsf, corresponding to lithostratigraphic Subunits IB and IC, respectively**.** The early drift and sub-drift sequence shows downhole increases in density and compaction. The brown mudstone unit, however, is of lower density than the chalk above and below. Temperature measurements yield a gradient of 51.9°C/km and an estimated heat-flow of 0.049 W/m^2.

Good logging results were obtained with all tools except the NMRS magnetic intensity instrument. All show signals of useful dynamic range, save magnetic susceptibility between 318 and 419 mbsf, which is of very low amplitude, paralleling the core values. These values correlate very well between core and log over the whole hole. The brown mudstone unit stands out sharply in gamma, porosity, seismic velocity, photoelectric effect and magnetic susceptibility. A 30-cm-thick layer at the correct position for the K/T boundary is evident in resistivity, magnetic susceptibility, and on the Formation MicroScanner display. The logs are vital for filling in the major features of a 17-m zero recovery interval just above 300 mbsf. The integrated travel times based on the sonic log suggest that reflector Y is most likely the top of the brown mudstones.

The organic carbon concentrations average 0.3% and are in the normal range for deep-sea sediments. Carbonate contents show a high variability with values between 0.1% and 88.3%, and thus reflect a varying combination of fluctuating biological productivity, dilution by non-carbonate hemipelagic sedimentary components, and postdepositional carbonate dissolution forced by

oxidation of organic matter.

The dominant chemical reactions that control the interstitial water element concentrations include organic matter degradation, carbonate dissolution/ precipitation, silica dissolution, chert formation, and reactions with clay minerals. The element profiles of alkalinity, phosphate, and ammonia are typical of a situation without active sulfate reduction, reflecting organic matter oxidation and carbonate precipitation. The behavior of Ca, Mg, and Sr in the bottom of the section reflects a chemical reaction other than carbonate diagenesis. The decrease of Sr is similar to the pattern of Li, which is related to Si utilization to form the chert in the lowermost part of the core. The low Si concentration in the middle of the section is attributed to poor preservation of biogenic siliceous sediments, probably caused by low paleoproductivity. The general chemical zonation of interstitial waters at Site 1124 can be related to the lithostratigraphic units, paleontological age divisions, and hiatuses.

This site will provide well dated and characterized material for paleoceanographic studies of the deeper levels of flow entering the southwest Pacific Ocean, though in places only bulk carbonate isotopic data may be possible.

Site 1125

Hole 1125A

Position: 42°32.9962´S, 178°9.9891´W
Start hole: 2248 hr, 2 October 1998
End hole: 2000 hr, 3 October 1998
Time on hole: 21.20 hr
Seafloor (drill pipe measurement from rig floor, mbrf): 1376.20
Distance between rig floor and sea level (m): 11.60
Water depth (drill pipe measurement from sea level, m): 1364.60
Total depth (from rig floor, mbrf): 1579.70
Total penetration (mbsf): 203.50
Coring totals: type: APC; number: 22; cored: 203.50 m; recovered: 102.74%
Formation: lithostratigraphic Subunit IA (0–70.8 mbsf): clayey nannofossil ooze interbedded with nannofossil-bearing silty clay
lithostratigraphic Subunit IB (70.8–203.52 mbsf): nannofossil-bearing silty clay intercalated clay-bearing nannofossil ooze

Hole 1125B

Position: 42°32.9791´S, 178°9.9876´W
Start hole: 2000 hr, 3 October 1998
End hole: 1730 hr, 6 October 1998
Time on hole: 69.50 hr
Seafloor (drill pipe measurement from rig floor, mbrf): 1377.20
Distance between rig floor and sea level (m): 11.60

Water depth (drill pipe measurement from sea level, m): 1365.60
Total depth (from rig floor, mbrf): 1929.30
Total penetration (mbsf): 552.10
Coring totals: type: APC; number: 20; cored: 188.80 m; recovered: 101.49%
type: XCB; number: 38; cored: 363.30 m; recovered: 88.09%
Formation: lithostratigraphic Subunit IA (0–74.8 mbsf): clayey nannofossil ooze interbedded with nannofossil-bearing silty clay
lithostratigraphic Subunit IB (74.8–245.2 mbsf): nannofossil-bearing silty clay intercalated clay-bearing nannofossil ooze
lithostratigraphic Subunit IIA (245.2–331.79 mbsf): clayey nannofossil chalk
lithostratigraphic Subunit IIB (331.79–552.10 mbsf): clayey nannofossil chalk

Site 1125 lies 610 km east of New Zealand's South Island at 1360 m depth on the north slope of Chatham Rise. It is in the Subtropical Convergence zone of high productivity and is swept by the East Cape Current which runs south along eastern North Island before turning east along the Rise. This current is also supplied with water (and sediment) by the Southland, which flows up the eastern South Island coast and turns to flow east in two branches, north and south of the Rise, partly through Mernoo Gap at the end of the Rise, before turning east. The area is thus richly supplied with both pelagic and hemipelagic material as well as volcanic ash from the Central Volcanic Zone.

The major targets of Site 1125 originally were to retrieve an unaltered sequence of lower Neogene and perhaps Paleogene sediments from the commencement of AAIW activity on the margin (i.e., penetrate back to the Oligocene). It appeared possible to achieve a high-quality oxygen isotopic record spanning the period of probable inception of both Antarctic glaciation and the consequent delivery of cold water into the deep circulation system, based on the appearance of a thin late Neogene section in seismic profiles. The recovered thick late Neogene sequence will provide a record of AAIW paleohydrography, changing paleoproductivity, and position of the Subtropical Convergence. It is a counterpart to DSDP Site 594 on the south side of Chatham Rise and at a similar depth (594 was at 1204 m). Site 1125 presently lies at the base of AAIW. In the North Atlantic, an intermediate water has been shown to increase both in depth range and speed during glaciations, concomitant with a decrease in North Atlantic Deep Water production in the Norwegian-Greenland Sea. Analogously, Pudsey et al. (1988) have argued that AABW production also diminished during glacials, in which case the thickness of AAIW may also have increased concomitantly. If the vigor of global deep circulation was decreased by these North Atlantic and Antarctic events, then during glacial times the Indian/Pacific upper Circumpolar Deep Water (CDW) should have become even more nutrient enriched and oxygen depleted than it is today. Material from Site 1125 (depth 1359 m) will be used for delta^{13}C and trace-element analysis (e.g., Cd/Ca in calcite and opal) to allow ocean paleochemistry to be used to determine whether during glaciations the site lay under severely nutrient-depleted AAIW or enriched CDW.

This site yielded the thickest double–piston-cored section (Table T7) of the leg with a complete

composite section for 238 mcd, extending back close to the Miocene/Pliocene boundary (Fig. F13). Correlation was difficult, being based on very low amplitude signals in reflectance and magnetic susceptibility. The correlations are not as firmly based as at other sites and the record will probably prove difficult to tune.

The recovered sequence is divided into two units distinguished primarily on inferred carbonate content and tephra. The upper unit of Pliocene to Pleistocene age shows cyclic alternations of more and less calcareous beds and has increasing tephra upward. Below 245 m, Unit II has higher carbonate content and is more uniform in appearance. An upper subunit has occasional thin sandy glauconitic layers. The underlying subunit, from 333 mbsf to the bottom of the hole at 552 mbsf, is of clayey nannofossil chalk with numerous tephra layers. Organic carbon values are awaited, but, judging from the sulfate and methane curves, they are probably relatively high. The lower part of the section represents rapid deposition of dominantly biogenic material under high-energy conditions. Biogenic sediment declined until rapid deposition resumed at 6 Ma. Halfway through this period, terrigenous sediment increased and biogenic material declined. This may have been a result of a circulation change bringing the sediment, abundantly available since the 6 Ma change of plate motion and uplift of the Southern Alps, from the South Island coast.

Well preserved and rich calcareous nannofossil, foraminiferal, and radiolarian floras and faunas are present throughout, and rich diatom floras are present below 160 mbsf. These have yielded 47 age datums from late Pleistocene to early Miocene, thus rendering a robust age-depth curve. The flora indicates subtropical high-productivity conditions, whereas the faunas show some mixing of warm and cool subtropical species. Some cyclicity in warm/cold faunas in light/dark layers is also apparent, but no subantarctic species have been found.

Magnetic intensities are weak in the upper 200 mbsf and below that decline to the noise level of the machine. A reasonable stratigraphy can be detected in the upper 200 mbsf, with most reversals down to the base of C3n.4n at 5.23 Ma. With shore-based work, this will significantly aid the development of a tuned age model for the Pliocene–Pleistocene.

Sedimentation rates show two periods of very rapid deposition, the early Tortonian (10.1–10.6 Ma) at 190 m/m.y., and Messinian (6–5 Ma) at 15 0 m/m.y., separated by lower accumulation rates. The late Tortonian rate was ~30 m/Ma and the Pliocene to Holocene rate declined from the Messinian high to a Quaternary average of 20 m/Ma, though this may contain a 0.5-m.y. hiatus.

Physical properties at this site are very uniform with slow and slight increases in density. Magnetic susceptibility is relatively featureless. The thermal gradient is 64.9°C/km and the calculated heat flow 0.071 W/m^2.

Because of severe time constraints, just one logging tool was run: the triple combination comprising gamma radiation, resistivity, and porosity/density sensors. Resistivity and density show little change over the top 500 m of the hole, but the latter jumps from 1950 to 2200 kg/m3 from around 510 mbsf to the bottom of the hole, accounting for very slow drilling encountered there. The gamma record exhibits more character which will be worth examining by spectral methods.

The upper part of the hole is marked by sulfate reduction with decline of SO_4 to zero at 200

mbsf and increase of methane to 500 mbsf in the zone of methanogenesis below. Most other properties are related to these processes - alkalinity and ammonia increase in the upper 200 m and resulting Ca decrease as a result of carbonate precipitation, followed by Ca increase and carbonate dissolution in the zone of methanogenesis. Silica increases steadily downhole but sharply decreases in the bottom 40 m where particularly hard mudstone is encountered, probably caused by incipient silica cementation.

Site 1125 proved the equal of the other sites on this leg in its capacity to surprise us. Two periods of an astonishing sedimentation rate over 150 m/m.y. ensured that in 550 m the middle Miocene was not reached. The prospect for high resolution study of productivity and intermediate water masses in the SW Pacific for the last 11 m.y. is excellent, however, and comparison of this site under subtropical water can be made with Site 594 just south of the Rise under subantarctic water.

CONCLUSIONS

ODP Leg 181 targeted drill sites located in the eastern New Zealand region and the key southwest Pacific gateway because:

1. The Pacific DWBC is today one of the largest single contributors to the deep waters of the world's oceans, and, therefore, deciphering its history is of fundamental importance to global ocean paleohydrography.

2. The stratigraphic record of the eastern New Zealand Plateau and its abyssal margins is the best available for deciphering the history of development of Pacific Southern Ocean water masses and of the sediment drifts that they deposited.

3. The gateway region includes two major oceanic fronts, the Subtropical Convergence and the Subantarctic Front (Fig. F1). Thus, the region is in a prime position to allow determination of the migration of these boundaries, the forcing processes that cause them to move, and the environmental response to their movement.

4. The stratigraphic record from ENZOSS is of interest in its own right, as a major geological and sedimentary system within which sources, sinks, and material fluxes can all be quantified. The ENZOSS record is also directly relevant to one of the most important unresolved problems of Cenozoic climatology, namely the timing and precise nature of the development of widespread glaciation on the Antarctic continent (e.g., Barrett, 1996). In turn, it is, of course, these same glacial events that contribute source water to the DWBC and its companion flow, the ACC, which forces the boundary current south of 49°S.

The Leg 181 drilling schedule included 51 days at sea with drilling operations at seven sites.

We began by drilling shallow-water sediment drifts on the upper continental slope near South Island New Zealand, moved south in difficult weather conditions to drill sites on the central Campbell Plateau, and, at its eastern foot, turned north to drill a deep hole through the levee sediments of the Bounty Fan, and finished by drilling two holes through sediment drifts on the north side of the Chatham Rise, and one into the shallow rise itself. Overall, we recovered 3600 m of core, and made over a million shipboard measurements. The material collected on Leg 181 will lead to a better understanding of the history and evolution of the Pacific ACC-DWBC system and related oceanic fronts and to the important role they play in global ocean circulation. Finally, that the stratigraphic and paleontologic information retrieved on the cruise contained many surprises was itself predictable, given the paucity of previous drilling in the Southwest Pacific area. This information will provide a vital database for the targeting of future drilling legs in the Southern Ocean.

REFERENCES

Barnes, P.M., 1992. Mid-bathyal current scours and sediment drifts adjacent to the Hikurangi deep-sea turbidite channel, eastern New Zealand: evidence from echo character mapping. *Mar. Geol.*, 106:169–187.

Barnes, P.M., 1994. Continental extension of the Pacific Plate at the southern termination of the Hikurangi subduction zone: the North Mernoo Fault Zone, offshore New Zealand. *Tectonics*, 13:735–754.

Barnes, P.M. and Mercier de Lepinay, B., 1997. Rates and mechanics of rapid frontal accretion along the very obliquely convergent southern Hikurangi margin, New Zealand. *J. Geophys. Res.*, 102:24931–24952.

Barrett, P.J., 1996. Antarctic paleoenvironment through Cenozoic times—a review. *Terra Antarct.*, 3:103–119.

Barron, J., Larsen, B., et al., 1989. *Proc. ODP, Init. Repts.*, 119: College Station, TX (Ocean Drilling Program).

Bishop, D.G., and Laird, M.G., 1976. Stratigraphy and depositional environment of the Kyeburn Formation (Cretaceous), a wedge of coarse terrestrial sediments in Central Otago. *J. R. Soc. N. Z.*, 6:55–71.

Boltovskoy, E., 1980. The age of the Drake Passage. *Alcheringa*, 4:289–297.

Broecker, W.S., Bond, G., Klas, M., Bonani, G., and Wolfi, W., 1990. A salt oscillator in the glacial Atlantic? I. The concept. *Paleoceanography*, 5:469–477.

Bryden, H.L. and Heath, R.A., 1985. Energetic eddies at the northern edge of the Antarctic Circumpolar Current in the Southwest Pacific. *Prog. Oceanogr.,* 14:65–87.

Campbell, H.J., Andrews, P.B., Beu, A.G., Maxwell, P.A., Edwards, R.A., Laird, M.G., Hornibrook, N. de B., Mildenhall, D.C., Watters, W.A., Buckeridge, J.S., Lee, D.E., Strong, C.P., Wilson, G.J., and Hayward, B.W., 1993. Cretaceous-Cenozoic Geology and Biostratigraphy of the Chatham Islands, New Zealand. *Inst. Geol. Nuc. Sci. Monog.*, 2:269.

Carter, L., and Carter, R.M., 1993. Sedimentary evolution of the Bounty Trough: a Cretaceous rift basin, southwestern Pacific Ocean. *In* Ballance, P., (Ed.), *Sedimentary Basins of the World-South Pacific: Amsterdam* (Elsevier), 51–67.

Carter, L., Carter, R.M., McCave, I.N., and Gamble, J., 1996. Regional sediment recycling in the abyssal Southwest Pacific Ocean. *Geology,* 24:735–738.

Carter, L., Garlick, R. D., Sutton, P., Chiswell, S, Oien, N. A., and Stanton, B.R., 1998. Ocean Circulation New Zealand. *NIWA Chart, Misc. Ser.,* 76.

Carter, L., and Herzer, R.H., 1979. The hydraulic regime and its potential to transport sediment on the Canterbury continental shelf. *Mem.— N. Z. Oceanogr. Inst.*, 83:1-33.

Carter, L., and McCave, I.N., 1994. Development of sediment drifts approaching an active plate margin under the SW Pacific deep western boundary current. *Paleoceanography,* 9:1061–1085.

Carter, L., and McCave, I.N., 1997. The sedimentary regime beneath the deep western boundary current inflow to the southwest Pacific Ocean. *J. Sed. Res.*, 67:1005–1017.

Carter, L., and Mitchell, J.S. 1987. Late Quaternary sediment pathways through the deep ocean, east of New Zealand. *Paleoceanography,* 2:409–422.

Carter, L., Nelson, C.S., Neil, H.L., and Froggatt, P.C., 1995. Correlation, dispersal, and preservation of the Kawakawa Tephra and other late Quaternary tephra layers in the Southwest Pacific Ocean. *N. Z. J. Geol. Geophys.*, 38:29–46.

Carter, L., and Wilkin, J., in press. Abyssal circulation around New Zealand: a comparison between observations and a global circulation model. *Mar. Geol.*

Carter, R.M., 1985. The mid-Oligocene Marshall Paraconformity, New Zealand: coincidence with

global eustatic sea-level fall or rise? *J. Geol.,* 93:359–371.

Carter, R.M., 1988a. Post-breakup stratigraphy of the Kaikoura Synthem (Cretaceous–Cenozoic), continental margin, southeastern New Zealand. *N. Z. J. Geol. Geophys.,* 31:405–429.

Carter, R.M., 1988b. Plate boundary tectonics, global sea-level changes and the development of the Eastern South Island Continental Margin, New Zealand, Southwest Pacific. *Mar. Pet. Geol.,* 5:90–107.

Carter, R.M., and Carter, L., 1996. The abyssal Bounty Fan and lower Bounty Channel: evolution of a rifted-margin sedimentary system. *Mar. Geol.,* 130:182–202.

Carter, R.M., Carter, L., and Davy, B., 1994. Geologic and stratigraphic history of the Bounty Trough, southwestern Pacific Ocean. *Mar. Pet. Geol.,* 11:79–93.

Carter, R.M., Carter, L., and McCave, I.N., 1996. Current controlled sediment deposition from the shelf to the deep ocean: the Cenozoic evolution of circulation through the SW Pacific gateway. *Geol. Rundsch.,* 85:438–451.

Carter, R.M., and Norris, R.J., 1976. Cainozoic history of southern New Zealand: an accord between geological observations and plate-tectonic predictions. *Earth Planet. Sci. Lett.,* 31:85–94.

Chiswell, S.M., 1994. Variability in sea surface temperature around New Zealand from AVHRR images. *N. Z. J. Mar. Freshwater Res.,* 28:179–192.

Cotton, C.A., 1955. Review of the Notocenozoic, or Cretaceo-Tertiary of New Zealand. *Trans. R. Soc. N. Z.,* 82:1071–1122.

Fenner, J., Carter, L., and Stewart, R., 1992. Late Quaternary paleoclimatic and paleoceanographic change over northern Chatham Rise, New Zealand. *Marine Geology,* 108:383–404.

Froggatt, P.C., and Lowe, D.J., 1990. A review of late Quaternary silicic and some other tephra formation from New Zealand: their stratigraphy, nomenclature, distribution, volume and age. *N. Z. J. Geol. Geophys.,* 33:89–109.

Froggatt, P.C., Nelson, C.S.,Carter, L., Griggs, G., and Black, K.P. 1986 An exceptionally large late Quaternary eruption from New Zealand. *Nature,* 319:578–582.

Gordon, A.I., 1986. Interocean exchange of thermocline water. *J. Geophys. Res.,* 91:5037-5046.

Howard, W.R., and Prell, W.L., 1992. Late Quaternary surface circulation of the southern Indian ocean and its relationship to orbital variations. *Paleoceanography,* 7:79–117.

Kennett, J.P., 1977. Cenozoic evolution of Antarctic glaciation, the circum-Antarctic Ocean, and their impact on global paleoceanography. *J. Geophys. Res.,* 82:3843–3860.

Kennett, J.P., Burns, R.E., Andrews, J.E., Churkin, M., Jr., Davies, T.A., Dumitrica, P., Edwards, A.R., Galehouse, J.S., Packham, G.H., and van der Lingen, G.J., 1972. Australian-Antarctic continental drift, paleocirculation change and Oligocene deep-sea erosion. *Nature,* 239:51-55.

Kennett, J.P., von der Borch, C.C., et al., 1986. *Init. Repts. DSDP,* 90: Washington (U.S. Govt. Printing Office).

Lawver, L., Gahagan, L., and Coffin, M., 1992. The development of paleoseaways around Antarctica. *Antarct. Res. Ser.,* 56:7–30.

Lewis, K.B.,1994. The 1500-km long Hikurangi Channel: trench-axis channel that escapes its trench, crosses a plateau, and feeds a fan-drift. *Geo-Marine Letters,* 14:19–28.

Lewis, K.B., and Kohn, B.P., 1973. Ashes, turbidites and rates of sedimentation on the continental slope off Hawkes Bay. *N. Z. J. Geol. Geophys.,* 16:439–454.

Lewis, K.B., Bennett, D.J., Herzer, R.H., and von der Borch, C.C., 1985. Seismic stratigraphy and structure adjacent to an evolving plate boundary, western Chatham Rise, New Zealand. *In* Kennett, J.P., von der Borch, C.C., et al., *Init. Repts. DSDP,* 90: Washington (U.S. Govt. Printing Office), 1325–1337.

Lonsdale, P., 1976. Abyssal circulation of the southeastern Pacific and some geological implications. *J. Geophys. Res.,* 81:1163-1176.

Lonsdale, P., 1988. Geography and history of the Louisville hotspot chain in the Southwest Pacific. *J. Geophys. Res.,* 93:3078–3104.

McCave, I.N., and Carter, L., 1997. Recent sedimentation beneath the Deep Western Boundary Current off northern New Zealand. *Deep-Sea Res.,* 44:1203–1237.

Milliman, J.D., and Syvitski, J.P.M., 1992. Geomorphic/tectonic control of sediment discharge to the ocean: the importance of small mountainous rivers. *J. Geol.,* 100:525–544.

Molnar, P., Atwater, T., Mammerickx, J., and Smith, S., 1975. Magnetic anomalies, bathymetry and the tectonic evolution of the South Pacific since the Late Cretaceous. *Geophys. J. R. Astron. Soc.*, 40:383-420.

Nelson, C. S., Froggatt, P. C., and Gosson, G. J., 1985. Nature, chemistry, and origin of late Cenozoic megascopic tephras in Leg 90 cores from the southwestern Pacific. *In* Kennett, J. P., von der Borch, C.C., et al., *Init. Repts. DSDP,* 90: Washington (U.S. Govt. Printing Office), 1161–1171.

Nelson, C.S., Hendy, C.H., Jarrett, G.R., and Cuthbertson, A.M., 1985. Near-synchroneity of New Zealand alpine glaciations and Northern Hemisphere continental glaciations during the past 750 kyr. *Nature*, 318:361–363.

Nelson, C.S., Hendy, C.H., Cuthbertson, A.M., and Jarrett, G.R.,1986. Late Quaternary carbonate and isotope stratigraphy, subantarctic Site 594, southwest Pacific. *In* Kennett, J.P., von der Borch, C.C., et al., *Init. Repts. DSDP*, 90: Washington (U.S. Govt. Printing Office), 1425–1436.

Nelson, C.S., Cooke, P.J., Hendy, C.H., and Cuthbertson, A.M., 1993. Oceanographic and climate changes over the past 150,000 years at Deep Sea Drilling Project Site 594 off southeastern New Zealand, southwest Pacific Ocean. *Paleoceanography*, 8:435–458.

Ninkovich, D., 1968. Pleistocene volcanic eruptions in New Zealand recorded in deep sea sediments. *Earth Planet. Sci. Lett.*, 4:89–102.

Norris, R.J., Carter, R.M., and Turnbull, I.M., 1978. Cainozoic sedimentation in basins adjacent to a major continental transform boundary in southern New Zealand. *J. Geol. Soc. London*, 135:191–205.

Oliver, R.L., Finlay, H.J., and Fleming, C.A., 1950. The geology of Campbell Island. *Cape Expedition Series, Bulletin, 3:* 1 map + 62 pp., DSIR, Wellington, New Zealand.

Orsi, A.H., Whitworth III, T., and Nowlin Jr, W.D., 1995. On the meridional extent and fronts of the Antarctic Circumpolar Current. *Deep-Sea Res.*, 42:641–673.

Pudsey, C.J., Barker, P.F., and Hamilton, N., 1988. Weddell Sea abyssal sediments: a record of Antarctic bottom water flow. *Mar. Geol.*, 81:289-314.

Schmitz, W.J., 1995. On the interbasin-scale thermohaline circulation. *Rev. Geophys.*,

33:151–173.

Schuur, C.L., Coffin, M.F., Frohlich, C., Mann, P., Massell, C.G., Karner, G.D., Ramsay, D., and Caress, D.W., in press. Sedimentary regimes at the Macquarie Ridge Complex: interaction of Southern Ocean circulation and plate boundary bathymetry. *Paleoceanography*.

Shackleton, N.J., and Kennett, J.P., 1975. Paleotemperature history of the Cenozoic and the initiation of Antarctic glaciation: oxygen and carbon isotope analyses in DSDP Sites 277, 279, and 281. *In* Kennett, J.P., Houtz, R.E., et al., *Init. Repts. DSDP,* 29: Washington (U.S. Govt. Printing Office), 743–755.

Shane, P. A. R., 1990. Correlation of some Pliocene tuffs in southern Wairarapa, New Zealand, and the comparison with biostratigraphic and magnetostratigraphic data. *N. Z. J. Geol. Geophys.,* 33:349–355.

Shane, P.A.R., and Froggatt, P.C., 1991. Glass chemistry, paleomagnetism and correlation of middle Pleistocene tuffs in southern North Island, New Zealand and western Pacific. *N. Z. J. Geol. Geophys.,* 34:203–211.

Shane, P.A.R., Black, T.M., Alloway, B.V., and Westgate, J.A., 1996. Early to middle Pleistocene tephrochronology of North Island, New Zealand: implications for volcanism, tectonism, and paleoenvironments. *Geol. Soc. Am. Bull.,* 108: 915–925.

Shane, P., Froggatt, P., Black, T., and Westgate, J., 1995. Chronology of Pliocene and Quaternary bioevents and climatic events from fission-track ages on tephra beds, Wairarapa, New Zealand. *Earth Planet. Sci. Lett.,* 130:141–154.

Suggate, R.P., Stevens, G.R., and Te Punga, M.T., 1978. *The Geology of New Zealand:* Wellington (New Zealand Govt. Printer).

Sutherland, R., 1995. The Australia-Pacific boundary and Cenozoic plate motions in the SW Pacific: some constraints from Geosat data. *Tectonics,* 14:819–831.

Thiede, J., Nees, S., Schulz, H., and De Deckker, P., 1997. Oceanic surface conditions recorded on the sea floor of the Southwest Pacific Ocean through the distribution of foraminifers and biogenic silica. *Palaeogeogr., Palaeoclimatol., Paleoecol.,* 131:207–239.

Turnbull, I.M., 1985. Sheet D42AC and Part Sheet D43 - Te Anau Downs. (1st ed.). *Geological Map of New Zealand 1:50 000, Map (1 sheet) and Notes:* Wellington (New Zealand Dept.Sci. Indust. Res.), 1–32.

van der Lingen, G.J., 1968. Volcanic ash in the Makara Basin (Upper Miocene), Hawkes Bay, New Zealand. *New Zealand Journal of Geology and Geophysics,* 11:693–705.

Vella, P., 1962. Age of the younger marine strata at upper Tengawai River (Appendix). *N. Z. J. Geol. Geophys.,* 5:172–174.

Walcott, R.I., 1998. Modes of oblique compression: late Cenozoic tectonics of the South Island of New Zealand. *Rev. Geophys.,* 36:1–26.

Ward, D.M., and Lewis, D.W., 1975. Paleoenvironmental implications of storm-scoured ichnofossiliferous mid-Tertiary limestones, Waihao district, South Canterbury, New Zealand. *N. Z. J. Geol. Geophys.,* 18:881–908.

Warren, B.A., 1973. TransPacific hydrographic sections at latitudes 435S and 285S; the SCORPIO Expedition—deep water. *Deep-Sea Res.,* 20:9–38.

Warren, B.A. 1981. Deep circulation of the world ocean. *In* Warren, B.A., and Wunsch, C. (Eds.), *Evolution of Physical Oceanography:* Cambridge, MA (MIT Press), 6–41.

Watkins, N.D., and Kennett, J.P., 1972. Regional sedimentary disconformities and upper Cenozoic changes in bottom water velocities between Australia and Antarctica. *Antarct. Res. Ser*., 19:317-334.

Weaver, P.P.E., Neil, H., and Carter, L., 1997. Sea surface temperature estimates from the Southwest Pacific based on planktonic foraminifera and oxygen isotopes. *Palaeogeogr., Palaeoclimatol., Paleoecol.,* 131:241–256.

Weaver, P.P.E., Carter, L., and Neil, H., 1998. Response of surface watermasses and circulation to late Quaternary climate change, east of New Zealand. *Paleoceanography,* 13:70–83.

TABLE CAPTIONS

Table T1. Site 1119 coring summary.

Table T2. Site 1120 coring summary.

Table T3. Site 1121 coring summary.

Table T4. Site 1122 coring summary.

Table T5. Site 1123 coring summary.

Table T6. Site 1124 coring summary.

Table T7. Site 1125 coring summary.

Core	Date (August 1998)	Time	Top depth (mbsf)	Bottom depth (mbsf)	Length cored (m)	Length recovered (m)	Recovery (%)
181-1119A-							
1H	23	1025	0.0	6.0	6.0	6.01	100.2
Coring totals:					6.0	6.01	100.17%
181-1119B-							
1H	23	1055	0.0	4.7	4.7	4.73	100.6
2H	23	1145	4.7	14.2	9.5	9.88	104.0
3H	23	1320	14.2	23.7	9.5	10.09	106.2
4H	23	1417	23.7	33.2	9.5	7.13	75.1
5H	23	1445	33.2	42.7	9.5	10.27	108.1
6H	23	1520	42.7	52.2	9.5	10.35	108.9
7H	23	1600	52.2	61.7	9.5	10.37	109.2
8H	23	1635	61.7	71.2	9.5	10.44	109.9
9H	23	1710	71.2	80.7	9.5	10.35	108.9
10H	23	1805	80.7	90.2	9.5	10.22	107.6
11H	23	1840	90.2	99.7	9.5	10.24	107.8
12H	23	1920	99.7	109.2	9.5	10.26	108.0
13H	23	2005	109.2	118.7	9.5	10.51	110.6
14H	23	2050	118.7	128.2	9.5	10.33	108.7
15H	23	2120	128.2	137.7	9.5	10.35	108.9
16H	23	2200	137.7	147.2	9.5	10.3	108.4
17H	23	2245	147.2	155.8	8.6	8.65	100.6
Coring totals:					155.8	164.47	105.56%
181-1119-C-							
1H	24	0105	0	8.3	8.3	8.27	99.6
2H	24	0135	8.3	17.8	9.5	9.35	98.4
3H	24	0215	17.8	27.3	9.5	10.08	106.1
4H	24	0245	27.3	36.8	9.5	10.24	107.8
5H	24	0315	36.8	46.3	9.5	10.32	108.6
6H	24	0345	46.3	55.8	9.5	10.4	109.5
7H	24	0415	55.8	65.3	9.5	10.67	112.3
8H	24	0450	65.3	74.8	9.5	10.27	108.1
9H	24	0525	74.8	84.3	9.5	10.48	110.3
10H	24	0600	84.3	93.8	9.5	10.15	106.8
11H	24	0630	93.8	103.3	9.5	10.5	110.5
12H	24	0705	103.3	112.8	9.5	10.19	107.3
13H	24	0745	112.8	122.3	9.5	10.31	108.5
14H	24	0820	122.3	131.8	9.5	10.53	110.8
15H	24	0900	131.8	141.3	9.5	10.28	108.2
16H	24	0935	141.3	150.8	9.5	11.12	117.1
17H	24	1020	150.8	160.3	9.5	10.41	109.6
18X	24	1220	160.3	168.7	8.4	9.9	117.9
19X	24	1315	168.7	178.3	9.6	7.97	83.0
20X	24	1345	178.3	187.9	9.6	9.62	100.2
21X	24	1425	187.9	197.6	9.7	8.67	89.4
22X	24	1500	197.6	207.2	9.6	9.28	96.7
Core	Date (August 1998)	Time	Top depth (mbsf)	Bottom depth (mbsf)	Length cored (m)	Length recovered (m)	Recovery (%)
23X	24	1530	207.2	216.8	9.6	10.0	104.2
24X	24	1605	216.8	226.4	9.6	0.0	0.0

Table 1

25X	24	1640	226.4	236.0	9.6	9.35	97.4
26X	24	1725	236.0	245.6	9.6	9.96	103.8
27X	24	1755	245.6	255.2	9.6	9.08	94.6
28X	24	1835	255.2	264.8	9.6	9.72	101.3
29X	24	1915	264.8	274.5	9.7	9.67	99.7
30X	24	1950	274.5	284.1	9.6	9.55	99.5
31X	24	2035	284.1	293.8	9.7	9.68	99.8
32X	24	2110	293.8	303.4	9.6	9.44	98.3
33X	24	2145	303.4	313.0	9.6	9.48	98.8
34X	24	2225	313.0	322.3	9.3	6.22	66.9
35X	24	2255	322.3	331.9	9.6	9.71	101.1
36X	24	2335	331.9	341.5	9.6	6.98	72.7
37X	25	0030	341.5	351.1	9.6	1.76	18.3
38X	25	0110	351.1	360.8	9.7	9.12	94.0
39X	25	0155	360.8	370.5	9.7	2.69	27.7
40X	25	0240	370.5	380.1	9.6	3.06	31.9
41X	25	0400	380.1	389.8	9.7	2.19	22.6
42X	25	0530	389.8	399.4	9.6	6.54	68.1
43X	25	0630	399.4	409.0	9.6	3.24	33.8
44X	25	0740	409.0	418.6	9.6	9.9	103.1
45X	25	0900	418.6	428.2	9.6	0.82	8.5
46X	25	1045	428.2	437.9	9.7	9.62	99.2
47X	25	1205	437.9	447.2	9.3	9.62	103.4
48X	25	1330	447.2	456.8	9.6	9.8	102.1
49X	25	1500	456.8	466.4	9.6	8.77	91.4
50X	25	1640	466.4	475.6	9.2	9.67	105.1
51X	25	1800	475.6	485.2	9.6	8.06	84.0
52X	25	1945	485.2	494.8	9.6	9.52	99.2
Coring totals:					494.8	442.23	89.38%

Table 1 (continued)

Core	Date (August 1998)	Time (mbsf)	Top depth (mbsf)	Bottom depth (m)	Length cored (m)	Length recovered (%)	Recovery
181-1120A-							
1H	28 Aug	0555	0.0	4.6	4.6	4.6	100
Coring totals:					4.6	4.6	100.00%
181-1120B-							
1H	28 Aug	0655	0.0	3.3	3.3	3.36	101.80
2H	28 Aug	0730	3.3	12.8	9.5	9.58	100.80
3H	28 Aug	0800	12.8	22.3	9.5	4.90	51.60
4H	28 Aug	0835	22.3	31.8	9.5	9.26	97.50
5H	28 Aug	0910	31.8	41.3	9.5	9.64	101.50
6H	28 Aug	1005	41.3	50.8	9.5	9.78	102.90
7H	28 Aug	1035	50.8	60.3	9.5	8.66	91.20
8H	28 Aug	1135	60.3	68.3	8.0	8.03	100.40
9X	28 Aug	1235	68.3	72.6	4.3	2.57	59.80
10X	28 Aug	1310	72.6	82.2	9.6	4.86	50.60
11X	28 Aug	1340	82.2	91.8	9.6	4.45	46.40
12X	28 Aug	1410	91.8	101.4	9.6	7.40	77.10
13X	28 Aug	1440	101.4	111.0	9.6	2.21	23.00
14X	28 Aug	1510	111.0	120.6	9.6	6.56	68.30
15X	28 Aug	1545	120.6	130.1	9.5	6.28	66.10
16X	28 Aug	1610	130.1	139.8	9.7	8.73	90.00
17X	28 Aug	1640	139.8	149.4	9.6	8.49	88.40
18X	28 Aug	1710	149.4	159.0	9.6	9.23	96.10
19X	28 Aug	1735	159.0	168.7	9.7	7.93	81.80
20X	28 Aug	1800	168.7	178.4	9.7	8.44	87.00
21X	28 Aug	1835	178.4	188.0	9.6	6.15	64.10
Coring totals:					188.0	146.51	77.93%
181-1120C-							
1H	30 Aug	300	0.0	6.6	6.6	6.59	99.8
2H	30 Aug	345	6.6	16.1	9.5	9.12	96.0
3H	30 Aug	415	16.1	25.6	9.5	9.51	100.1
4H	30 Aug	455	25.6	35.1	9.5	9.95	104.7
5H	30 Aug	1055	35.1	44.6	9.5	9.78	102.9
Coring totals:					44.6	44.95	100.78%
181-1120D-							
1	31 Aug	2045	0.0	157.4	0.0	0.0	N/A
1X	31 Aug	2125	157.4	167.0	9.6	9.63	100.3
2X	31 Aug	2155	167.0	176.7	9.7	9.73	100.3
3X	31 Aug	2225	176.7	186.3	9.6	8.28	86.3
4X	31 Aug	2255	186.3	195.9	9.6	8.48	88.3
5X	31 Aug	2320	195.9	205.5	9.6	7.77	80.9
6X	31 Aug	2359	205.5	210.1	4.6	8.72	189.6
7X	1 Sept	0035	210.1	215.1	5.0	3.55	71.0
8X	1 Sept	0110	215.1	218.7	3.6	6.75	187.5
9X	1 Sept	0140	218.7	220.7	2.0	3.26	163.0
Coring totals:					63.3	66.17	104.53%

Table 2

Core	Date (August 1998)	Time	Top depth (mbsf)	Bottom depth (mbsf)	Length cored (m)	Length recovered (m)	Recovery (%)
181-1121A-							
1H	2	1620	0.0	8.4	8.4	8.37	99.6
Coring totals:				8.4	8.37	99.64%	
181-1121B-							
1H	2	1740	0.0	9.5	9.5	9.92	104.4
2H	2	1855	9.5	19.0	9.5	9.93	104.5
3H	2	2025	19.0	23.0	4.0	9.83	245.8
4X	2	2240	23.0	23.5	0.5	0.28	56.0
5X	3	0040	23.5	32.7	9.2	0.27	2.9
6X	3	0150	32.7	42.3	9.6	4.58	47.7
7X	3	0255	42.3	52.0	9.7	8.35	86.1
8X	3	0400	52.0	61.6	9.6	9.06	94.4
9X	3	0455	61.6	71.2	9.6	9.68	100.8
10X	3	0620	71.2	80.9	9.7	6.18	63.7
11X	3	0740	80.9	90.5	9.6	6.32	65.8
12X	3	1045	90.5	100.1	9.6	3.81	39.7
13X	3	1300	100.1	109.7	9.6	0.39	4.1
14X	3	1530	109.7	119.4	9.7	0.56	5.8
15X	3	1745	119.4	126.0	6.6	2.93	44.4
16X	3	2000	126.0	130.0	4.0	1.30	32.5
17X	3	2355	130.0	139.7	9.7	4.47	46.1
Coring totals:					139.7	87.86	62.89%

Table 3

Core	Date (August 1998)	Time	Top depth (mbsf)	Bottom depth (mbsf)	Length cored (m)	Length recovered (m)	Recovery (%)
181-1122A-							
1H	6	1240	0.0	9.3	9.3	9.32	100.2
2H	6	1355	9.3	18.8	9.5	9.66	101.7
3H	6	1500	18.8	28.3	9.5	9.77	102.8
4H	6	1625	28.3	37.8	9.5	10.05	105.8
5H	6	1730	37.8	47.3	9.5	8.82	92.8
6H	6	1830	47.3	56.8	9.5	9.06	95.4
7H	6	1935	56.8	66.3	9.5	9.13	96.1
8H	6	2045	66.3	75.8	9.5	7.69	80.9
9X	6	2205	75.8	85.4	9.6	0.81	8.4
10X	6	2305	85.4	95.0	9.6	0.44	4.6
11X	7	0025	95.0	104.7	9.7	1.92	19.8
12X	7	0135	104.7	114.3	9.6	5.02	52.3
13X	7	0240	114.3	123.9	9.6	5.77	60.1
Coring totals:					123.9	87.46	70.59%
181-1122B-							
1H	2	1740	0.0	9.5	9.5	9.92	104.4
2H	2	1855	9.5	19.0	9.5	9.93	104.5
3H	2	2025	19.0	23.0	4.0	9.83	245.8
4X	2	2240	23.0	23.5	0.5	0.28	56.0
5X	3	0040	23.5	32.7	9.2	0.27	2.9
6X	3	0150	32.7	42.3	9.6	4.58	47.7
7X	3	0255	42.3	52.0	9.7	8.35	86.1
8X	3	0400	52.0	61.6	9.6	9.06	94.4
9X	3	0455	61.6	71.2	9.6	9.68	100.8
10X	3	0620	71.2	80.9	9.7	6.18	63.7
11X	3	0740	80.9	90.5	9.6	6.32	65.8
12X	3	1045	90.5	100.1	9.6	3.81	39.7
13X	3	1300	100.1	109.7	9.6	0.39	4.1
14X	3	1530	109.7	119.4	9.7	0.56	5.8
15X	3	1745	119.4	126.0	6.6	2.93	44.4
16X	3	2000	126.0	130.0	4.0	1.30	32.5
17X	3	2355	130.0	139.7	9.7	4.47	46.1
Coring totals:					139.7	87.86	62.89%
181-1122C-							
1H	7	0805	0.0	2.5	2.5	2.5	100.4
2H	7	0930	2.5	9.5	7.0	9.8	139.3
3H	7	1035	9.5	14.0	4.5	7.6	169.8
4H	7	1155	14.0	23.5	9.5	9.7	102.1
5H	7	1310	23.5	33.0	9.5	9.0	94.2
6H	7	1355	33.0	42.5	9.5	9.2	96.4
7H	7	1500	42.5	52.0	9.5	8.7	91.8
8H	7	1610	52.0	61.5	9.5	9.4	99.4
9H	7	1710	61.5	71.0	9.5	8.7	91.3
10H	7	1830	71.0	80.5	9.5	9.4	99.3
Core	Date (August 1998)	Time	Top depth (mbsf)	Bottom depth (mbsf)	Length cored (m)	Length recovered (m)	Recovery (%)
11H	7	2000	80.5	86.9	6.4	6.5	101.3
12H	7	2100	86.9	94.9	8.0	7.9	98.8

Table 4

13H	7	2210	94.9	103.7	8.8	8.8	100.0
14X	7	2330	103.7	108.0	4.3	4.3	100.5
15X	8	0025	108.0	117.6	9.6	3.4	35.2
16X	8	0135	117.6	127.2	9.6	5.4	56.0
17X	8	0240	127.2	136.9	9.7	6.3	64.4
18X	8	0345	136.9	146.5	9.6	3.7	38.6
19X	8	0445	146.5	156.1	9.6	4.1	42.5
20X	8	0545	156.1	165.7	9.6	5.2	54.3
21X	8	0645	165.7	175.3	9.6	2.4	25.4
22X	8	0745	175.3	185.0	9.7	1.7	17.8
23X	8	0850	185.0	194.7	9.7	2.4	24.5
24X	8	0950	194.7	204.3	9.6	0.8	8.5
25X	8	1125	204.3	214.0	9.7	0.7	6.9
26X	8	1230	214.0	223.7	9.7	4.1	42.2
27X	8	1335	223.7	233.3	9.6	3.5	36.6
28X	8	1430	233.3	242.9	9.6	4.5	46.7
29X	8	1530	242.9	252.5	9.6	4.8	50.3
30X	8	1625	252.5	261.7	9.2	6.7	73.2
31X	8	1725	261.7	271.3	9.6	4.7	48.9
32X	8	1830	271.3	280.7	9.4	2.6	27.1
33X	8	1930	280.7	290.4	9.7	7.3	75.6
34X	8	2040	290.4	300.0	9.6	7.4	77.5
35X	8	2150	300.0	309.6	9.6	8.0	83.4
36X	8	2255	309.6	319.3	9.7	8.7	89.7
37X	9	0010	319.3	328.9	9.6	9.1	94.5
38X	9	0120	328.9	338.5	9.6	4.5	46.7
39X	9	0230	338.5	348.2	9.7	5.3	54.2
40X	9	0340	348.2	357.9	9.7	3.3	33.6
41X	9	0445	357.9	367.5	9.6	2.1	21.7
42X	9	0550	367.5	377.2	9.7	4.7	48.4
43X	9	0700	377.2	386.9	9.7	0.4	4.4
44X	9	0805	386.9	396.6	9.7	5.7	59.2
45X	9	0925	396.6	406.2	9.6	6.0	62.6
46X	9	1035	406.2	415.9	9.7	6.3	65.4
47X	9	1140	415.9	425.5	9.6	5.7	59.5
48X	9	1250	425.5	435.2	9.7	7.0	72.3
49X	9	1400	435.2	444.8	9.6	9.3	97.0
50X	9	1510	444.8	454.4	9.6	7.4	77.2
51X	9	1655	454.4464.19.				

Core	Date (August 1998)	Time	Top depth (mbsf)	Bottom depth (mbsf)	Length cored (m)	Length recovered (m)	Recovery (%)
58X	10	0510	521.5	531.2	9.7	2.1	21.4
59X	10	0705	531.2	540.7	9.5	0.1	1.3
60X	10	0850	540.7	550.4	9.7	0.5	4.7
61X	10	1030	550.4	560.0	9.6	5.2	54.1
62X	10	1215	560.0	569.6	9.6	3.4	35.5
63X	10	1355	569.6	579.3	9.7	1.7	17.7
64X	10	1545	579.3	588.9	9.6	1.6	16.7
65X	10	1735	588.9	598.5	9.6	1.8	18.5
66X	10	1920	598.5	608.2	9.7	1.0	9.8
67X	10	2100	608.2	617.8	9.6	1.0	10.5
68X	10	2245	617.8	627.4	9.6	0.1	0.5
Coring totals:					627.4	351.44	56.02%

Table 4 (continued)

Core	Date (August 1998)	Time	Top depth (mbsf)	Bottom depth (mbsf)	Length cored (m)	Length recovered (m)	Recovery (%)
181-1123A-							
1H	14	0445	0.0	6.1	6.1	6.1	100
2H	14	0545	6.1	15.6	9.5	9.61	101.2
3H	14	0640	15.6	25.1	9.5	7.71	81.2
4H	14	0825	25.1	34.6	9.5	9.7	102.1
5H	14	0930	34.6	44.1	9.5	9.69	102
6H	14	1025	44.1	53.6	9.5	9.72	102.3
7H	14	1125	53.6	63.1	9.5	9.65	101.6
8H	14	1225	63.1	72.6	9.5	8.97	94.4
9H	14	1325	72.6	82.1	9.5	9.83	103.5
10H	14	1420	82.1	91.6	9.5	9.83	103.5
11H	14	1515	91.6	101.1	9.5	9.64	101.5
12H	14	1610	101.1	110.6	9.5	9.76	102.7
13H	14	1700	110.6	120.1	9.5	9.14	96.2
14H	14	1800	120.1	129.6	9.5	9.66	101.7
15H	14	1855	129.6	139.1	9.5	9.99	105.2
16H	14	1955	139.1	148.6	9.5	9.61	101.2
17H	14	2250	148.6	158.1	9.5	10.02	105.5
Coring totals:					158.1	158.63	100.34%
181-1123B-							
1H	15	0130	0.0	3.4	3.4	3.36	98.8
2H	15	0220	3.4	12.9	9.5	9.45	99.5
3H	15	0315	12.9	22.4	9.5	9.84	103.6
4H	15	0415	22.4	31.9	9.5	9.8	103.2
5H	15	0535	31.9	41.4	9.5	9.77	102.8
6H	15	0630	41.4	50.9	9.5	9.78	102.9
7H	15	0750	50.9	60.4	9.5	10.12	106.5
8H	15	0845	60.4	69.9	9.5	9.79	103.1
9H	15	0945	69.9	79.4	9.5	9.76	102.7
10H	15	1045	79.4	88.9	9.5	9.79	103.1
11H	15	1155	88.9	98.4	9.5	9.91	104.3
12H	15	1255	98.4	107.9	9.5	9.76	102.7
13H	15	1350	107.9	117.4	9.5	9.88	104.0
14H	15	1445	117.4	126.9	9.5	9.58	100.8
15H	15	1540	126.9	136.4	9.5	9.91	104.3
16H	15	1855	136.4	145.9	9.5	9.46	99.6
17H	15	2040	145.9	155.4	9.5	9.78	102.9
18X	15	2145	155.4	162.7	7.3	8.39	114.9
19X	15	2225	162.7	172.3	9.6	9.59	99.9
20X	15	2330	172.3	181.9	9.6	9.65	100.5
21X	16	0735	181.9	191.6	9.7	9.47	97.6
22X	16	0840	191.6	201.2	9.6	9.87	102.8
23X	16	0955	201.2	210.8	9.6	7.76	80.8
24X	16	1110	210.8	220.4	9.6	9.75	101.6
25X	16	1220	220.4	230.0	9.6	9.7	101.0
26X	16	1330	230.0	239.6	9.6	4.18	43.5
Core	Date (August 1998)	Time	Top depth (mbsf)	Bottom depth (mbsf)	Length cored (m)	Length recovered (m)	Recovery (%)
27X	16	1440	239.6	249.2	9.6	9.82	102.3
28X	16	1545	249.2	258.8	9.6	9.59	99.9

Table 5

29X	16	1820	258.8	268.4	9.6	9.79	102.0
30X	16	1940	268.4	278.1	9.7	9.65	99.5
31X	16	2045	278.1	287.7	9.6	9.49	98.9
32X	16	2145	287.7	297.3	9.6	8.71	90.7
33X	16	2305	297.3	306.9	9.6	9.65	100.5
34X	17	0010	306.9	316.5	9.6	9.78	101.9
35X	17	0120	316.5	325.9	9.4	9.62	102.3
36X	17	0230	325.9	335.5	9.6	9.67	100.7
37X	17	0350	335.5	345.1	9.6	9.8	102.1
38X	17	0510	345.1	354.7	9.6	9.79	102.0
39X	17	0625	354.7	364.4	9.7	9.88	101.9
40X	17	0740	364.4	374.1	9.7	9.76	100.6
41X	17	1020	374.1	383.7	9.6	8.2	85.4
42X	17	1145	383.7	393.4	9.7	4.84	49.9
43X	17	1335	393.4	403.0	9.6	6.22	64.8
44X	17	1525	403.0	412.6	9.6	5.42	56.5
45X	17	1710	412.6	422.2	9.6	4.06	42.3
46X	17	1855	422.2	431.8	9.6	6.21	64.7
47X	17	2045	431.8	441.5	9.7	5.26	54.2
48X	17	2255	441.5	450.8	9.3	4.25	45.7
49X	18	0220	450.8	460.4	9.6	6.41	66.8
50X	18	0420	460.4	470.0	9.6	8.35	87.0
51X	18	0625	470.0	479.3	9.3	9.72	104.5
52X	18	0835	479.3	489.0	9.7	9.36	96.5
Coring totals:					489	451.4	92.31%
181-1123C-							
1H	19	1155	0.0	9.0	9.0	9.02	100.2
2H	19	1250	9.0	18.5	9.5	9.53	100.3
3H	19	1355	18.5	28.0	9.5	9.79	103.1
4H	19	1450	28.0	37.5	9.5	9.59	100.9
5H	19	1545	37.5	47.0	9.5	8.85	93.2
6H	19	1645	47.0	56.5	9.5	9.91	104.3
7H	19	1740	56.5	66.0	9.5	9.85	103.7
8H	19	1845	66.0	75.5	9.5	9.82	103.4
9H	19	1935	75.5	85.0	9.5	8.65	91.1
10H	19	2035	85.0	94.5	9.5	9.94	104.6
11H	19	2130	94.5	104.0	9.5	9.71	102.2
12H	19	2225	104.0	113.5	9.5	9.87	103.9
13H	19	2325	113.5	123.0	9.5	9.74	102.5
14H	20	0025	123.0	132.5	9.5	10.05	105.8
15H	20	0125	132.5	142.0	9.5	9.59	100.9
16H	20	0240	142.0	151.5	9.5	9.79	103.1
170	20	0630	151.5	230.0	0.0	0.00	N/A
17X	20	0740	230.0	239.6	9.6	6.39	66.6
Core	Date (August 1998)	Time	Top depth (mbsf)	Bottom depth (mbsf)	Length cored (m)	Length recovered (m)	Recovery (%)
180	20	1945	239.6	484.0	0.0	0.00	N/A
18X	20	2125	484.0	488.5	4.5	4.95	110.0
19X	20	2310	488.5	498.1	9.6	9.7	101.0
20X	21	0115	498.1	507.7	9.6	8.44	87.9
21X	21	0320	507.7	517.4	9.7	9.41	97.0
22X	21	0510	517.4	527.0	9.6	9.81	102.2
23X	21	0710	527.0	536.6	9.6	9.81	102.2
24X	21	0905	536.6	546.2	9.6	9.76	101.7

Table 5 (continued)

25X	21	1050	546.2	555.7	9.5	9.66	101.7
26X	21	1230	555.7	565.4	9.7	9.67	99.7
27X	21	1410	565.4	575.1	9.7	9.66	99.6
28X	21	1555	575.1	584.7	9.6	8.78	91.5
29X	21	1815	584.7	594.3	9.6	8.71	90.7
30X	21	2035	594.3	603.9	9.6	5.44	56.7
31X	21	2305	603.9	613.6	9.7	7.28	75.1
32X	21	0340	613.6	623.2	9.6	5.61	58.4
33X	22	0710	623.2	632.8	9.6	2.66	27.7
Coring totals:					309.9	289.44	93.40%

Table 5 (continued)

Core	Date (August 1998)	Time	Top depth (mbsf)	Bottom depth (mbsf)	Length cored (m)	Length recovered (m)	Recovery (%)
181-1124A-							
1H	26 Sept	0325	0.0	9.5	9.5	9.51	100.1
Coring totals:					9.5	9.51	100.11%
181-1124B-							
1H	26 Sept	0530	0.0	5.4	5.4	5.41	100.2
2H	26 Sept	1740	5.4	9.9	4.5	4.48	99.6
Coring totals:					9.9	9.89	99.90%
181-1124C-							
10	27 Sept	0325	0.0	8.0	0.0	0.0	N/A
1X	27 Sept	0330	8.0	17.6	9.6	1.51	15.7
2X	27 Sept	0430	17.6	27.2	9.6	7.68	80.0
3H	27 Sept	0540	27.2	36.7	9.5	10	105.3
4H	27 Sept	0645	36.7	46.2	9.5	9.74	102.5
5H	27 Sept	0810	46.2	55.7	9.5	9.99	105.2
6H	27 Sept	0915	55.7	65.2	9.5	9.58	100.8
7H	27 Sept	1040	65.2	74.7	9.5	9.99	105.2
8H	27 Sept	1155	74.7	84.2	9.5	9.75	102.6
9H	27 Sept	1315	84.2	93.7	9.5	10.04	105.7
10H	27 Sept	1420	93.7	103.2	9.5	9.12	96.0
11H	27 Sept	1535	103.2	112.7	9.5	9.85	103.7
12H	27 Sept	1640	112.7	122.2	9.5	9.15	96.3
13H	27 Sept	1745	122.2	131.7	9.5	9.91	104.3
14H	27 Sept	1850	131.7	141.2	9.5	9.51	100.1
15H	27 Sept	1955	141.2	150.7	9.5	9.45	99.5
16H	27 Sept	2100	150.7	159.2	8.5	8.72	102.6
17X	27 Sept	2220	159.2	168.8	9.6	9.6	100.0
18X	27 Sept	2325	168.8	178.4	9.6	9.58	99.8
19X	28 Sept	0040	178.4	188.0	9.6	9.87	102.8
20X	28 Sept	0145	188.0	197.7	9.7	9.67	99.7
21X	28 Sept	0250	197.7	207.3	9.6	9.76	101.7
22X	28 Sept	0400	207.3	216.9	9.6	9.76	101.7
23X	28 Sept	0505	216.9	226.5	9.6	9.79	102.0
24X	28 Sept	0615	226.5	236.2	9.7	9.66	99.6
25X	28 Sept	0720	236.2	245.8	9.6	9.78	101.9
26X	28 Sept	0830	245.8	255.4	9.6	9.7	101.0
27X	28 Sept	0935	255.4	265.1	9.7	9.65	99.5
28X	28 Sept	1040	265.1	274.7	9.6	9.62	100.2
29X	28 Sept	1150	274.7	284.3	9.6	1.81	18.9
30X	28 Sept	1300	284.3	294.0	9.7	0.15	1.5
31X	28 Sept	1410	294.0	303.6	9.6	9.18	95.6
32X	28 Sept	1520	303.6	313.3	9.7	9.45	97.4
33X	28 Sept	1625	313.3	322.9	9.6	9.48	98.8
34X	28 Sept	1740	322.9	332.6	9.7	9.69	99.9
35X	28 Sept	1850	332.6	342.2	9.6	9.84	102.5
36X	28 Sept	2000	342.2	351.9	9.7	9.61	99.1
Core	Date (August 1998)	Time	Top depth (mbsf)	Bottom depth (mbsf)	Length cored (m)	Length recovered (m)	Recovery (%)
37X	28 Sept	2110	351.9	361.5	9.6	9.74	101.5
38X	28 Sept	2225	361.5	371.2	9.7	9.66	99.6

Table 6

39X	28 Sept	2330	371.2	380.8	9.6	9.85	102.6
40X	29 Sept	0040	380.8	390.4	9.6	9.37	97.6
41X	29 Sept	0200	390.4	400.1	9.7	9.57	98.7
42X	29 Sept	0315	400.1	409.7	9.6	9.74	101.5
43X	29 Sept	0450	409.7	419.3	9.6	9.05	94.3
44X	29 Sept	0635	419.3	429.0	9.7	9.77	100.7
45X	29 Sept	0820	429.0	438.7	9.7	9.72	100.2
46X	29 Sept	1005	438.7	448.3	9.6	7.18	74.8
47X	29 Sept	1145	448.3	457.9	9.6	9.26	96.5
48X	29 Sept	1350	457.9	467.4	9.5	5.52	58.1
49X	29 Sept	1620	467.4	473.1	5.7	5.72	100.4
Coring totals:					465.1	433.79	93.27%
181-1124D-							
10	30 Sept	2050	0.0	22.6	0.0	0.0	N/A
1H	30 Sept	2150	22.6	32.1	9.5	9.56	100.6
2H	30 Sept	2255	32.1	41.6	9.5	7.75	81.6
3H	30 Sept	2355	41.6	51.1	9.5	8.97	94.4
4H	1 Oct	0100	51.1	60.6	9.5	8.52	89.7
5H	1 Oct	0205	60.6	70.1	9.5	9.77	102.8
6H	1 Oct	0315	70.1	79.6	9.5	9.3	97.9
7H	1 Oct	0420	79.6	89.1	9.5	9.95	104.7
8H	1 Oct	0525	89.1	98.6	9.5	9.01	94.8
9H	1 Oct	0630	98.6	108.1	9.5	9.88	104.0
10H	1 Oct	0730	108.1	117.6	9.5	9.72	102.3
11H	1 Oct	0835	117.6	127.1	9.5	9.89	104.1
12H	1 Oct	0940	127.1	136.6	9.5	9.73	102.4
13H	1 Oct	1040	136.6	146.1	9.5	10.04	105.7
14H	1 Oct	1155	146.1	155.6	9.5	9.75	102.6
Coring totals:					133	131.84	99.13%

Table 6 (continued)

Core	Date (August 1998)	Time	Top depth (mbsf)	Bottom depth (mbsf)	Length cored (m)	Length recovered (m)	Recovery (%)
181-1125A-							
1H	3	0405	0.0	4.3	4.3	4.31	100.2
2H	3	0445	4.3	13.8	9.5	9.17	96.5
3H	3	0515	13.8	23.3	9.5	9.9	104.2
4H	3	0550	23.3	32.8	9.5	9.63	101.4
5H	3	0640	32.8	42.3	9.5	9.88	104.0
6H	3	0715	42.3	51.8	9.5	9.42	99.2
7H	3	0805	51.8	61.3	9.5	10.07	106.0
8H	3	0840	61.3	70.8	9.5	9.18	96.6
9H	3	0930	70.8	80.3	9.5	10.06	105.9
10H	3	1015	80.3	89.8	9.5	9.71	102.2
11H	3	1055	89.8	99.3	9.5	10.12	106.5
12H	3	1130	99.3	108.8	9.5	9.88	104.0
13H	3	1215	108.8	118.3	9.5	10.09	106.2
14H	3	1250	118.3	127.8	9.5	9.91	104.3
15H	3	1335	127.8	137.3	9.5	10.0	105.3
16H	3	1415	137.3	146.8	9.5	9.45	99.5
17H	3	1455	146.8	156.3	9.5	9.99	105.2
18H	3	1535	156.3	165.8	9.5	9.82	103.4
19H	3	1620	165.8	175.3	9.5	9.92	104.4
20H	3	1650	175.3	184.8	9.5	9.72	102.3
21H	3	1730	184.8	194.3	9.5	9.62	101.3
22H	3	1820	194.3	203.5	9.2	9.22	100.2
Coring totals:					203.5	209.07	102.74%
181-1125B-							
1H	3	2145	0.0	8.3	8.3	8.30	100.00
2H	3	2210	8.3	17.8	9.5	9.65	101.60
3H	3	2245	17.8	27.3	9.5	9.51	100.10
4H	3	2320	27.3	36.8	9.5	9.38	98.70
5H	3	2355	36.8	46.3	9.5	9.86	103.80
6H	4	0035	46.3	55.8	9.5	9.73	102.40
7H	4	0110	55.8	65.3	9.5	9.95	104.70
8H	4	0145	65.3	74.8	9.5	9.12	96.00
9H	4	0230	74.8	84.3	9.5	9.85	103.70
10H	4	0305	84.3	93.8	9.5	8.50	89.50
11H	4	0345	93.8	103.3	9.5	9.93	104.50
12H	4	0420	103.3	112.8	9.5	9.65	101.60
13H	4	0455	112.8	122.3	9.5	9.90	104.20
14H	4	0535	122.3	131.8	9.5	9.94	104.60
15H	4	0620	131.8	141.3	9.5	9.92	104.40
16H	4	0755	141.3	150.8	9.5	9.97	104.90
17H	4	0840	150.8	160.3	9.5	10.06	105.90
18H	4	0920	160.3	169.8	9.5	9.39	98.80
19H	4	1005	169.8	179.3	9.5	9.98	105.10
20H	4	1100	179.3	188.8	9.5	9.03	95.10
21X	4	1235	188.8	197.2	8.4	9.74	116.00
Core	Date (August 1998)	Time	Top depth (mbsf)	Bottom depth (mbsf)	Length cored (m)	Length recovered (m)	Recovery (%)
22X	4	1315	197.2	206.8	9.6	9.81	102.20
23X	4	1400	206.8	216.4	9.6	9.47	98.60

24X	4	1435	216.4	226.0	9.6	7.50	78.10
25X	4	1520	226.0	235.6	9.6	8.82	91.90
26X	4	1600	235.6	245.2	9.6	9.72	101.30
27X	4	1640	245.2	254.8	9.6	8.75	91.10
28X	4	1725	254.8	264.4	9.6	9.74	101.50
29X	4	1810	264.4	274.1	9.7	9.64	99.40
30X	4	1900	274.1	283.7	9.6	8.23	85.70
31X	4	1945	283.7	293.3	9.6	4.68	48.80
32X	4	2030	293.3	303.0	9.7	9.82	101.20
33X	4	2110	303.0	312.6	9.6	9.79	102.00
34X	4	2205	312.6	321.9	9.3	8.44	90.80
35X	4	2255	321.9	331.5	9.6	9.89	103.00
36X	4	2340	331.5	341.1	9.6	1.28	13.30
37X	5	0055	341.1	350.7	9.6	7.31	76.10
38X	5	0150	350.7	360.4	9.7	9.77	100.70
39X	5	0235	360.4	370.1	9.7	9.69	99.90
40X	5	0320	370.1	379.7	9.6	9.02	94.00
41X	5	0405	379.7	389.4	9.7	9.76	100.60
42X	5	0450	389.4	399.0	9.6	6.67	69.50
43X	5	0535	399.0	408.6	9.6	7.83	81.60
44X	5	0620	408.6	418.3	9.7	3.53	36.40
45X	5	0735	418.3	427.9	9.6	9.61	100.10
46X	5	0830	427.9	437.5	9.6	9.82	102.30
47X	5	0915	437.5	446.8	9.3	9.63	103.50
48X	5	1030	446.8	456.4	9.6	4.07	42.40
49X	5	1145	456.4	466.0	9.6	9.60	100.00
50X	5	1255	466.0	475.2	9.2	9.15	99.50
51X	5	1405	475.2	484.9	9.7	9.80	101.00
52X	5	1515	484.9	494.5	9.6	9.69	100.90
53X	5	1625	494.5	504.1	9.6	9.13	95.10
54X	5	1755	504.1	513.8	9.7	8.73	90.00
55X	5	2005	513.8	523.4	9.6	7.28	75.80
56X	5	2230	523.4	533.0	9.6	9.59	99.90
57X	6	0030	533.0	542.6	9.6	9.32	97.10
58X	6	0315	542.6	552.1	9.5	5.72	60.20
Coring totals:					552.1	511.66	92.68%

Table 7 (continued)

FIGURE CAPTIONS

Figure F1. A. The bathymetry of the eastern New Zealand region, with the positions of major fronts at the ocean surface (summer temperatures) and the Antarctic Circumpolar (ACC) and Pacific Deep Western Boundary (DWBC) currents indicated. For other abbreviations, see Table T3. **B.** Meridional salinity cross section through the Pacific Ocean (data after Levitus, 1976), with location of the Leg 181 sites projected onto the plane of section. For abbreviations, see Table T3.

Figure F2. Bathymetric map of the eastern New Zealand region, southwest Pacific Ocean, showing the location of previous DSDP sites, and the location of all sites drilled during Leg 181.

Figure F3. Plate tectonic reconstructions of the southern hemisphere continents in polar projection for 50, 30 and 20 Ma (after Lawver et al., 1992), with position of inferred currents indicated with arrows.

Figure F4. Geologic cross sections **A.** through the eastern South Island and adjacent shelf, and **B.** from the shelf-edge across the Campbell Plateau to the southwest Pacific abyssal plain.

Figure F5. West to east cross section through the major water masses of the southwest Pacific Ocean at ~45_S, with position of ODP Leg 181 sites projected on to the plane of section. For abbreviations, see Table T3.

Figure F6. The Eastern New Zealand Oceanic Sedimentary System (ENZOSS), showing the location of the main areas of current scour, sediment supply, and drift deposition related to the ACC-DWBC (after Carter et al., 1997).

Figure F7. Summary log for Site 1119.

Figure F8. Summary log for Site 1120.

Figure F9. Summary log for Site 1121.

Figure F10. Summary log for Site 1122.

Figure F11. Summary log for Site 1123.

Figure F12. Summary log for Site 1124.

Figure F13. Summary log for Site 1125.

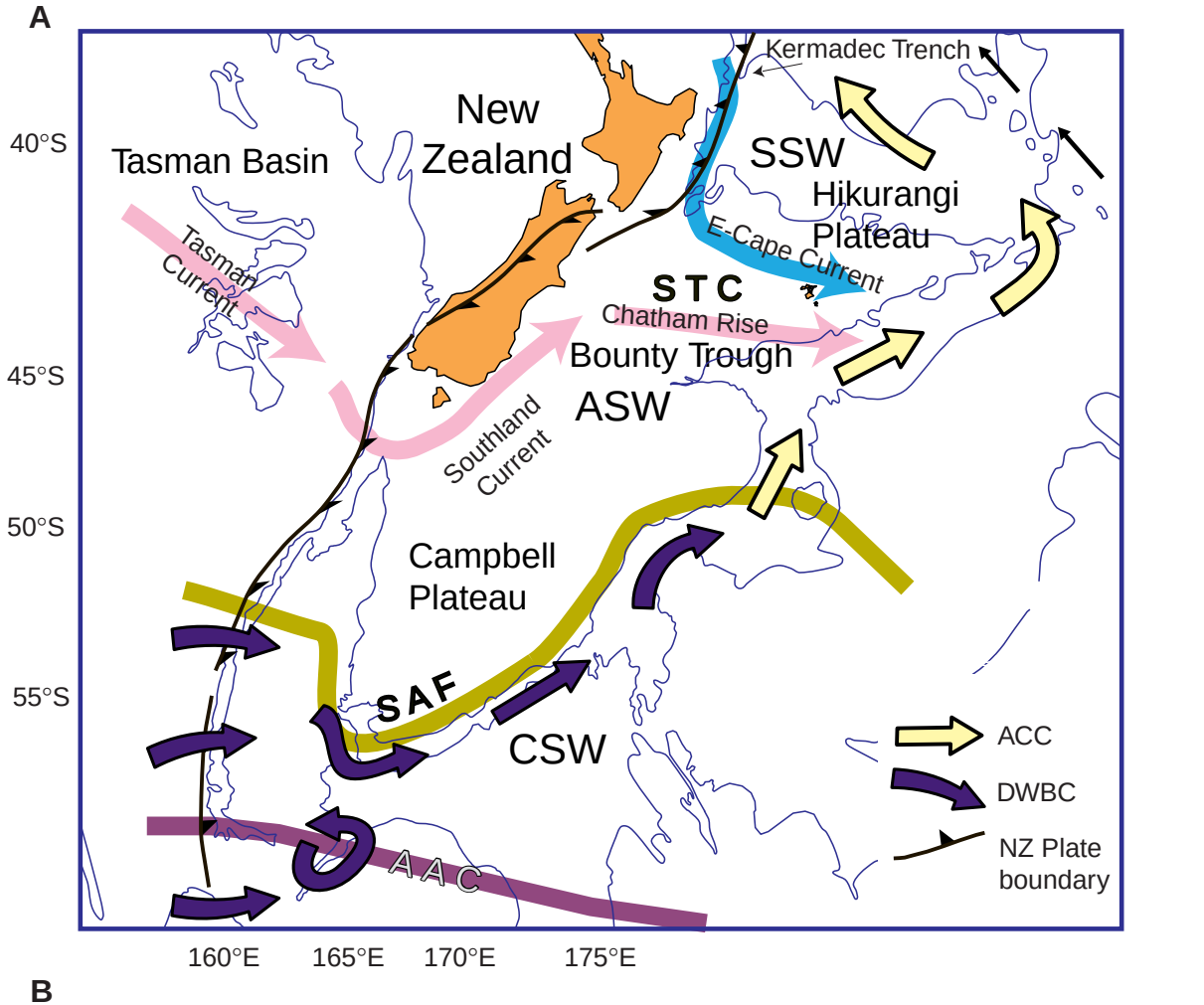
A
40°S
45°S
50°S
55°S
160°E
165°E
170°E
175°E
Tasman Basin
New Zealand
Kermadec Trench
SSW
Hikurangi Plateau
E-Cape Current
Tasman Current
STC
Chatham Rise
Bounty Trough
ASW
Southland Current
Campbell Plateau
SAF
CSW
AAC
ACC
DWBC
NZ Plate boundary

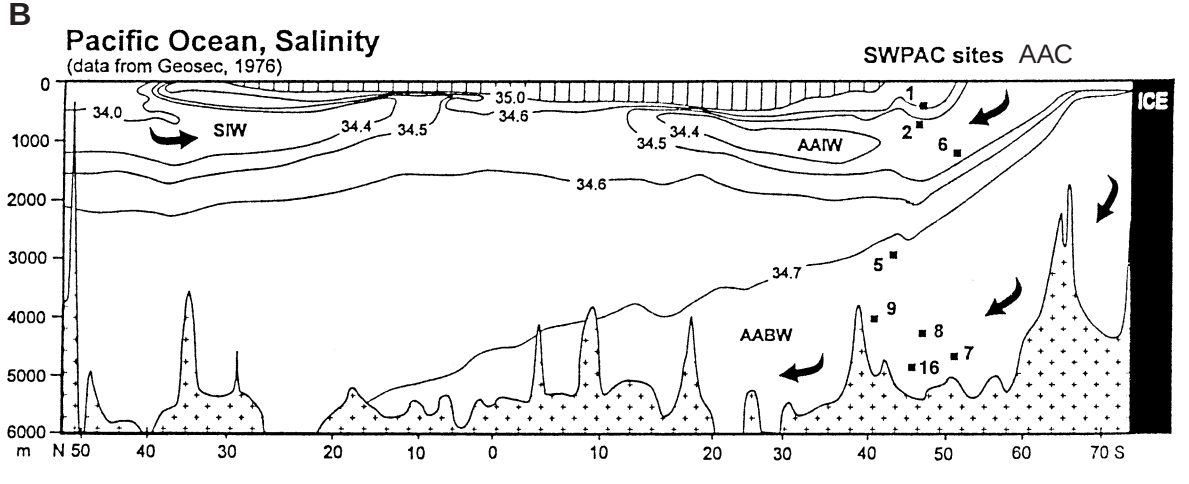
B
Pacific Ocean, Salinity
(data from Geosec, 1976)
SWPAC sites AAC
ICE
SIW
AAIW
AABW
34.0
34.4
34.5
35.0
34.6
34.7
0
1000
2000
3000
4000
5000
6000
m
N 50
40
30
20
10
0
10
20
30
40
50
60
70 S

Figure 1

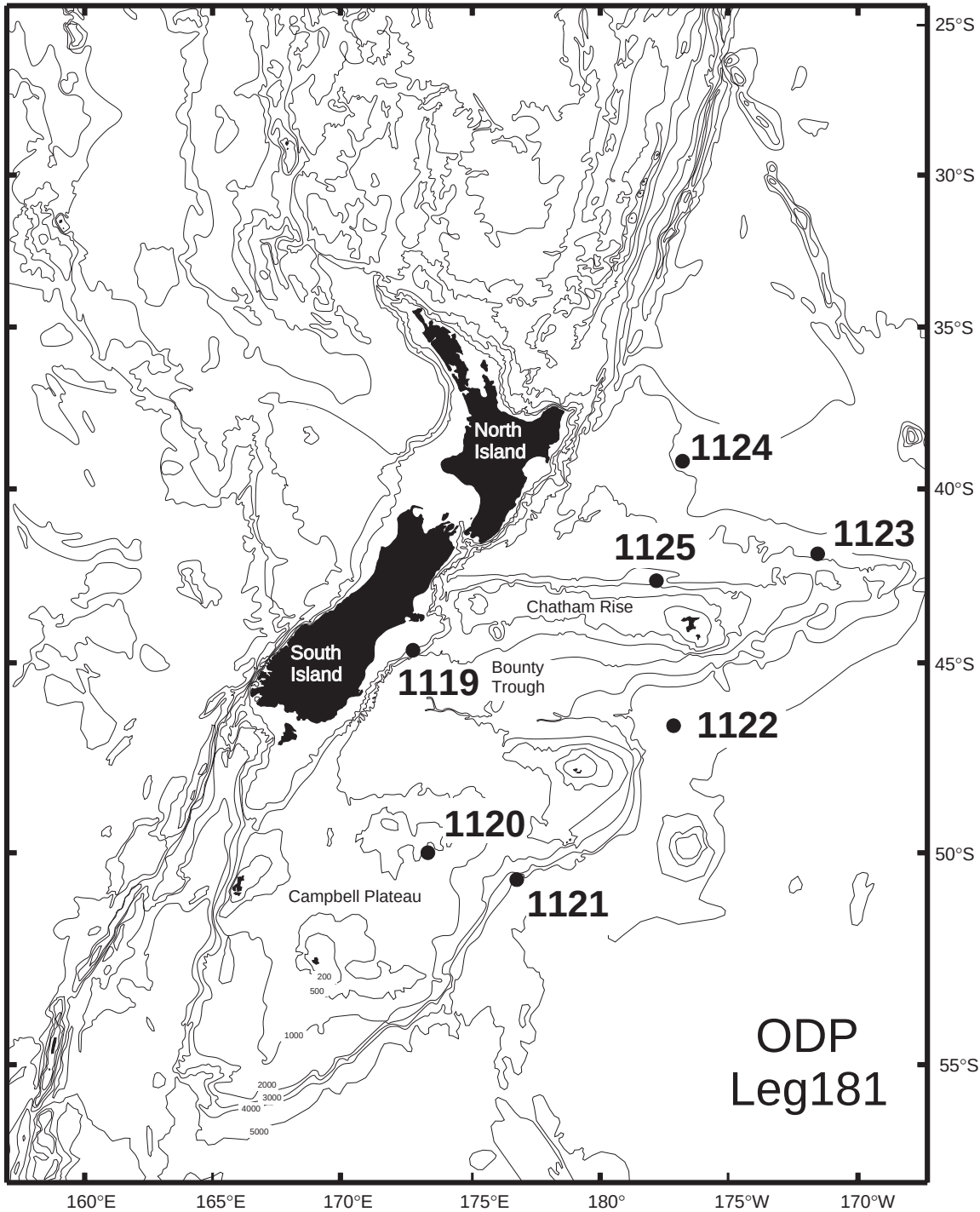
25°S
30°S
35°S
40°S
45°S
50°S
55°S
160°E
165°E
170°E
175°E
180°
175°W
170°W
North Island
South Island
1124
1123
1125
Chatham Rise
1119
Bounty Trough
1122
1120
1121
Campbell Plateau
200
500
1000
2000
3000
4000
5000
ODP Leg181

Figure 2

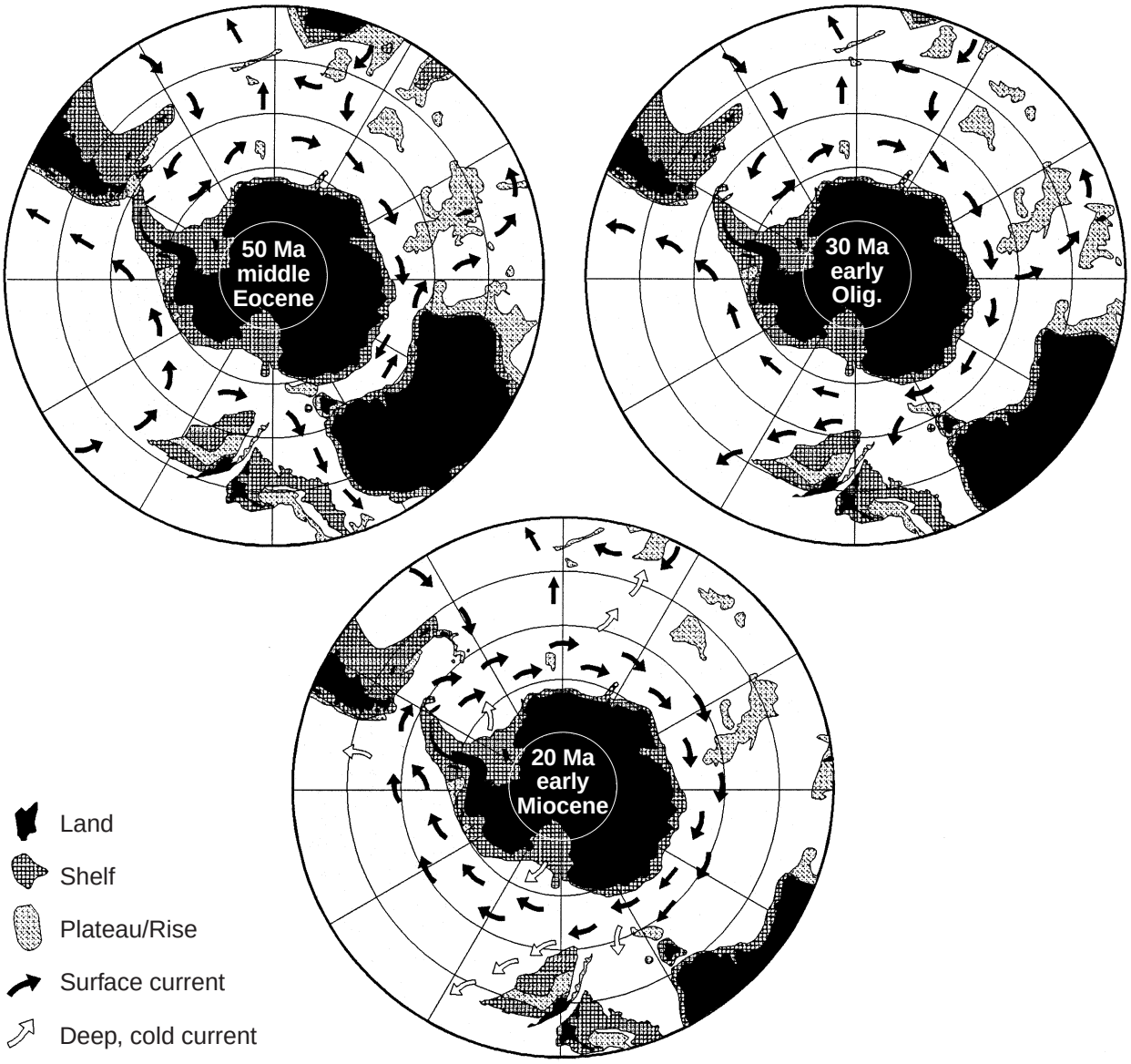
50 Ma
middle
Eocene
30 Ma
early
Olig.
20 Ma
early
Miocene
Land
Shelf
Plateau/Rise
Surface current
Deep, cold current

Figure 3

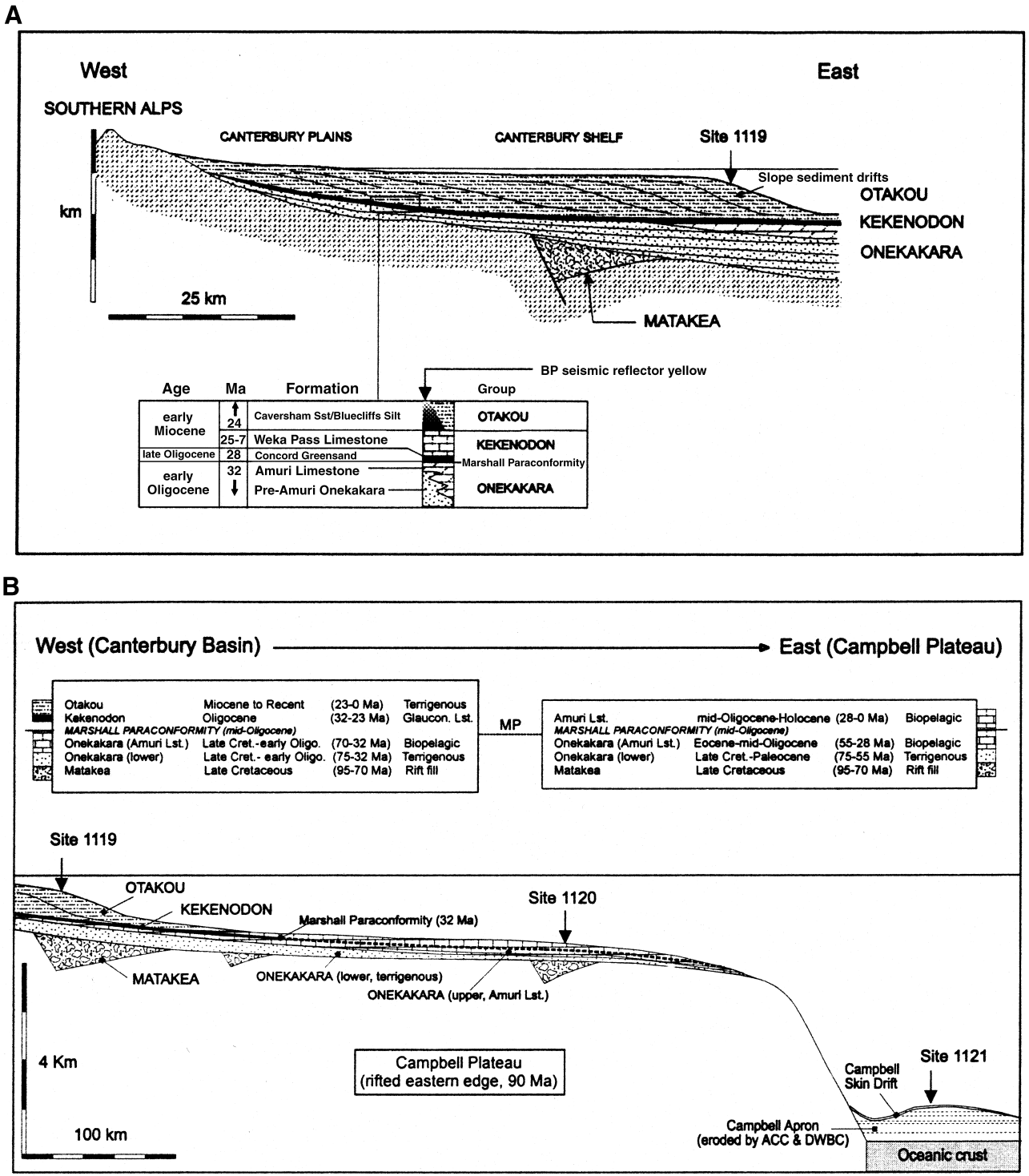
A
West
East
SOUTHERN ALPS
CANTERBURY PLAINS
CANTERBURY SHELF
Site 1119
Slope sediment drifts
OTAKOU
KEKENODON
ONEKAKARA
km
25 km
MATAKEA
BP seismic reflector yellow
Age
Ma
Formation
Group
early Miocene
24
Caversham Sst/Bluecliffs Silt
OTAKOU
25-7
Weka Pass Limestone
KEKENODON
late Oligocene
28
Concord Greensand
Marshall Paraconformity
early Oligocene
32
Amuri Limestone
Pre-Amuri Onekakara
ONEKAKARA
B
West (Canterbury Basin)
East (Campbell Plateau)
Otakou
Miocene to Recent
(23-0 Ma)
Terrigenous
Kekenodon
Oligocene
(32-23 Ma)
Glaucon. Lst.
MARSHALL PARACONFORMITY (mid-Oligocene)
Onekakara (Amuri Lst.)
Late Cret.-early Oligo.
(70-32 Ma)
Biopelagic
Onekakara (lower)
Late Cret.- early Oligo.
(75-32 Ma)
Terrigenous
Matakea
Late Cretaceous
(95-70 Ma)
Rift fill
MP
Amuri Lst.
mid-Oligocene-Holocene
(28-0 Ma)
Biopelagic
MARSHALL PARACONFORMITY (mid-Oligocene)
Onekakara (Amuri Lst.)
Eocene-mid-Oligocene
(55-28 Ma)
Biopelagic
Onekakara (lower)
Late Cret.-Paleocene
(75-55 Ma)
Terrigenous
Matakea
Late Cretaceous
(95-70 Ma)
Rift fill
Site 1119
OTAKOU
KEKENODON
Marshall Paraconformity (32 Ma)
Site 1120
MATAKEA
ONEKAKARA (lower, terrigenous)
ONEKAKARA (upper, Amuri Lst.)
4 Km
100 km
Campbell Plateau
(rifted eastern edge, 90 Ma)
Site 1121
Campbell
Skin Drift
Campbell Apron
(eroded by ACC & DWBC)
Oceanic crust

Figure 4

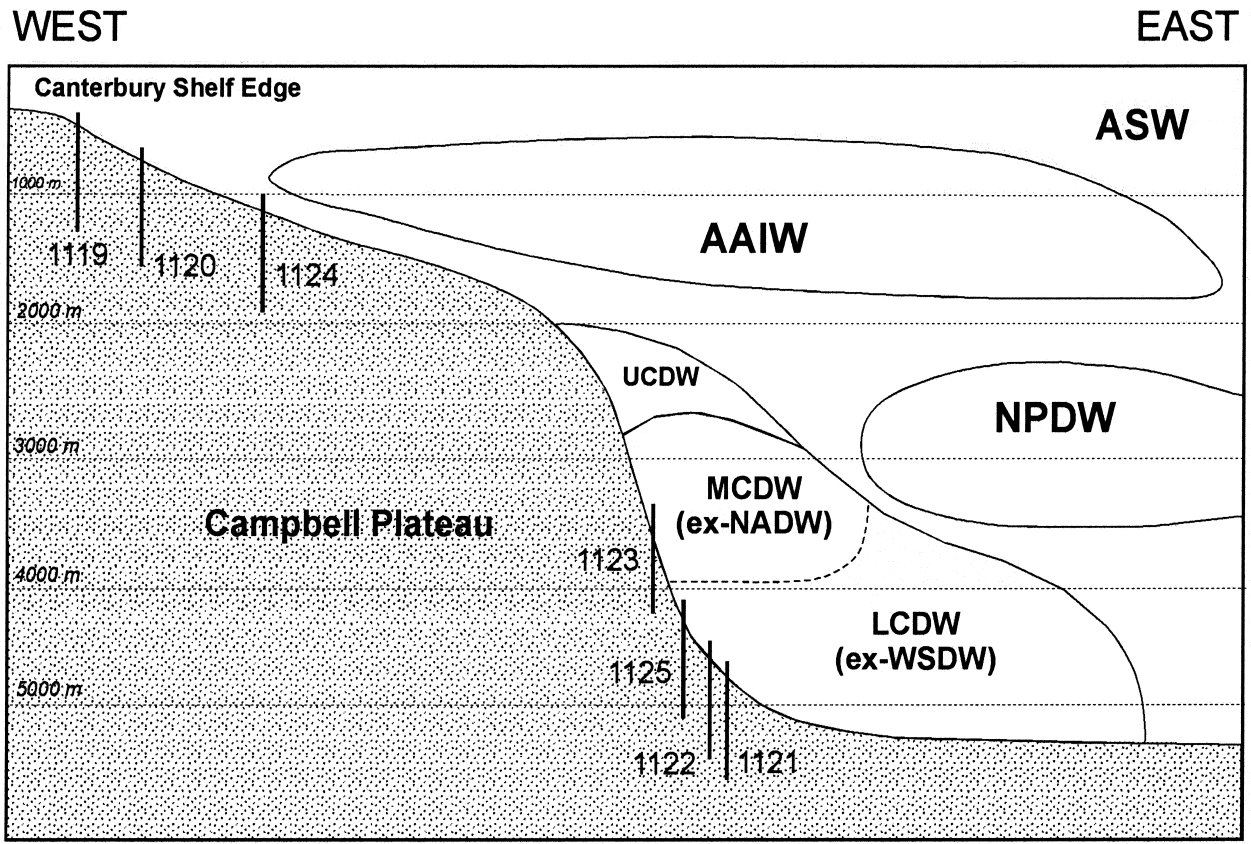
WEST
EAST
Canterbury Shelf Edge
ASW
AAIW
1000 m
2000 m
3000 m
4000 m
5000 m
1119
1120
1124
UCDW
NPDW
MCDW
(ex-NADW)
Campbell Plateau
1123
LCDW
(ex-WSDW)
1125
1122
1121

Figure 5

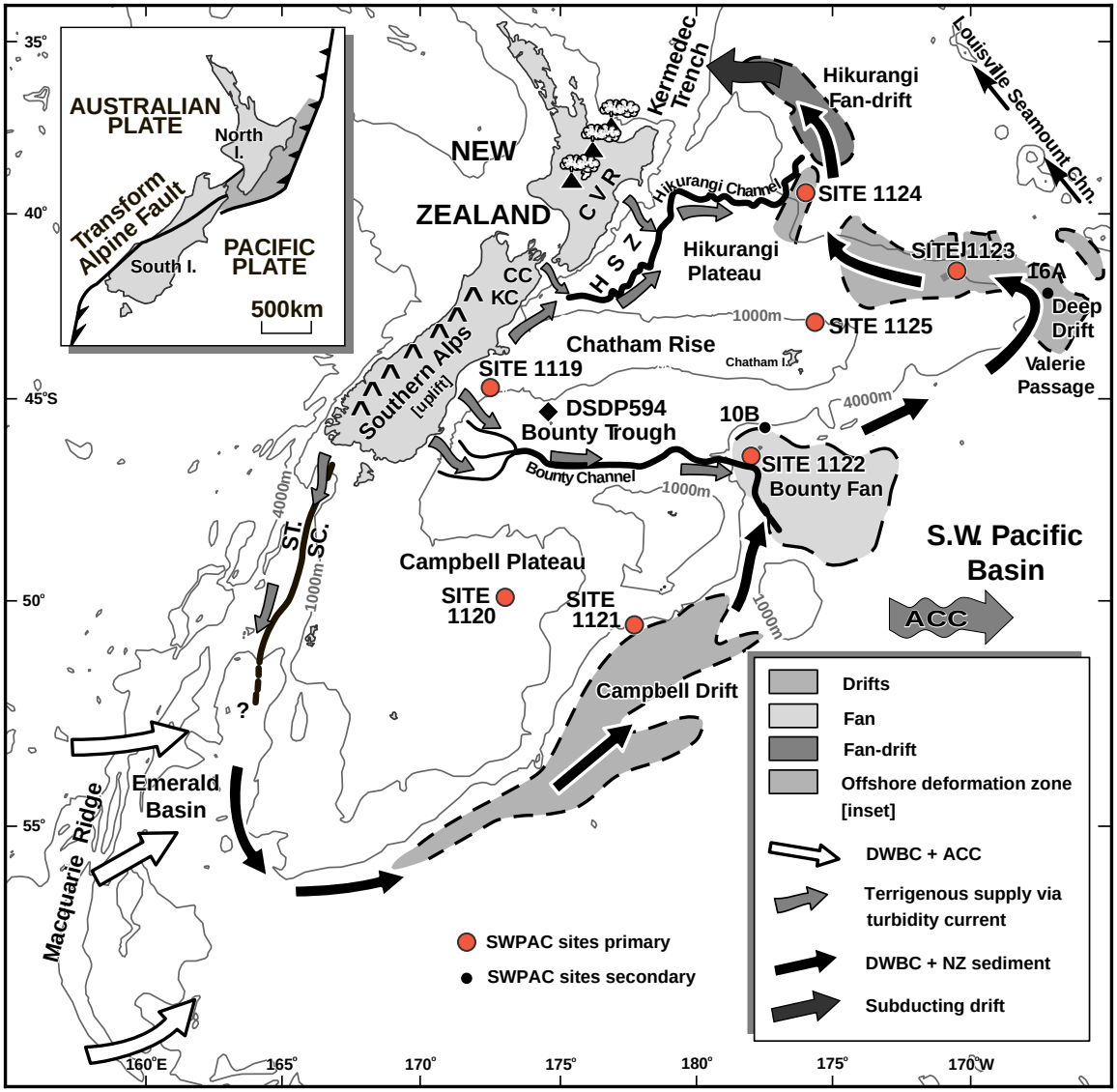
AUSTRALIAN PLATE
North I.
Transform Alpine Fault
South I.
PACIFIC PLATE
500km
NEW ZEALAND
Kermedec Trench
Louisville Seamount Chn.
Hikurangi Fan-drift
SITE 1124
Hikurangi Channel
CVR
HSZ
Hikurangi Plateau
SITE 1123
16A
Deep Drift
Valerie Passage
CC
KC
1000m
SITE 1125
Chatham Rise
Chatham I.
SITE 1119
Southern Alps
[uplift]
DSDP594
Bounty Trough
10B
4000m
Bounty Channel
SITE 1122
Bounty Fan
S.W. Pacific Basin
ACC
ST.
SC.
Campbell Plateau
SITE 1120
SITE 1121
Campbell Drift
Emerald Basin
Macquarie Ridge
Drifts
Fan
Fan-drift
Offshore deformation zone [inset]
DWBC + ACC
Terrigenous supply via turbidity current
DWBC + NZ sediment
Subducting drift
SWPAC sites primary
SWPAC sites secondary
35°
40°
45°S
50°
55°
160°E
165°
170°
175°
180°
175°
170°W

Figure 6

Leg: 181 Site: 1119

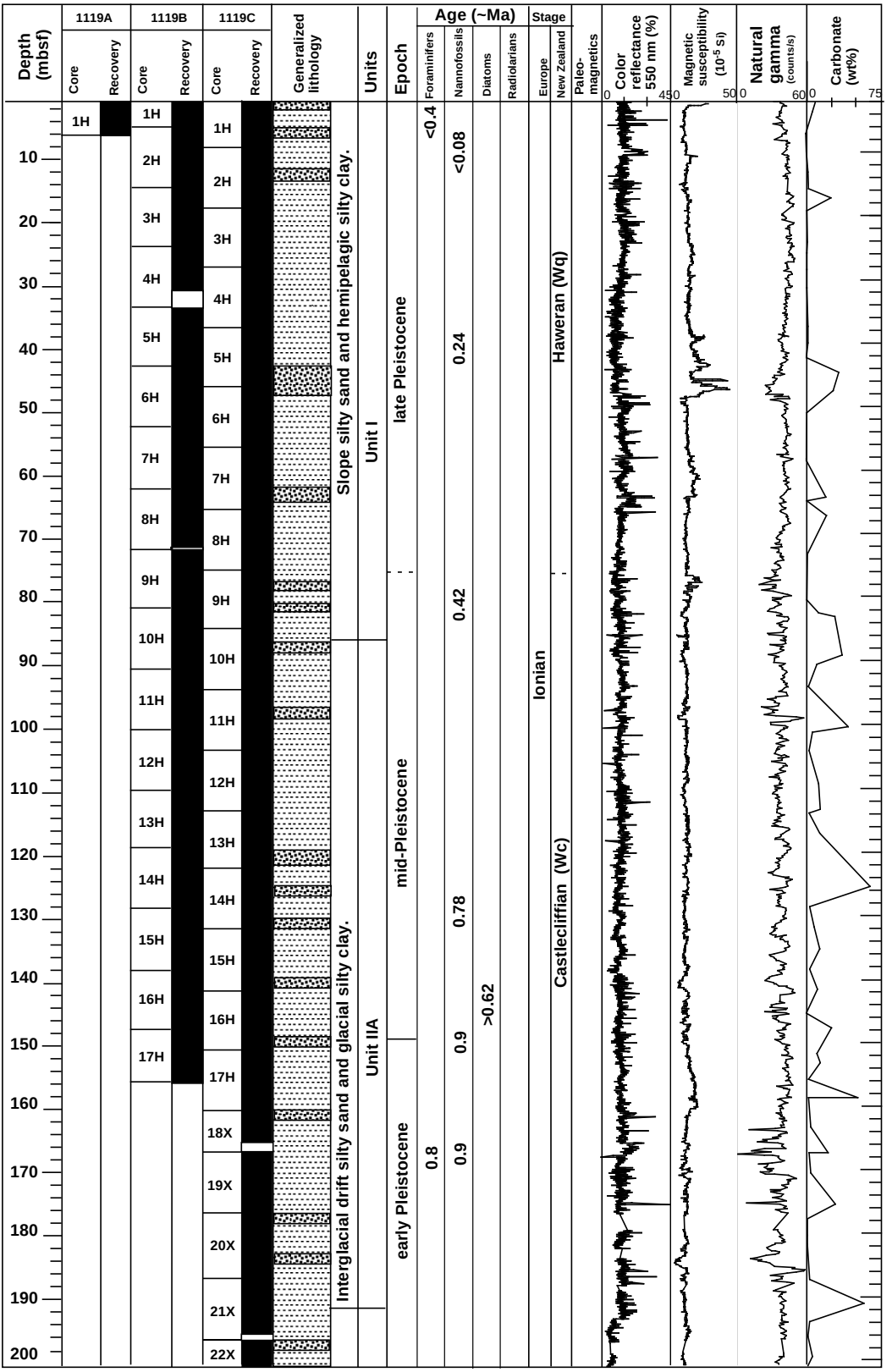

Figure 7

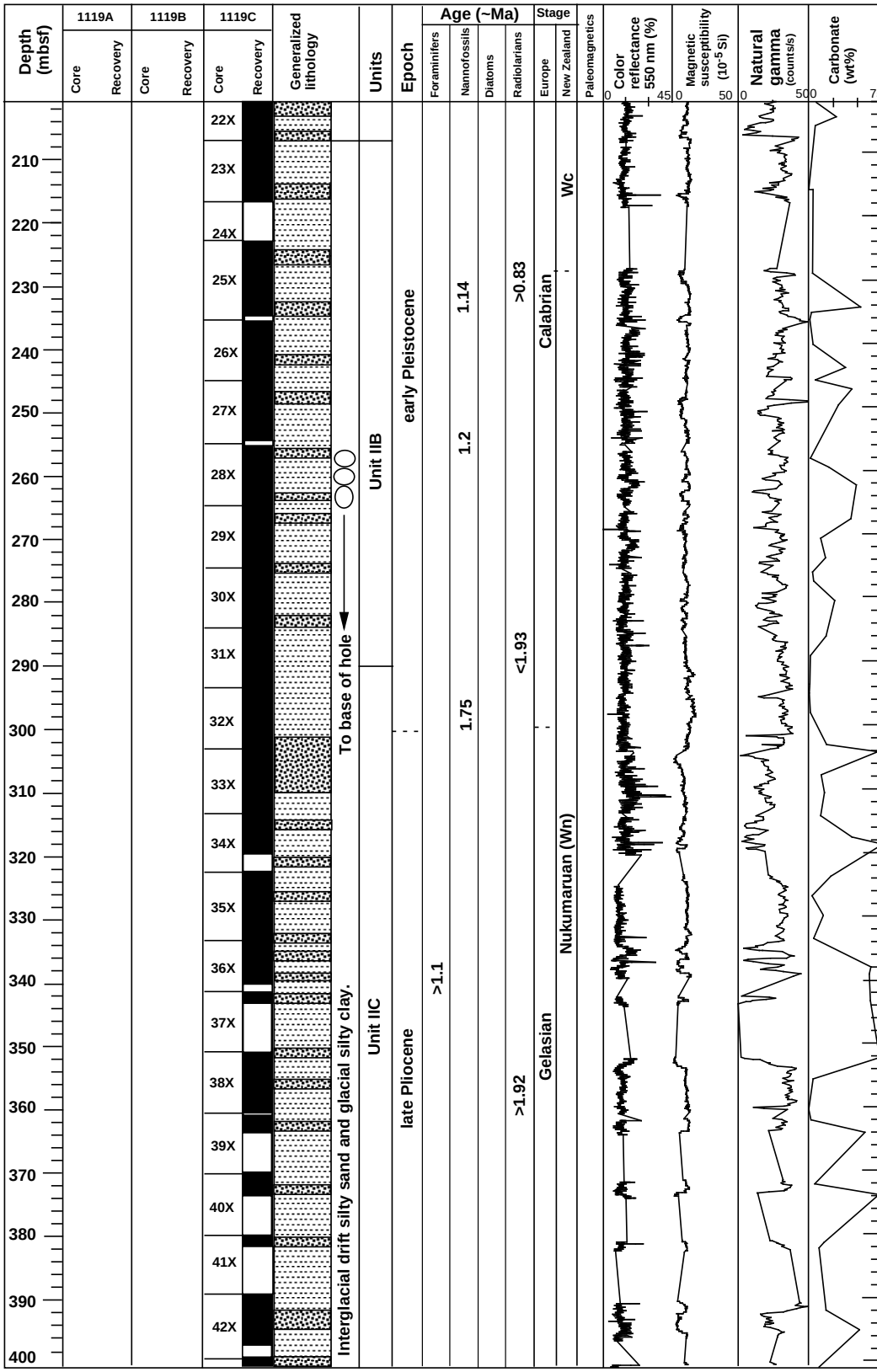

Figure 7 (continued)

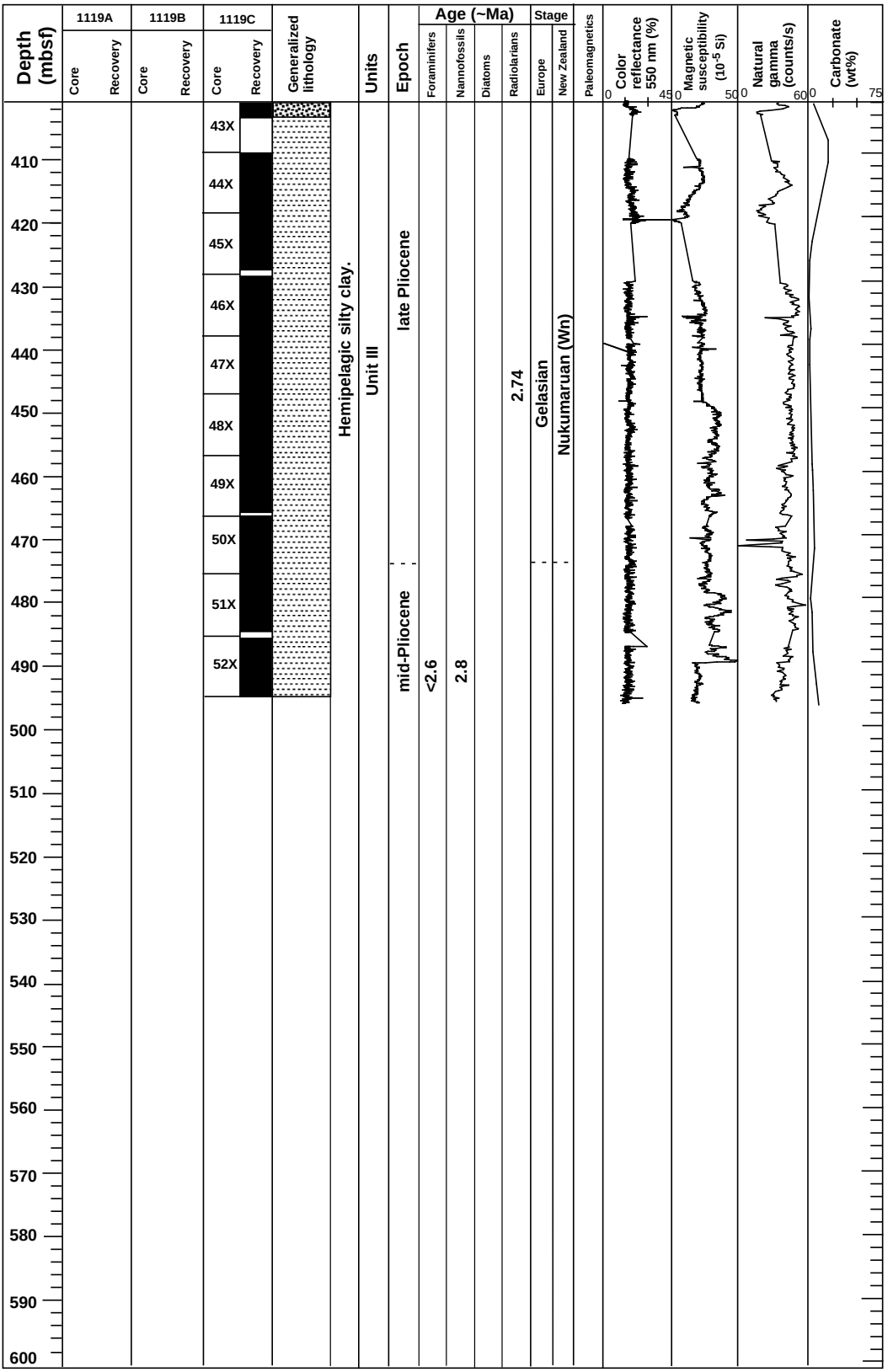

Figure 7 (continued)

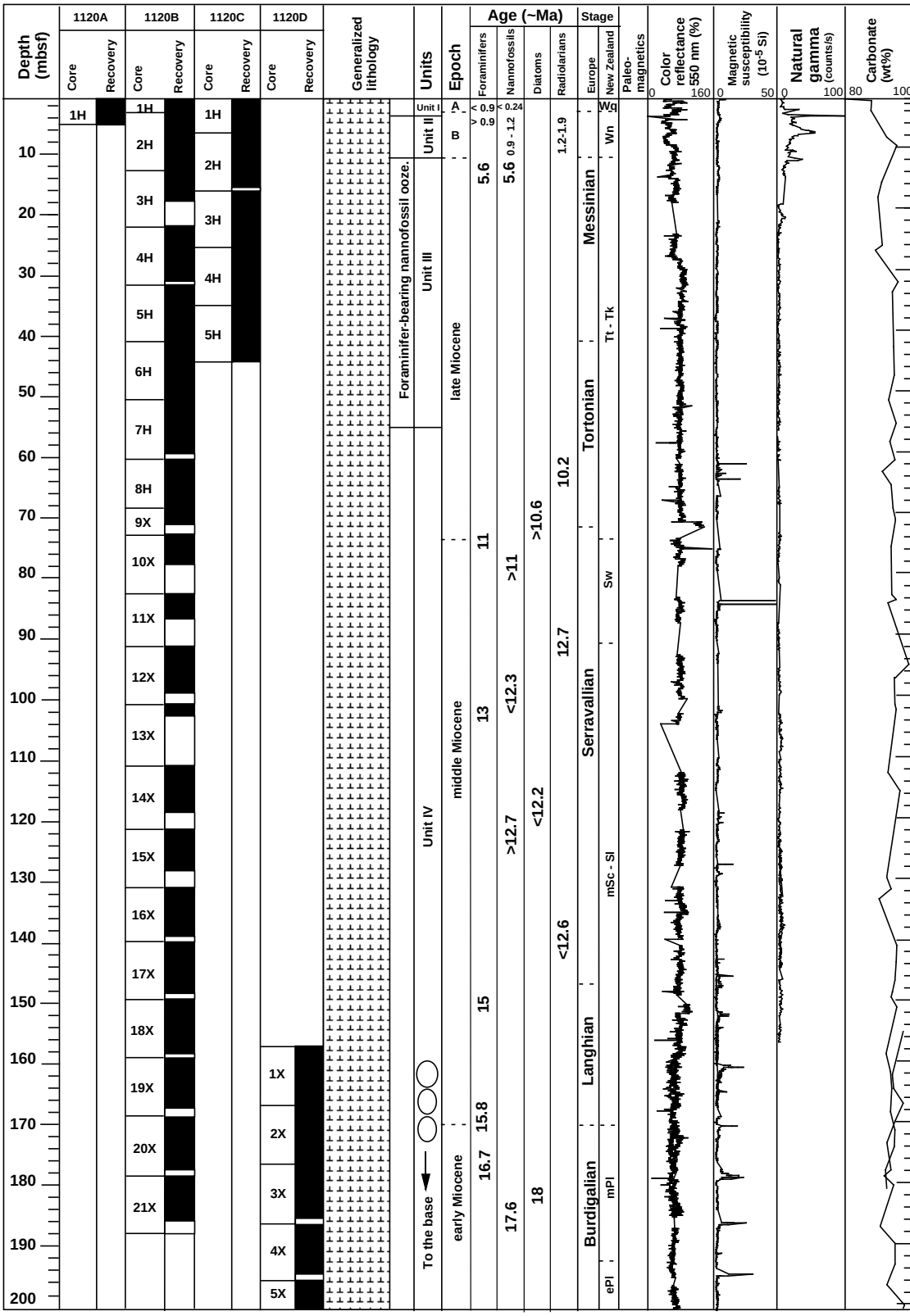
Leg: 181 Site: 1120
A= Latest Pleistocene
B= Early Pleistocene
Depth (mbsf)
1120A
1120B
1120C
1120D
Core
Recovery
Generalized lithology
Units
Unit I
Unit II
Unit III
Unit IV
Foraminifer-bearing nannofossil ooze.
To the base
Epoch
early Miocene
middle Miocene
late Miocene
Age (~Ma)
Foraminifers
Nannofossils
Diatoms
Radiolarians
Stage
Europe
New Zealand
Paleo-magnetics
Burdigalian
Langhian
Serravallian
Tortonian
Messinian
Color reflectance 550 nm (%)
Magnetic susceptibility (10-5 SI)
Natural gamma (counts/s)
Carbonate (wt%)

Figure 8

Figure 8 (continued)

Leg: 181 Site: 1121

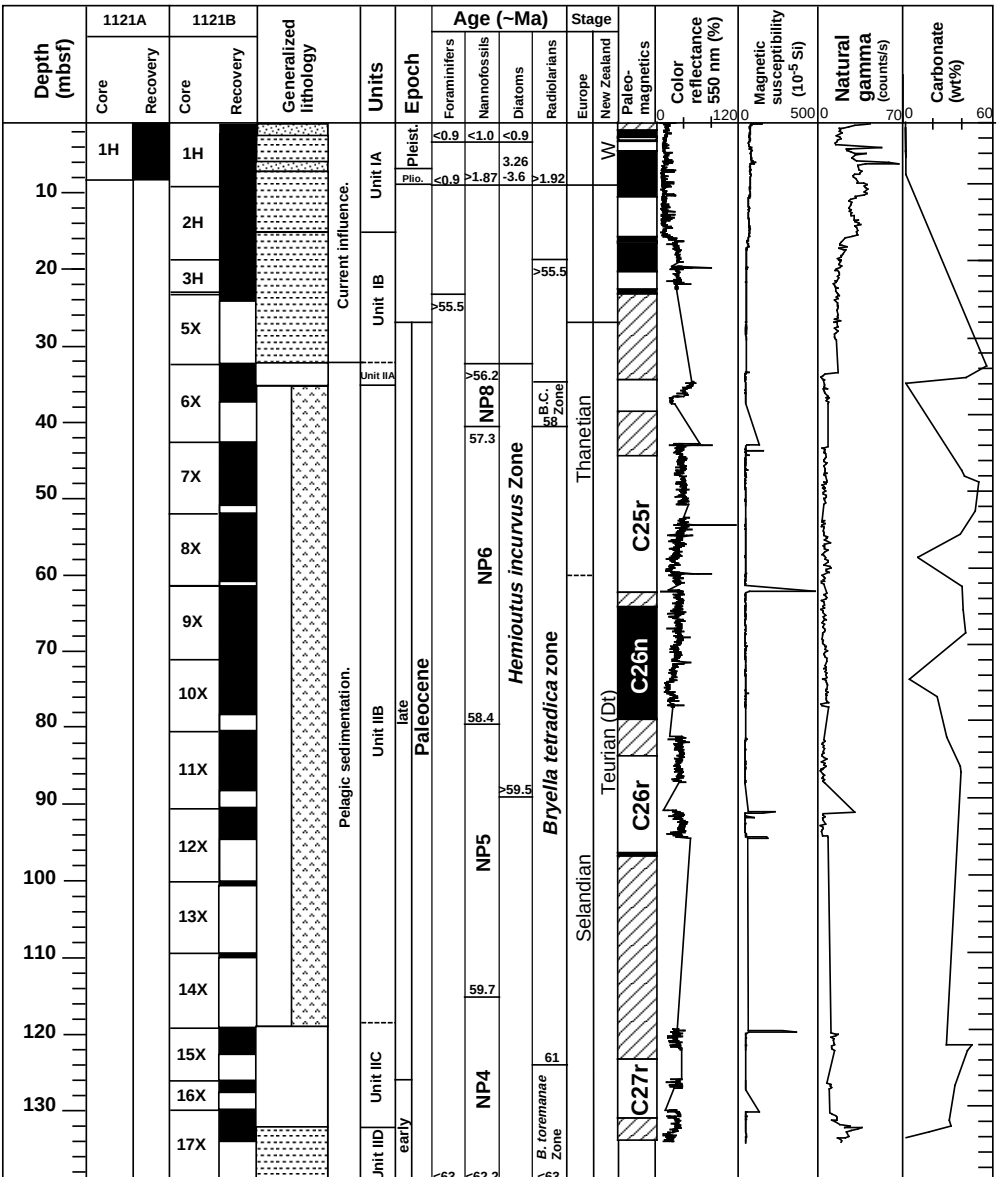

Figure 9

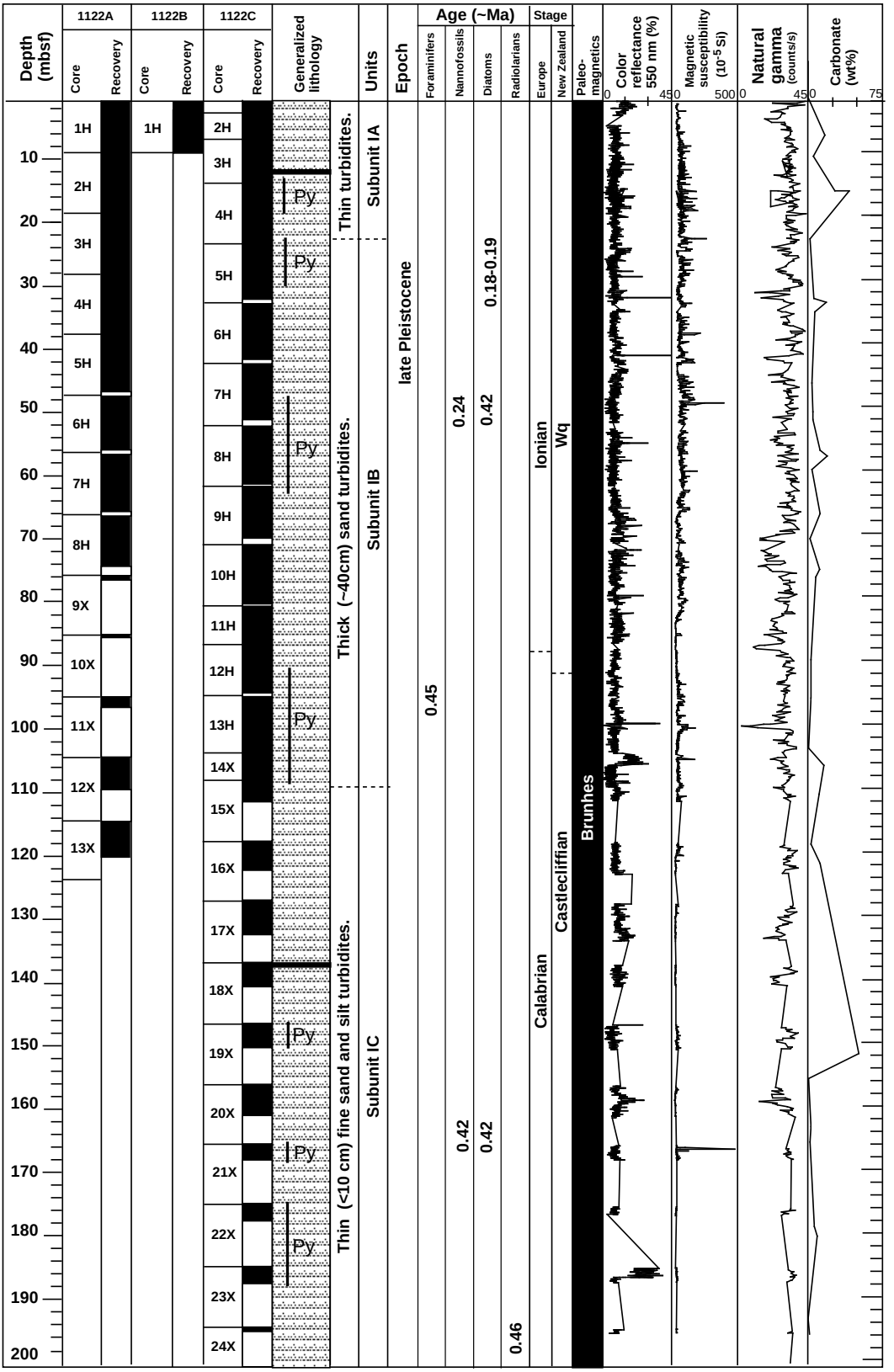
Leg: 181 Site: 1122
Depth (mbsf)
1122A
1122B
1122C
Core
Recovery
Generalized lithology
Units
Epoch
Age (~Ma)
Foraminifers
Nannofossils
Diatoms
Radiolarians
Stage
Europe
New Zealand
Paleo-magnetics
Color reflectance 550 nm (%)
Magnetic susceptibility (10⁻⁵ SI)
Natural gamma (counts/s)
Carbonate (wt%)
Thin turbidites.
Subunit IA
Thick (~40cm) sand turbidites.
Subunit IB
Thin (<10 cm) fine sand and silt turbidites.
Subunit IC
late Pleistocene
0.45
0.24
0.42
0.18-0.19
0.42
0.42
0.46
Ionian
Wq
Calabrian
Castlecliffian
Brunhes
Py

Figure 10

Figure 10 (continued)

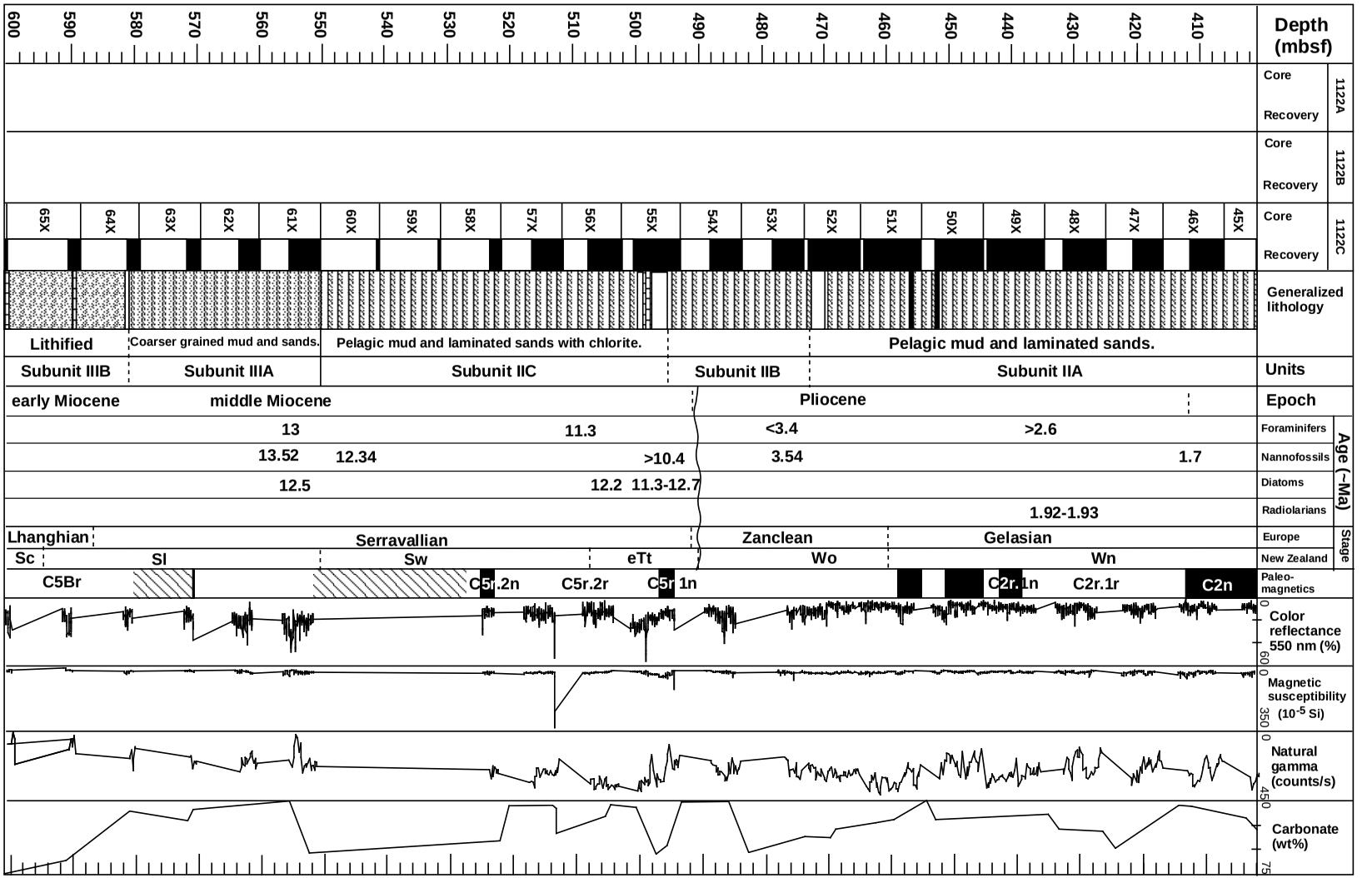

Figure 10 (continued)

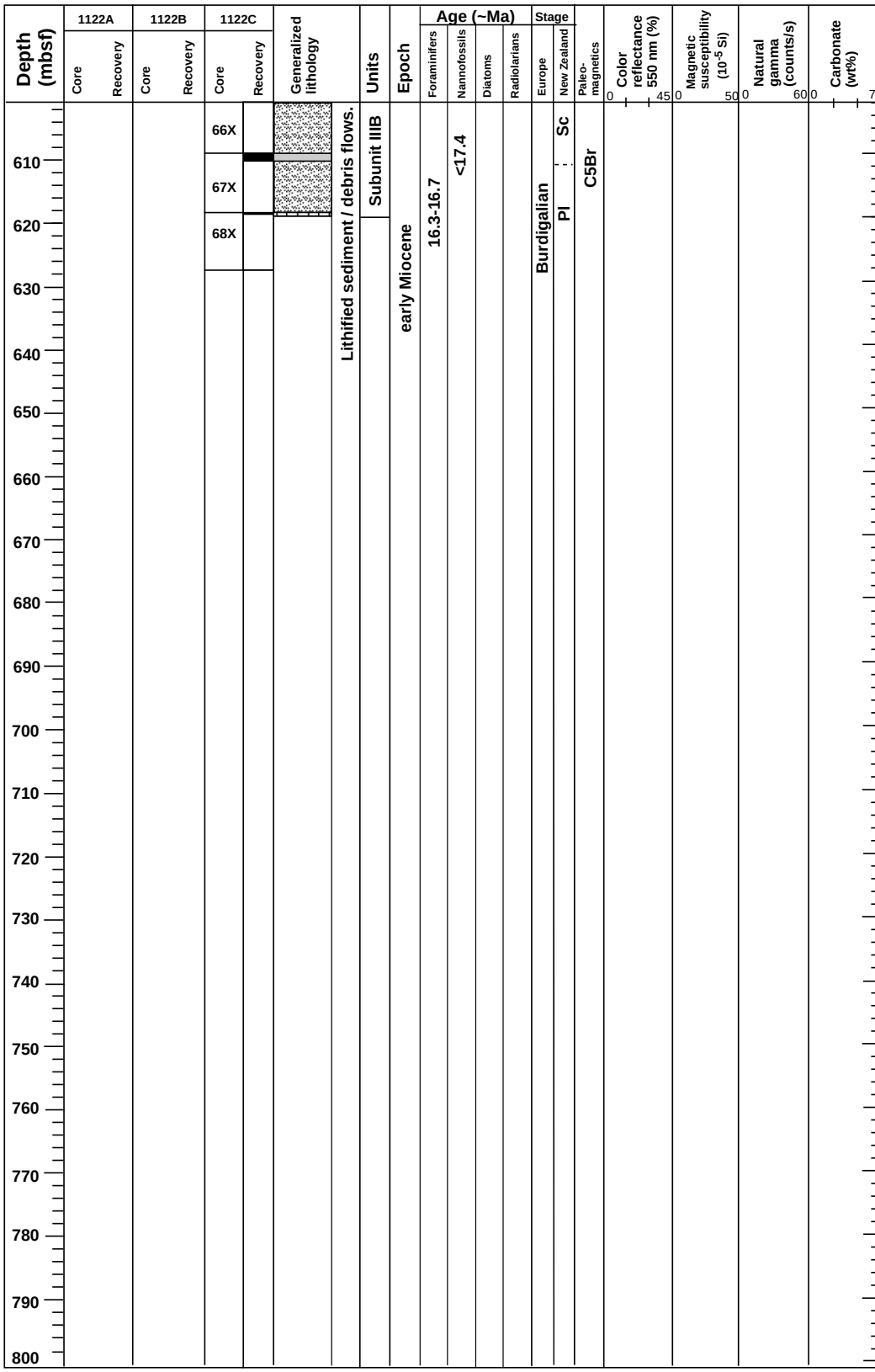

Figure 10 (continued)

Leg: 181 Site: 1123

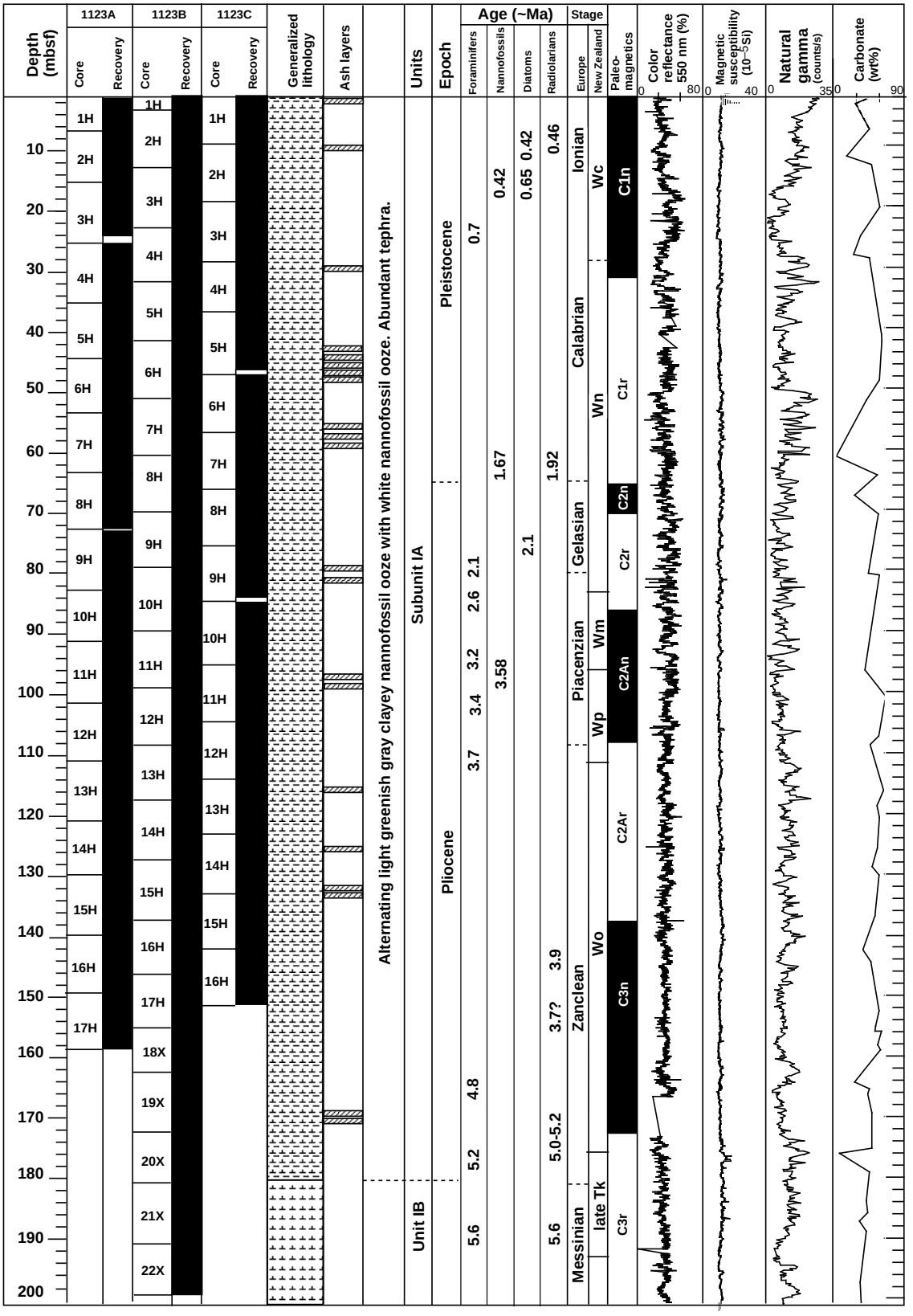

Figure 11

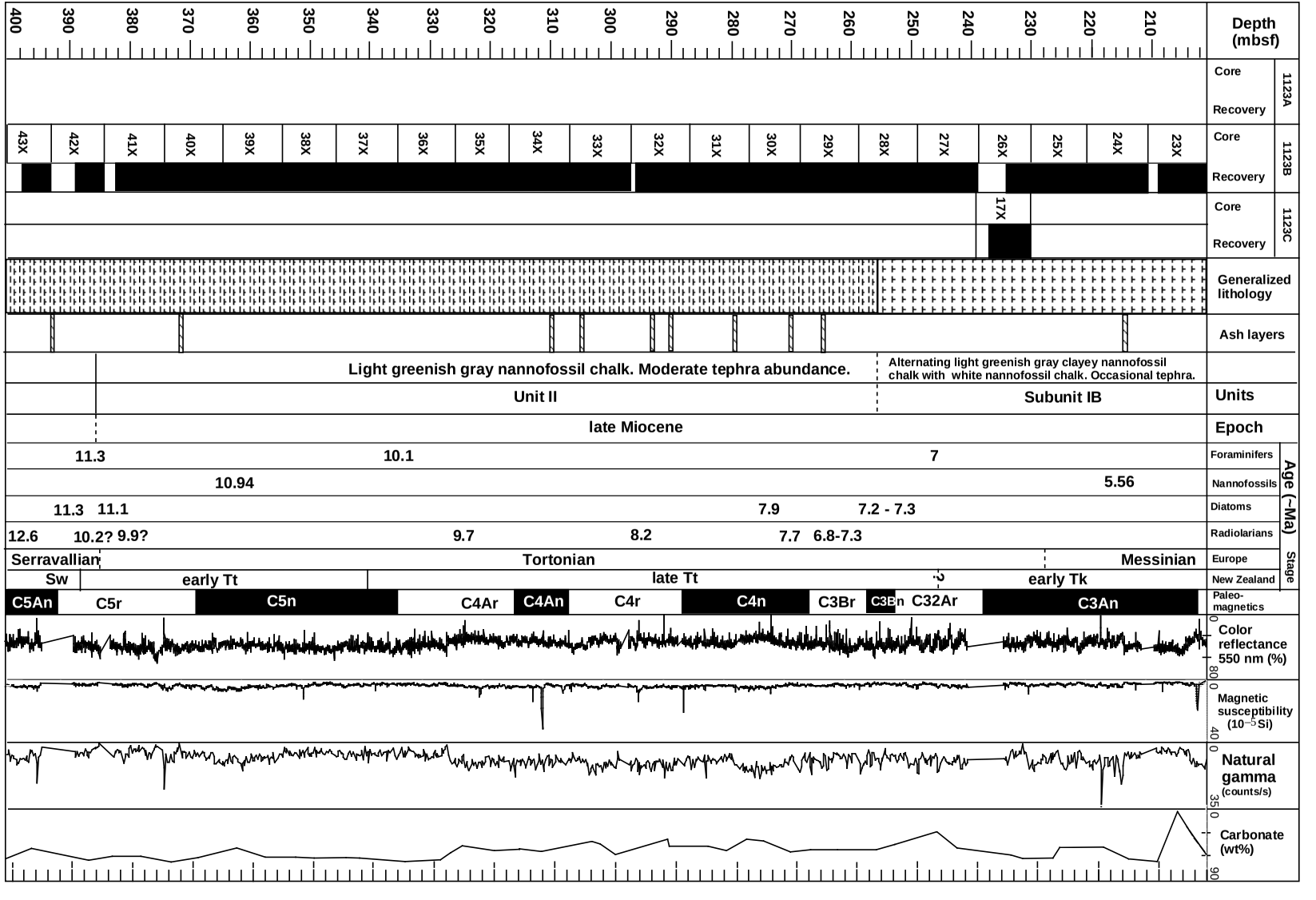

Figure 11 (continued)

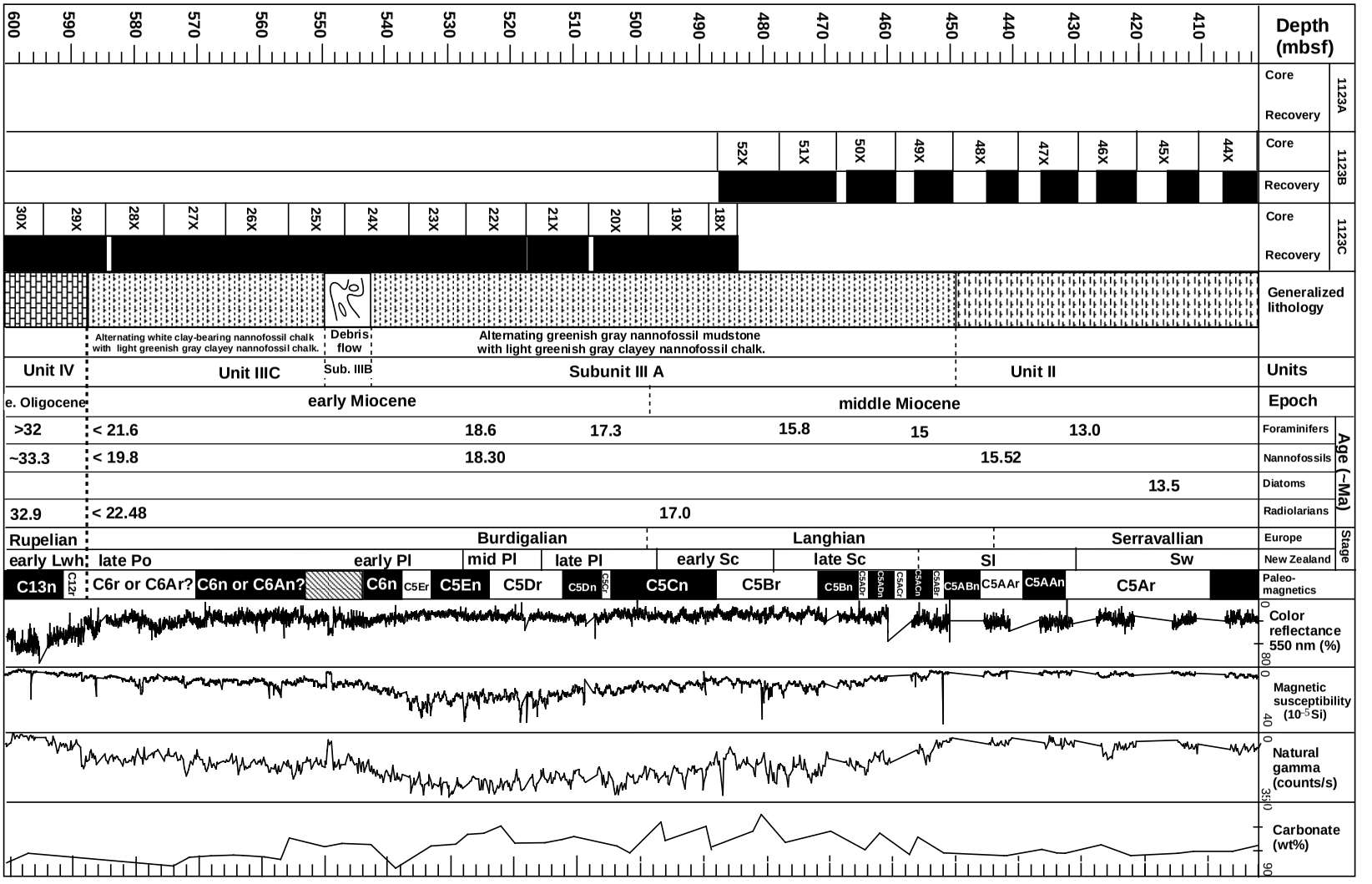

Figure 11 (continued)

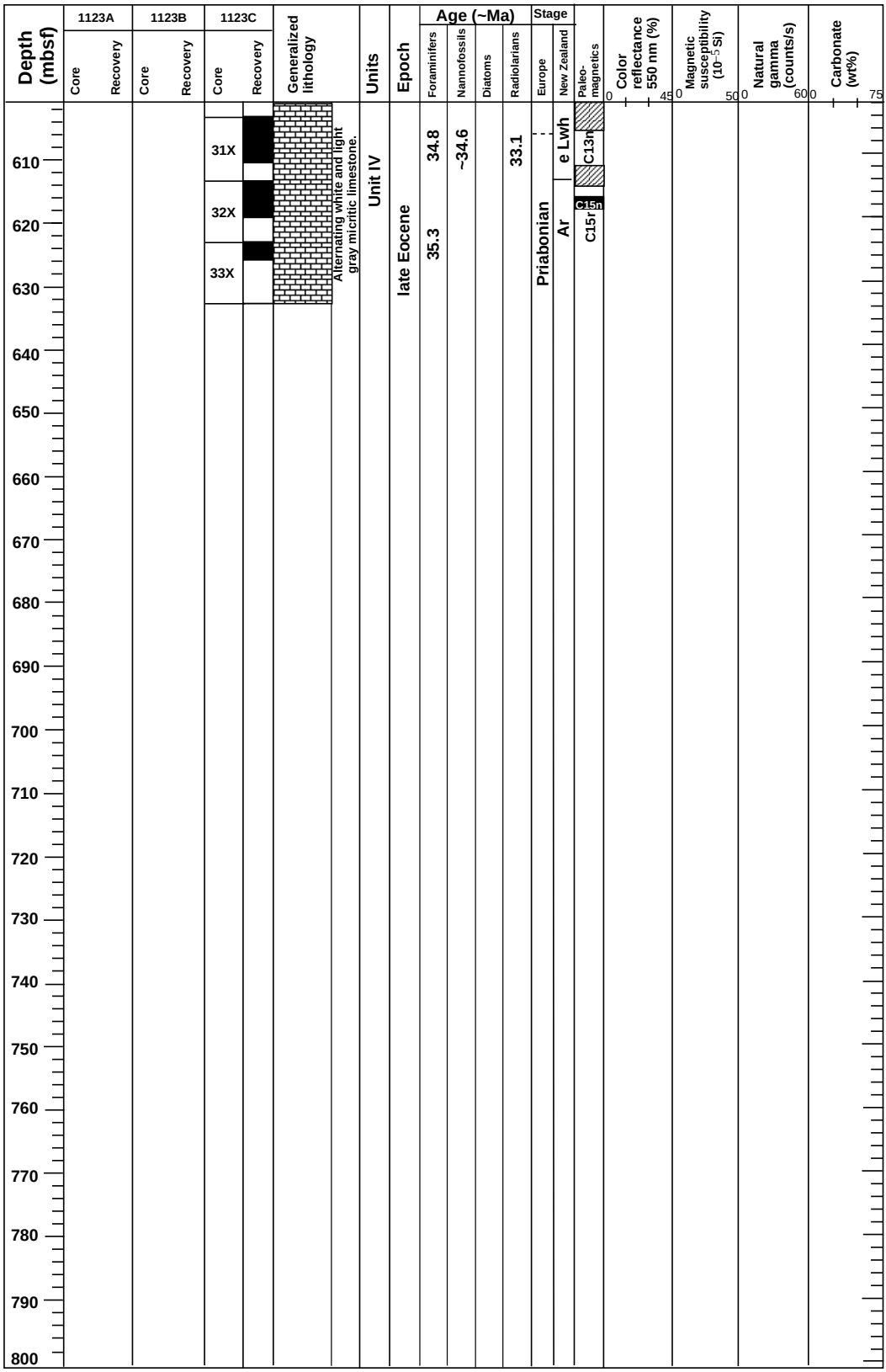

Figure 11 (continued)

Leg: 181 Site: 1124
Depth (mbsf)
1124A
1124B
1124C
1124D
Core
Recovery
Generalized lithology
Ash layers
Alternating light greenish gray clay-bearing nannofossil ooze with greenish gray nannofossil silty clay containing foraminifers and biosiliceous microfossils and frequent tephras, up to 90 cm thick.
Light greenish gray clay-bearing nannofossil ooze with greenish gray nannofossil-bearing silty clay and frequent tephras, less than 50 cm thick.
Units
Subunit IA
Subunit IB
Epoch
Pleistocene
Pliocene
Miocene
Age (~Ma)
Foraminifers
Nannofossils
Diatoms
Radiolarians
Stage
Europe
New Zealand
Paleo-magnetics
Calabrian
Gelasian
Piacenzian
Zanclean
Messinian
Tortonian
late Tt
Ionian
Wc
Wn
Wm
Wp
Wo
late Tk
C1n
C1r
C2n
C2r
C2An
C2Ar
C3n
C3r
C3An
C3Ar
C3Bn
C3Br
C4n
C4r
C4An
C4Ar
Color reflectance 550 nm (%)
Magnetic susceptibility (10^{-5}SI)
Natural gamma (counts/s)
Carbonate (wt%)

Figure 12

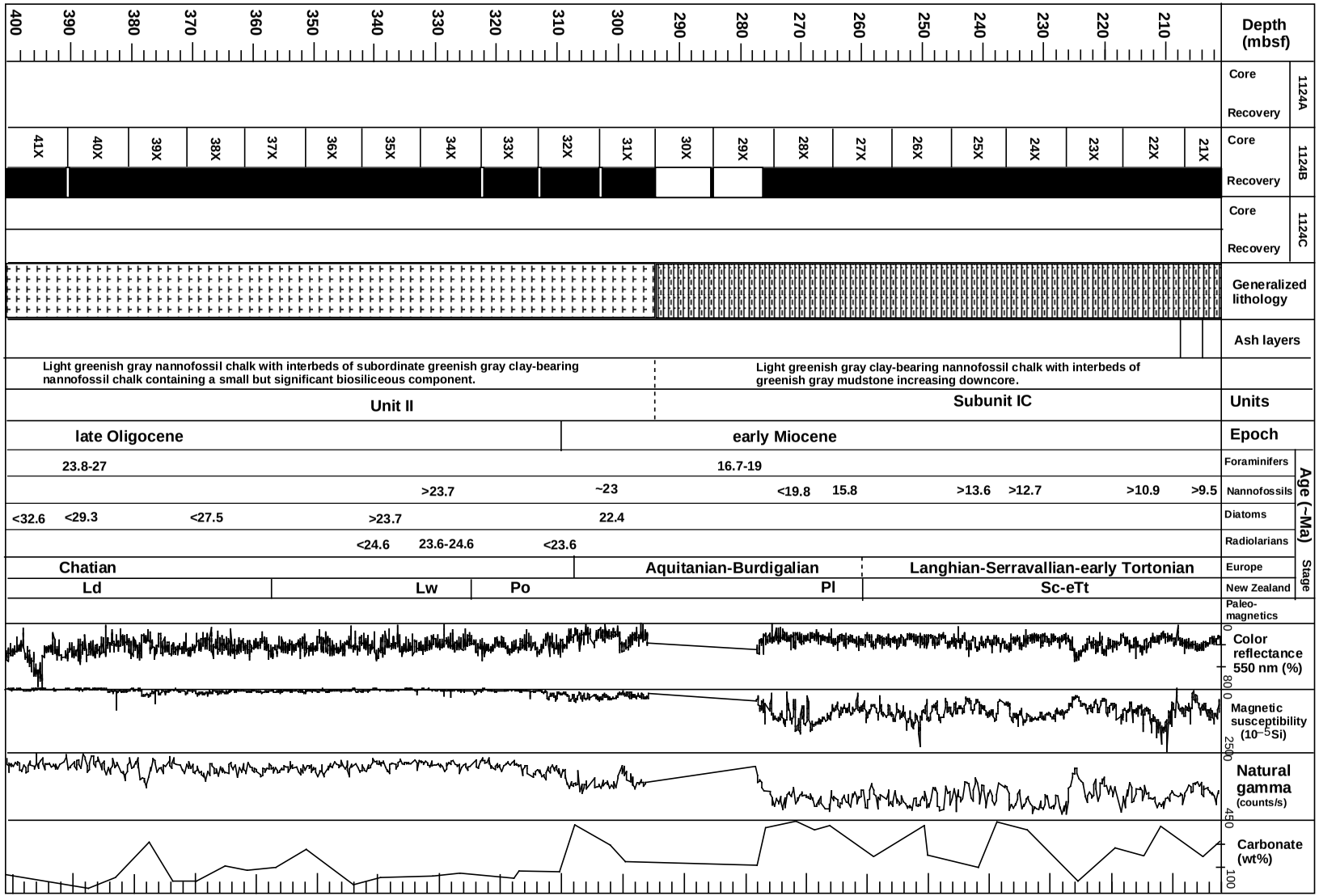

Figure 12 (continued)

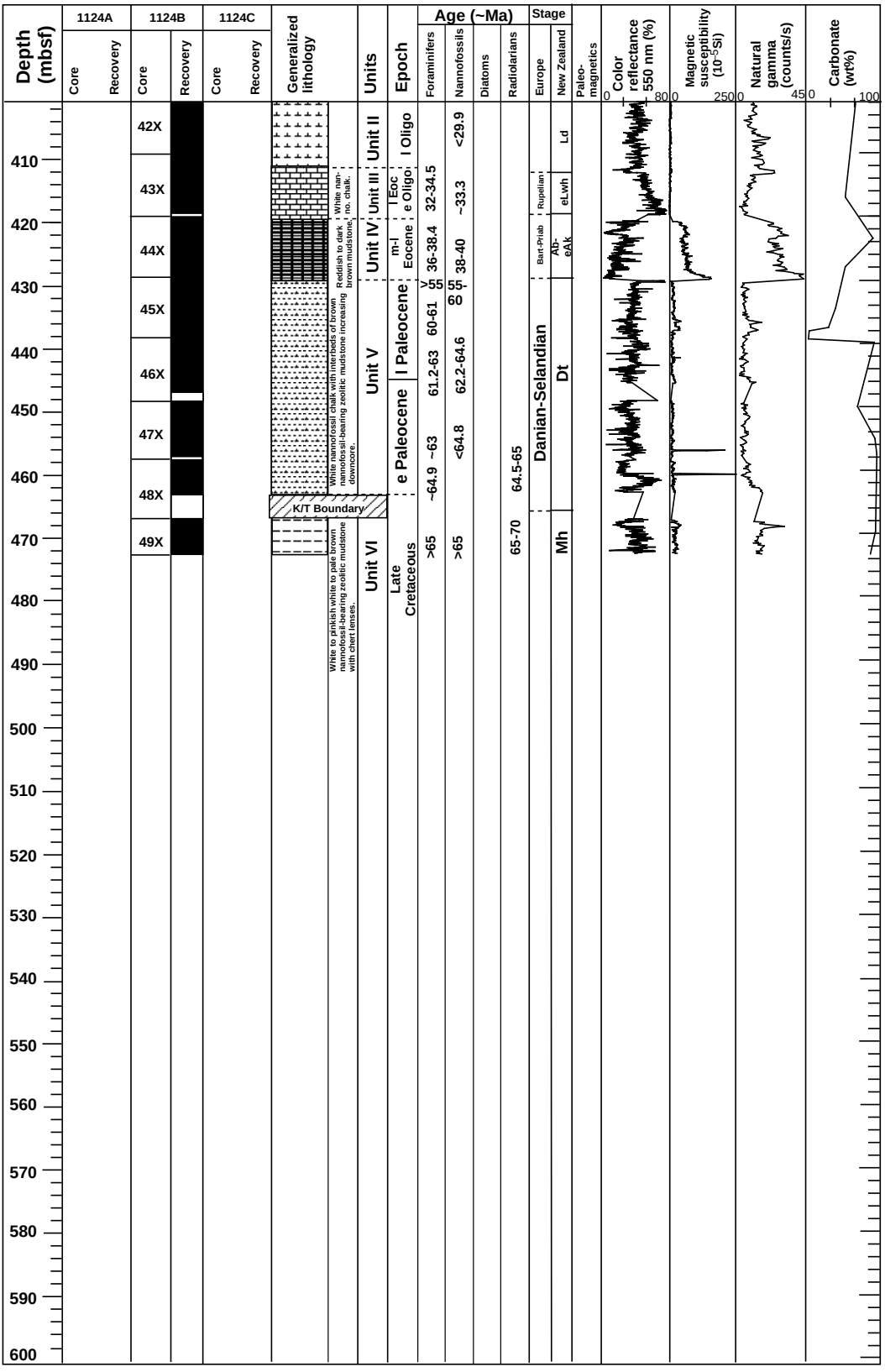

Figure 12 (continued)

Leg: 181 Site: 1125

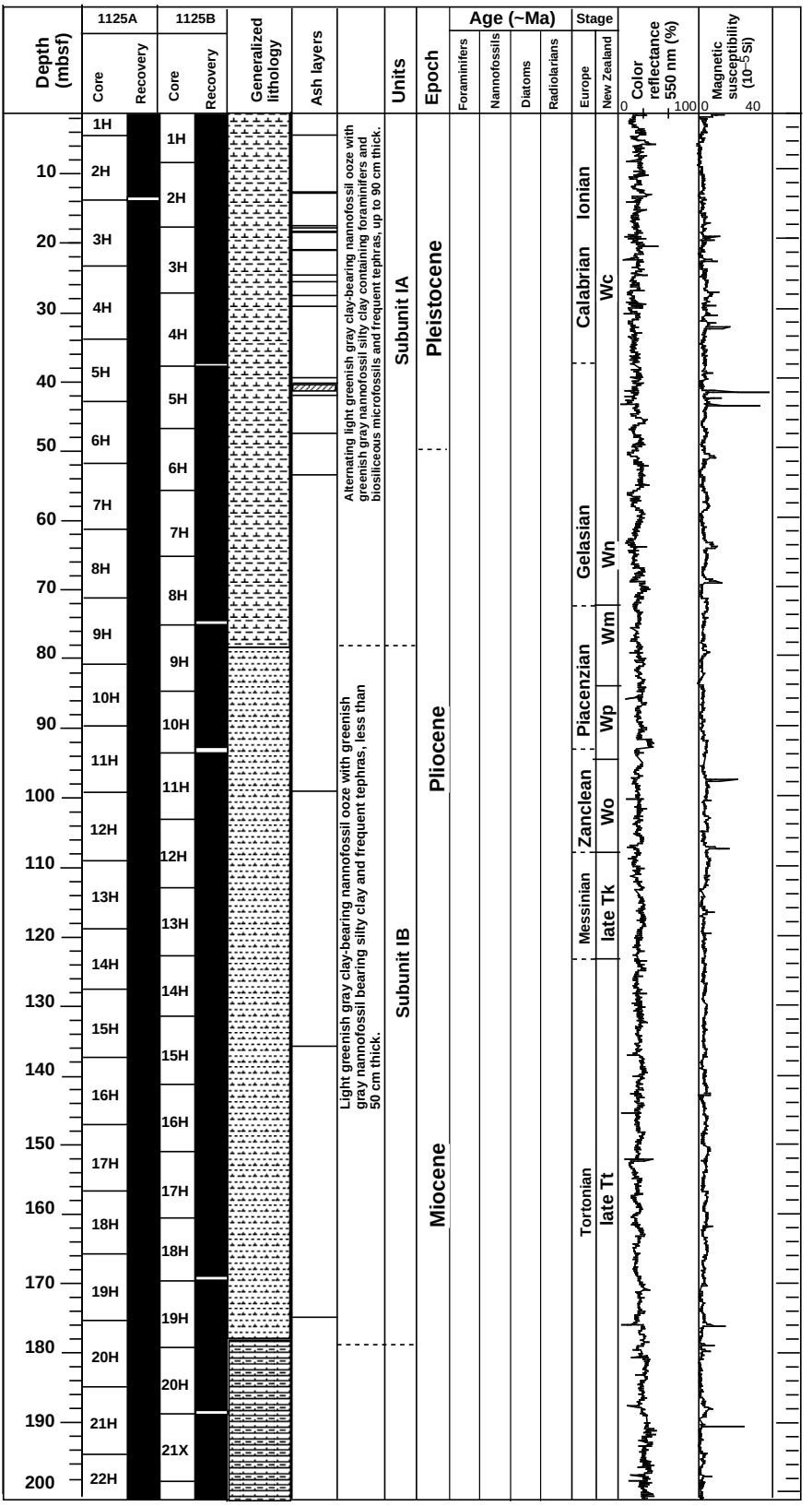

Figure 13

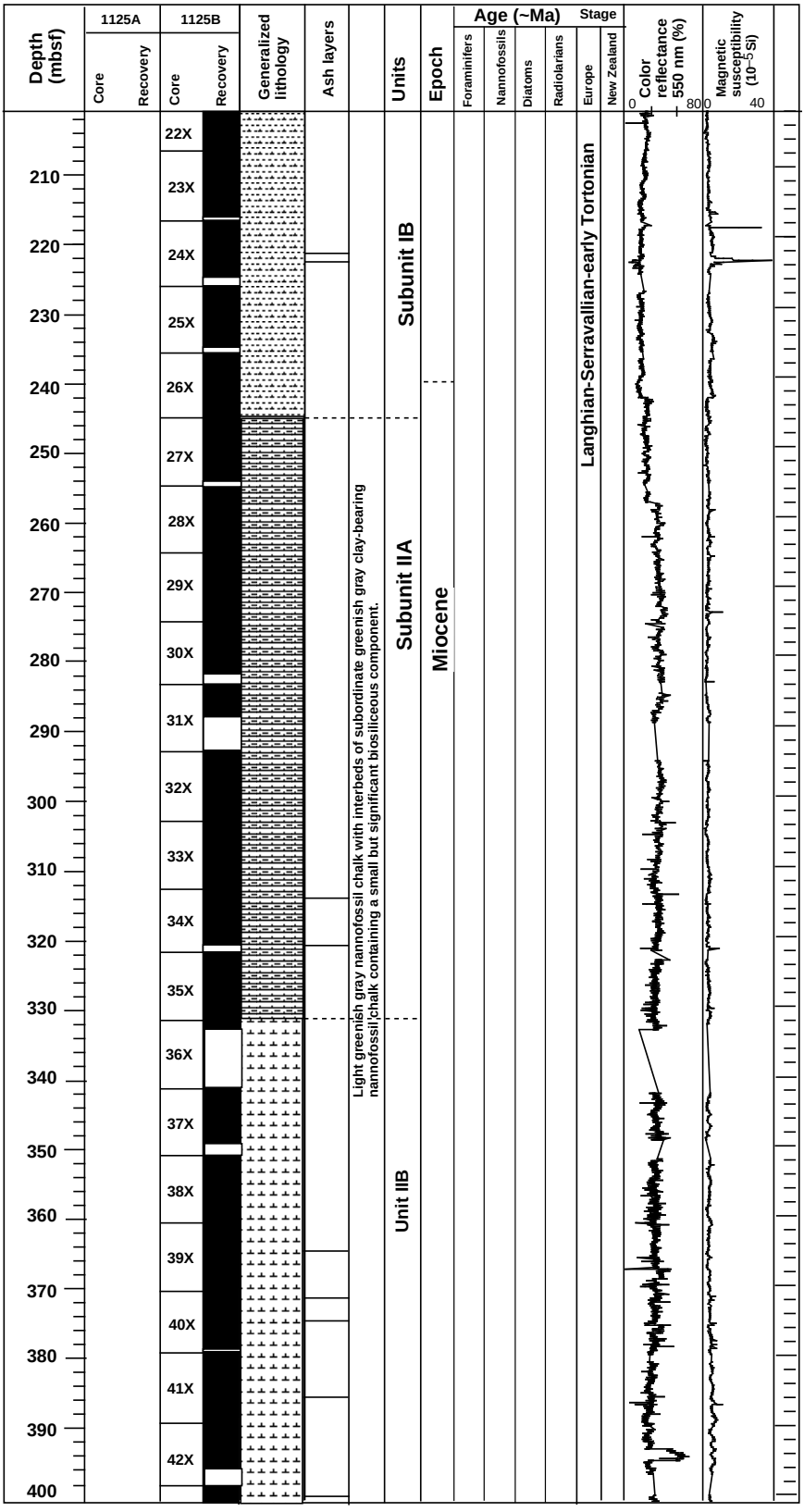

Figure 13 (continued)

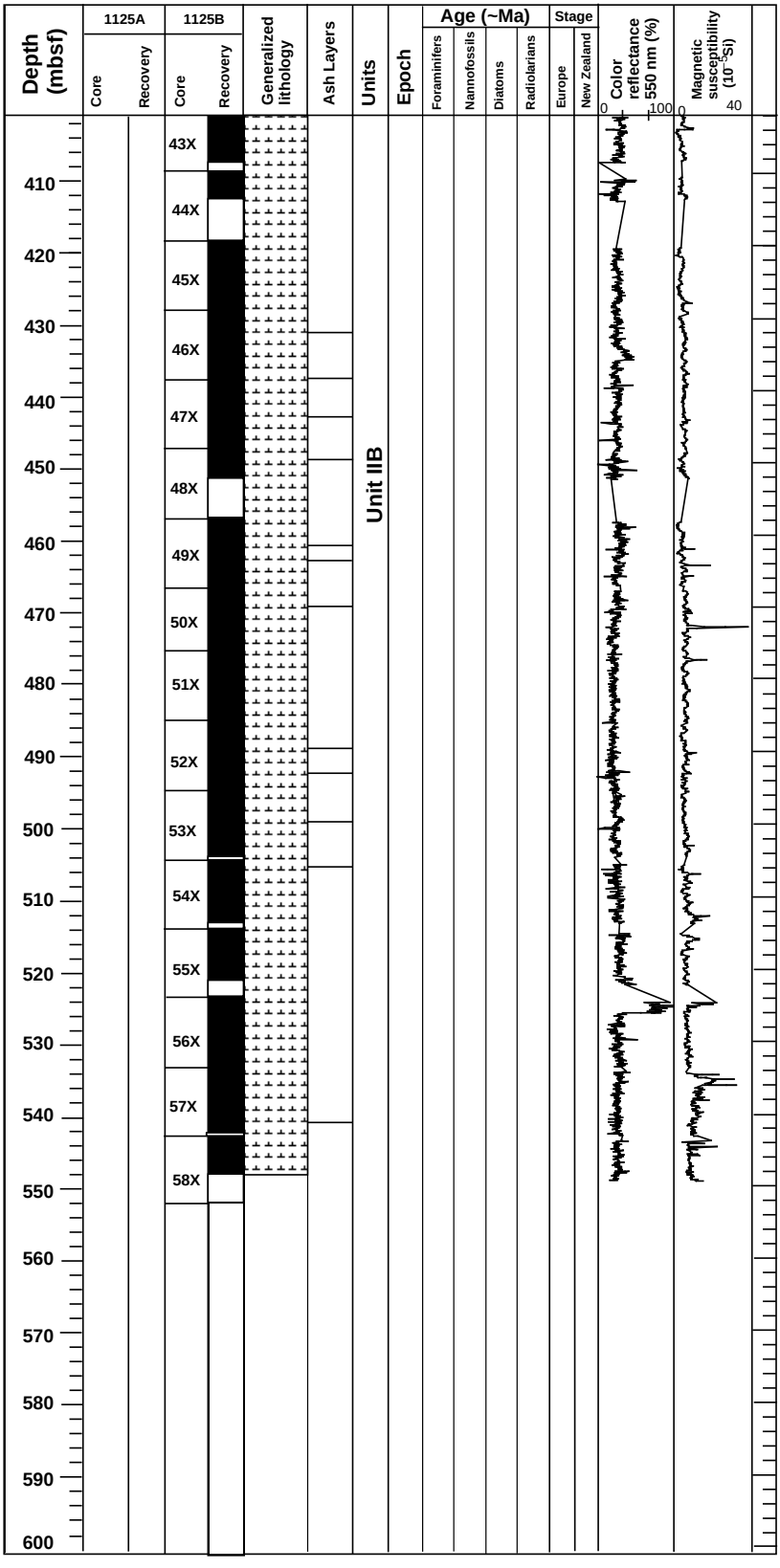

Figure 13 (continued)

OPERATIONS SYNOPSIS

The operations and engineering personnel aboard *JOIDES Resolution* for Leg 181 were:

ODP Operations Manager:	Ron Grout
Schlumberger Engineer:	Steve Kittredge

SUMMARY OF LEG 181 ENGINEERING AND DRILLING OPERATIONS

Sydney to Site 1119

The last line in Sydney cleared the dock at 0839 hr local time on 17 August 1998. The sea voyage to Site 1119 (proposed site SWPAC-1C) required 136.8 hr at an average speed of 9.7 kt. The planned track was to proceed on a southeasterly course, pass through Cook Strait between the North and South Islands of New Zealand, and then proceed directly south to Site 1119. However, because of heavy seas and bad weather that course was abandoned, and the vessel steered a southerly heading, taking the *JOIDES Resolution* around the southern tip of the South Island and then north to the site location.

The sizeable southern swell caused the voyage across the Tasman Sea to be slower than expected (9.6 kt average speed) and less comfortable than hoped for. When the vessel cleared the Foveaux Strait between the South Island and Stewart Island and turned northeast, the seas calmed and the vessel speed increased to 12 kt. Because no seismic survey was required, the vessel proceeded directly to the Global Positioning System (GPS) coordinates of the location.

Hole 1119A

The positioning beacon was dropped at 0342 hr on 23 August 1998. The APC/XCB bottom-hole assembly (BHA) was assembled using an 11-7/16-in used RBI C-3 bit with a lockable float valve (LFV) and deployed. Hole 1119A was spudded with the APC at 1015 hr on 23 August. The recovery indicated that the water depth referenced to the dual elevator stool (DES) was 406.5 meters below rig floor (mbrf), equivalent to 395.50 meters below sea level (mbsl). Hole 1119A is a single core hole designated for mudline sampling.

Hole 1119B

The second hole of the site was spudded with the APC at 1050 hr on 23 August without offsetting the vessel. The seafloor depth inferred from recovery was 407.8 mbrf (396.8 mbsl). APC coring proceeded to 155.8 meters below seafloor (mbsf) when Core 181-1119B-17H did not achieve full stroke. Cores were oriented starting with 181-1119B-3H. Heat-flow measurements were attempted with the Adara heat-flow shoe at 33.2 mbsf (4H), 61.7 mbsf (7H), 90.2 mbsf (10H), and 118.7 mbsf (13H), but could not be retrieved because the instrument had an electronic failure. The drill bit cleared the seafloor at 0020 hr on 24 August.

Hole 1119C

The vessel was offset 20 m to the east and the bit was lowered 3 m before the initial mud line attempt to provide stratigraphic overlap in the sedimentary record. The seafloor depth inferred from recovery was 407.2 mbrf (396.2 mbsl). APC coring advanced to 160.3 mbsf where piston coring was concluded when Core 181-1119C-17H failed to achieve a full stroke. XCB coring deepened the hole to the depth objective of 494.8 mbsf. No hole problems were encountered.

Logging Operations at Hole 1119C

After pumping down the aluminum "go-devil," the hole was flushed with 60 barrels of high viscosity mud. The drill string was pulled back in the hole to logging depth where the bit was positioned at 95.0 mbsf. Three logging measurements were scheduled for this hole. Logging operations began at ~2300 hr on 25 August. Three standard tool-string configurations were run: the triple combination, the Formation MicroScanner (FMS) with a sonic sensor (two passes), and the Geologic High Resolution Magnetic Tool (GHMT). Logging was conducted below the pipe at 80 mbsf to a hole obstruction at ~40 m above the bottom of the hole. The hole quality was poor, with an uneven borehole wall and many breakouts and ledges. The NUMRS tool (total magnetic field) on the GHMT suite failed to collect data for unknown reasons.

After logging was concluded by 1330 hr on 26 August, the Schlumberger equipment was dismantled. The drill pipe was lowered to 454 mbsf and the circulating head made up to the pipe. After filling the hole with 170 barrels of 12 pounds per gallon (1438 kg/m^3) heavy mud, the drill string was pulled out of the hole. While the drill string was being retrieved, the beacon was released and recovered, and the hydrophones and thrusters retracted and secured. At 1915 hr on 26 August, the vessel was under way to Site 1120.

Site 1120

Hole 1120A

The 319-nmi voyage to Site 1120 (proposed site SWPAC-6B) was accomplished through calm seas at an average speed of 11.0 kt. The vessel proceeded directly to the GPS coordinates of the location. The positioning beacon was dropped at 0045 hr on 28 August 1998. The APC/XCB BHA was assembled using a 9 7/8" PDC bit with an LFV and deployed. Hole 1120A was spudded with the APC at 0550 hr on 28 August. The recovery indicated that the water depth was 542.9 mbsl. The hole was scheduled for only a mudline sample and the single APC Core 181-1120A-1H was taken from 0 to 4.6 mbsf.

Hole 1120B

The second hole of the site was spudded with the APC at 0650 hr on 28 August. The seafloor depth inferred from recovery was 544.2 mbsl. APC coring advanced to 68.3 mbsf when Core 181-1121B-8H did not achieve a full stroke. Cores were oriented starting with 181-1120B-3H. Coring was continued with the XCB and deepened the hole to 188.0 mbsf when operations were put on standby because of excessive heave (2 m with an occasional 3 m event) generated by 2.0–2.5-m seas combined with a 4.0–5.5 m swell from the southwest. The hole was abandoned, the bit clearing the seafloor at 2020 hr on 28 August.

Hole 1120C

A force 9 gale with sustained winds up to 45 kt and gusts to 60 kt (force 10) prevailed in the drilling area from the evening of 28 August until 0045 hr on 30 August when it was decided to continue site operations even through environmental conditions were borderline for shallow-water

operations. After positioning the bit at 543 mbsl, Hole 1120C was spudded with the APC at 0613 hr on 30 August. The seafloor depth based upon recovery was 545.9 mbsl. Piston coring advanced to 44.6 mbsf when an incomplete stroke was encountered at Core 181-1120C-5H. While recovering the core, the wireline broke. In an attempt to fish the parted wireline, monel sinker bars, and APC assembly, the drill pipe was pulled back. The bit cleared the seafloor at 0613 hr on 31 August.

A wireline spear was made up and run in the pipe. It tagged the broken wireline at 183 mbsl. Attempts to work the broken wireline back up the pipe were unsuccessful and the spear slipped off. The drill pipe was pulled back in stands until the broken end of the wireline was found. After the broken wireline was recovered, the APC core barrel containing Core 181-1120C-5H was retrieved at 1055 hr. Environmental conditions were too extreme to continue and operations were placed in standby mode waiting on weather to improve.

Hole 1120D

At 1600 hr on 31 August, Hole 1120D was spudded and drilled ahead to 157.4 mbsf where XCB coring was initiated. XCB coring advanced from 157.4 to 220.7 mbsf when operations again had to be terminated because of excessive heave. It was decided to discontinue coring at this location and move on to Site 1121. As the drill string was being retrieved, the beacon was recalled and recovered. At 0600 hr on 1 September, the vessel began the transit to Site 1121.

Site 1121

Hole 1121A

The 95-nmi voyage to Site 1121 (proposed site SWPAC-7B) was accomplished at an average speed of 10.4 kt. The vessel proceeded directly to the GPS coordinates of the location. The positioning beacon was dropped at 2025 hr on 1 September. A backup beacon with a higher output setting had to be launched because the first beacon signal was marginal. The hydrophones and thrusters were lowered and the APC/XCB BHA was assembled using a 9-7/8-in PDC bit and deployed. A drill pipe swab (pig) was pumped down the pipe to clean out rust that had accumulated in the additional drill pipe that was brought for this deep-water site. Hole 1121A was spudded with the APC at 1554 hr on 2 September. The recovery indicated that the water depth was 4492 mbsl. The hole was scheduled for only a mudline sample and the single APC Core 181-1121A-1H was taken from 0 to 8.4 mbsf.

Hole 1121B

The second hole of the site was spudded with the APC at 1710 hr on 2 September. The sea-floor depth inferred from recovery was 4487.9 mbsl. APC coring advanced to 23.0 mbsf when Core 181-1121B-3H did not achieve a full stroke. The XCB barrel was run in with a soft formation cutting shoe and experienced considerable difficulty advancing with high torque and a very low penetration rate. After advancing only 0.5 m in 30 min of rotation, the core barrel was recovered to investigate why the coring was so difficult. The core proved to contain chert fragments. A hard-formation cutting shoe was deployed, and coring continued with the XCB in slow and occasionally difficult conditions.

XCB coring deepened the hole to 139.7 mbsf when operations were terminated because the scientific objectives were reached. The bit cleared the seafloor at 0120 hr on 4 September, ending operations at Hole 1121B. The bit was at the plane of the rotary table at 1040 hr and by 1045 hr the drilling equipment was secured for the voyage to the next site. Both beacons were recalled and recovered. At 1045 hr on 4 September, the vessel was under way on a northeasterly course to Site 1122.

Site 1122

Hole 1122A

The 341-nmi voyage to Site 1122 (proposed site SWPAC-8A) was accomplished at an average speed of 9.6 kt. The vessel proceeded directly to the GPS coordinates of the location. The positioning beacon was dropped at 2254 hr on 5 September. The hydrophones and thrusters were extended and the vessel settled on location. The APC/XCB BHA was assembled using a 9 7/8" PDC bit. Hole 1122A was spudded with the APC at 1210 hr on 6 September. The recovery indicated that the water depth was 4435.00 mbsl. Piston coring advanced to refusal at 75.8 mbsf and Core 181-1122A-1H through 8H were taken. The hole was deepened with the XCB to 124.0 mbsf, which was considered the objective for the initial hole of the site. APC cores were oriented starting with Core 181-1122A-3H. The bit cleared the seafloor at 0415 hr on 7 September, ending operations at Hole 1122A.

Hole 1122B

The vessel was offset 20 m to the west and the second hole of the site was spudded with the APC at 0615 hr on 7 September. To obtain a stratigraphic overlap for interhole correlation, the bit was positioned 5 m higher than at Hole 1122A. However, the recovered core barrel was full, which required another attempt to obtain a mudline core.

Hole 1122C

The bit was raised at the same location by an additional 5 m and Hole 1122C was spudded with the APC at 0740 hr. The mudline core indicated that the water depth was 4431.80 mbsl. The APC was advanced by recovery to 103.7 mbsf and Cores 181-1122C-1H through 13H were

obtained. The last three cores (181-1122C-11H, -12H, and -13H) did not achieve a full stroke.

Coring was switched to the XCB and advanced without incident to 204 mbsf with good to poor recovery. Very rapid XCB coring continued with recovery ranging from 1%–97% from 204 to 627 mbsf. After making a drill pipe connection following the retrieval of Core 181-1122C-68X (617.8 to 627.4 mbsf), the drill string became stuck and could not be rotated with up to 700 amps of top drive current. For over an hour, the driller worked the pipe with overpulls as large as 200 kips (200,000 lb), while maintaining a circulation rate of 1000 gallons/min at 2200 psi pressure. After working the pipe for over an hour, the drill string became free. It was considered imprudent to attempt to deepen the hole past this depth, and preparations for logging operations were started.

Logging Operations at Hole 1122C

In preparation for logging, the hole was swept with 60 barrels of high viscosity mud. The bit was pulled back in the hole to 520 mbsf and the hole was displaced with 175 barrels of sepiolite mud. The bit was then pulled back and positioned at 83 mbsf. At 0700 hr on 11 September, the logging equipment was rigged up and the first tool suite (triple combination: DITE/HLDS/APC/HNGS) was deployed in the drill pipe. The tool string was unable to pass the bit more than 12 m and after repeated attempts by the logging winch operator, it was decided to recover the logging tool in rapidly deteriorating weather conditions. After the logging tool was disassembled, we terminated operations at the site because of heavy seas and high winds. The combined sea state was exceeding 10 m and wind gusts were recorded as high as 55 kt.

When overpulls as large as 200 kips were unable to free the drill string, the top drive was picked up. For two hours, the stuck drill pipe was worked with 200 kips of overpull while maintaining a circulating rate of 1000 gallons/min. At 1530 hr on 11 September, the pipe was free and the drill string was recovered. The bit cleared the seafloor at 1625 hr. By 0800 hr the drilling equipment was secured for the voyage to the next site and the beacon was recalled and recovered. At 0800 hr on 12 September, the vessel was under way on a northeasterly course to Site 1123 (SWPAC-5B).

Site 1123

Hole 1123A

The 384-nmi voyage to Site 1123 (proposed site SWPAC-5B) was accomplished at an average speed of 11.1 kt. The vessel proceeded directly to the GPS coordinates of the location. The positioning beacon was deployed at 1848 hr on 13 September. The hydrophones and thrusters were lowered and the APC/XCB BHA was assembled using a 9-7/8-in PDC bit and deployed. Hole 1123A was spudded with the APC at 0425 hr on 14 September. The recovery indicated that the water depth was 3290.1 mbsl. APC coring advanced to refusal at 158.1 mbsf. The bit cleared the seafloor at 2355 hr on 14 September.

Hole 1123B

To obtain stratigraphic overlap with the previous hole, the bit was raised by 3 m from the

spudding depth of Hole 1123A, and Hole 1123B was spudded with the APC at 0110 hr on 15 September. The recovery of the mudline core indicated a seafloor depth of 3289.9 mbsl. APC Cores 181-1123B-1H through 15H were recovered from 0 to 136.4 mbsf. While attempting to retrieve Core 181-1123B-16H from a depth of 145.9 mbsf, the wireline parted at the sinker bar assembly socket. An eight-finger hard formation core catcher was used as an overshot in order to latch onto the core barrel. The overshot was run in and engaged on the first attempt and the core barrel was retrieved to the surface. Piston coring resumed in Hole 1123B with a full stroke of Core 181-1123B-17H. The core barrel could not be extracted from the sediment and had to be drilled over. The Adara heat-flow shoe was deployed with Cores 181-1123B-5H (41.4 mbsf), 6H (60.4 mbsf), 7H (79.4 mbsf), and 11H (98.4 mbsf). These runs failed to provide heat-flow data because of the frictional heat that was generated by the vertical motion of the vessel (heave). Coring was switched to the XCB and advanced without incident to 182.0 mbsf with >100% recovery. While retrieving Core 181-1123B-21X the core-winch operator noticed that the line on the drum was slack and that there was no line tension on the weight indicator. This was an obvious indication that the wireline and sinker bars were caught on an obstruction in the drill pipe. The obstruction turned out to be the core barrel which had stuck in the pipe 124 m below the drill floor. As a result of running into the core barrel, the wireline on the drum backlashed. After respooling the line and after various attempts to free the stuck XCB barrel the drill string had to be retrieved to the level of the stuck core barrel. There was nothing found on the inside of the drill pipe to suggest the cause of the jamming. The drill string was run back in to the bottom and XCB operations recommenced at 0545 hr on 16 September. Coring advanced to 374.1 mbsf. While pumping down the XCB core barrel to cut Core 181-1123B-41X, the barrel stopped at an obstruction in the bore of the drill pipe at 645 mbrf. On tagging the stuck barrel with the sinker assembly, a number of loose wraps were produced on the forward core winch drum before the brakes could be applied. Approximately 50 m of wire was spooled from the drum to remove the loose wraps. A fishing assembly was deployed, and the core barrel was tagged at 645 mbrf. After the first hit of the wireline jars, the stuck core barrel was freed and recovered to the rig floor. XCB coring again resumed at 0900 hr on 17 September and advanced to 489 mbsf, which was the revised depth objective for this hole.

Logging Operations in Hole 1123B

In preparation for logging, an aluminum go-devil was dropped and the hole swept with 60 barrels of high viscosity mud. The bit was pulled back in the hole to 520 mbsf and the hole was displaced with 175 barrels of sepiolite mud. The bit was then positioned at the logging depth of 83 mbsf. Logging operations began at 1100 hr and lasted for 20 hr. Logging was conducted from the bottom of the hole at 489 mbsf to the bit at 84 mbsf. Three standard tool-string configurations were run: the triple combination, the FMS-sonic (two passes), and the GHMT. The NMRS (total field) tool on the GHMT failed to work. The condition of the borehole was good and the quality of the data was excellent. After the logging equipment was disassembled, the bit was pulled out of the hole and cleared the seafloor at 0955 hr on 19 September, ending operations at Hole 1123B.

Hole 1123C

The vessel was offset by 30 m to the north and Hole 1123C was spudded with the APC at 1130 hr. Piston coring advanced to 151.5 mbsf. A core barrel with a center bit was dropped and the hole was deepened by drilling ahead to 230.0 mbsf. The center bit was retrieved and one XCB core (Core 181-1123C-17X) was obtained from 230.0 to 239.6 mbsf with 67% recovery to provide overlap with an interval of poor recovery in Hole 1123B. Following the recovery of the XCB core barrel, the center bit was dropped again and the hole was drilled ahead from 239.6 to 484.0 mbsf. After the center bit was recovered, XCB coring resumed and advanced from 484.0 mbsf to the modified depth objective of 632.8 mbsf (Cores 181-1123C-18X to 33X), with excellent recovery.

Logging Operations in Hole 1123C

In preparation for logging, an aluminum go-devil was dropped and the hole swept with 60 barrels of high viscosity mud. The bit was pulled back in the hole to 629 mbsf and the hole was displaced with 213 barrels of sepiolite mud. The bit was then pulled back to logging depth of 68 mbsf. By the time the drill crew was preparing to rig up for logging, there were wind gusts of over 60 kt, seas of 3–4 m, and up to 12-m-high swells, which forced the decision to abandon planned logging. At 1050 hr on 22 September, the bit was pulled clear of the seafloor. The pipe was partially recovered, but by 1300 hr the maximum vessel pitch was over 9°. Pipe tripping was suspended because of the hazard to men and material, and operations were placed in weather standby. The storm abated by 0330 hr on 24 September, which allowed the drill crew to recover the drill string and beacon. By 1000 hr the drilling equipment was secured and the thrusters and hydrophones retracted as the vessel began the 269-nmi transit to Site 1124.

Site 1124

Hole 1124A

The vessel proceeded directly to the GPS coordinates of proposed site SWPAC-9B where the positioning beacon was deployed and the hydrophones and thrusters were lowered. The APC/XCB BHA was assembled using a 9-7/8-in PDC bit and deployed. Hole 1124A was spudded with the APC at 0610 hr on 26 September. The core barrel was full and required a second attempt to recover a mudline.

Hole 1124B

The bit was positioned at 3962.5 mbsl, which was 5 m higher than the bit position of Hole 1124A. The initial attempt at a mud-line core on this hole was thwarted when the core barrel was recovered with a shattered liner and no core. Another core barrel was deployed and Hole 1124B was spudded with the APC at 0507 hr on 26 September. At 0610 hr the second piston core in Hole 1124B was shot with the bit at 3972.0 mbsl (5.4 mbsf). Because of an incomplete stroke, the drill string pressure had to be manually bled off. The core barrel could not be retrieved with 10 kilopounds (kips) of overpull being applied. Various attempts at freeing the stuck core barrel

proved unsuccessful. After the sinker bar assembly was recovered with the wireline the top drive was racked and the BHA with the stuck APC barrel was brought back to the surface. At 1745 hr on 26 September, the bit was at the rotary table. The APC corer was found in a fully stroked out position and the bottom section of the inner barrel was extended below the bit and bent ~1 m below the BHA, which prevented the core barrel being retrieved through the bit.

We concluded that the piston corer hit a thick layer of volcanic ash at a shallow depth, which forced the BHA to displace horizontally and bend the core barrel. Because of the shallow penetration (5 mbsf), the sediment provided very little lateral support to the BHA when the the piston corer advanced into the hard layer of ash. The situation can be compared to trying to balance a full bottle of soda in the air with a plastic straw.

Hole 1124C

Because of the incident in Hole 1124B, we decided to drill the first two cores in Hole 1124C with the XCB. Hole 1124C was spudded at 0220 hr on 27 September and washed to 8.0 mbsf where XCB coring was initiated. XCB coring advanced from 8.0 to 27.2 mbsf with 74% recovery. The coring system was then switched to the APC and piston coring advanced from 27.2 to 159.2 mbsf, which was considered APC refusal. The Adara heat-flow shoe was affixed to the APC corer for Cores 181-1124C-5H (55.7 mbsf), 7H (74.7 mbsf), 9H (93.7 mbsf), and 11H (112.7 mbsf). The data from the last three runs were used to compute a temperature gradient of 51.9_C/km.

XCB coring deepened the hole from 159.2 to 473.1 mbsf, which was considered the depth objective for this hole.

Logging Operations in Hole 1124C

To prepare for logging, an aluminum go-devil was dropped and the hole swept with 60 barrels of high-viscosity mud. The bit was pulled back in the hole to 447 mbsf and the hole was displaced with 175 barrels of sepiolite mud. The bit was then positioned at the logging depth of 96 mbsf.

Logging operations began at 2100 hr on 29 September and lasted for 19 hr. Logging was conducted from the bottom of the hole at 474 mbsf to the bit at 78 mbsf (picked up from 96 mbsf). Three standard tool-string configurations were run: the triple combination, the FMS-sonic, and the GHMT (Geological High Resolution Magnetic Tool). The NMRS tool on the GHMT failed to operate. The condition of the borehole was good and the quality of the data was excellent. By 1545 hr on 30 September, the Schlumberger logging equipment was disassembled and the drill bit cleared the seafloor at 1630 hr.

Hole 1124D

The vessel was offset 30 m to the north of Hole 1124C. An attempt was made to wash down to 13 mbsf but was given up when very hard formation (possibly cemented ash) was encountered. The vessel was offset an additional 10 m to the west where Hole 1124D was spudded with the XCB at 1917 hr on 30 September. The bit was drilled ahead to 22.6 mbsf with no difficulty and the XCB wash barrel was recovered. APC coring was initiated at this depth and continued to the

planned depth objective of 155.6 mbsf.

The drill string was pulled to the surface with the bit clearing the sea floor at 1325 hr. As soon as the bit cleared the seafloor, the beacon was recalled. After the BHA was inspected, the drilling equipment was secured and the vessel was under way to Site 1125, the last site of Leg 181, at 2330 hr on 1 October.

Site 1125

Hole 1125A

The 198-nmi voyage to Site 1125 (proposed site SWPAC-3A) was accomplished at an average speed of 9.0 kt. The vessel proceeded directly to the GPS coordinates of the location. The hydrophones and thrusters were lowered and the APC/XCB BHA was assembled using a 9 7/8" PDC bit and deployed. Hole 1125A was spudded with the APC at 0352 hr on 3 October. The recovery indicated a water depth of 1364.6 mbsl. APC coring advanced without incident to refusal, which was at 203.5 mbsf when Core 181-1125A-22H failed to achieve full stroke. The Adara heat-flow shoe was deployed at 42.5 mbsf (5H), 61.3 mbsf (7H), 80.3 mbsf (9H), 99.3 mbsf (11H), and 118.3 mbsf (13H). The computed heat-flow gradient was 70.7°C/km. The bit was pulled back to 168.0 mbsf where the top drive was set back. The drill string was pulled out in stands clearing the seafloor at 2000 hr on 3 October, ending operations at Hole 1125A.

Hole 1125B

The vessel was offset 30 m to the north. To obtain stratigraphic overlap with the previous hole, the bit was lowered by 5 m from the spudding depth of Hole 1123A, and Hole 1125B was spudded with the APC at 2130 hr on 3 October. The recovery indicated a seafloor depth of 1365.6 mbsl. APC coring advanced without incident to 188.8 mbsf. Cores were oriented starting with Core 181-1125B-3H. The hole was deepened with the XCB to 552.1 mbsf, when coring time expired for the leg at 0315 hr on 6 October.

Logging Operations in Hole 1125B

In preparation for logging, an aluminum go-devil was dropped and the hole was circulated with a 60-barrel flush of high-viscosity mud and displaced with 186 barrels of sepiolite. The bit was pulled back to 512 mbsf and the top drive set back. The bit was placed at the logging depth of 96 mbsf. Logging operations began at 0600 hr on 6 October and ended at 1300 hr the same day. Logging operations were limited to only one full pass of the triple combination because of time constraints. There was ~1–2 m of heave throughout operations and the wireline heave compensator was used during all measurements. The hole was logged from the bottom at 524 mbsf to the bit at 78 mbsf (picked up from 96 mbsf). The condition of the borehole was good and the quality of the data was excellent. The hole had a fairly uniform diameter of 12 inches throughout, except near the top where the hole widened to >18 inches.

Following the rigging down from logging, the drill string was recovered and the BHA disassembled for secure stowage during the final transit of the leg. Following the recovery of the

beacon, the hydrophones and thrusters were retracted, and the vessel began the transit to Wellington, New Zealand, at 1730 hr on 6 October.